2. Iron

Annie K. Powell

CONTENTS

0010-8545/94/$26.00
SSDI 0010-8545 (94) 04000–N

INTRODUCTION

Since the field of iron coordination chemistry is so vast, with a dominance of the +2 and +3 oxidation states, this review has been divided up into subject areas based on the categories of compound type which are found in Nature, which is reflected by the fact that much of the current interest in the preparation of iron coordination compounds lies in the area of biomimetic chemistry. In such systems it is the interplay of oxidation and spin states which can result in iron centres specifically capable of catalysing certain reactions, or recognising certain substrates. These themes are also important in the synthetic complexes reported here, and have led to the production of an exciting variety of compounds often designed with the lessons from Nature in mind. In general, the review does not cover organometallic compounds nor catalytic systems, although a few organometallic compounds which may be of interest to coordination chemists have been included, and some of the catalytic reactions of models for enzyme systems covered. The sheer size of the subject area probably precludes a fully comprehensive coverage, but I hope I have at least highlighted the themes of current importance.

The sources for the literature discussed are the following journals for 1991: *Acta Chem. Scand., Angew. Chem., Int. Ed. Engl., Aust. J. Chem., Bull. Acad. Sci. USSR (English translation of Iz. Akad. Nauk. SSSR, Ser. Khim.), Bull. Chem. Soc. Jpn., Bull. Soc. Chim. Belg., Bull. Soc. Chim. France, Can. J. Chem., Chem. Ber., Chem. Lett., Chimia, Eur. J. Solid State Inorg. Chem., Gazz. Chim. Ital., Helv. Chim. Acta, Inorg. Chem., Inorg. Chim. Acta, J. Am. Chem. Soc, J. Chem. Soc., Chem. Commun., J. Chem. Soc., Dalton Trans., J. Coord. Chem. A, J. Struct. Chem. (English translation of Zh. Strukt. Khim.), Polyhedron, Recueil Trav. Chim. Pays-Bas, Revue Roumaine Chim., Russian J. Inorg. Chem. (English translation of Zh. Neorg. Khim.), Transition Metal Chem., Z. Anorg. Allg. Chem., Z. Naturforsch, Teil B.* Additionally, *Chemical Abstracts* was searched on-line for 1991.

I would like to thank Sarah Heath and Richard Henderson for their help in preparing the diagrams and the final form of the text. I would also like to thank the SERC for the provision of the Chemical Database Service at Daresbury, which provided the crystallographic coordinates for a large number of the figures.

2.1 IRON(II) COMPOUNDS

Iron(II) complexes are generally stabilised by relatively strong-field donors, and this is reflected by the dominance of nitrogen-donor complexes. In addition, the nature of the ligands can have a subtle effect on the spin-state of the iron(II) and there are many instances of "spin crossover" behaviour. With the increasing availability of variable temperature magnetic studies and the rekindled interest in magnetic properties per se it has become difficult to make more than an arbitrary distinction between compounds displaying "unusual magnetic properties" and simple coordination compounds. Those compounds which have been subjected to detailed magnetic investigations are given their own section, but the reader will also find other examples of mixed spin-state systems elsewhere, particularly in amongst the substituted aromatic nitrogen donors.

2.1.1 *Complexes with oxygen donor ligands*

The racemic ligand (±)-1,1'-binaphthyl-2,2'-diyl hydrogenphosphate reacts with iron(II) ions, as well as cobalt(II) and copper(II), in methanol to give mononuclear products [1]. On the basis of the X-ray diffraction study on the copper(II) complex and a comparison of the properties of the complexes, it is concluded that the bonding in the iron(II) and copper(II) complexes is similar. The structure consists of an octahedrally coordinated metal system with four equatorial methanol molecules and two axial water molecules; the hydrogenphosphate ligand is not directly bound to the metal ion.

Iron(II) alkoxides $[Fe(O(CH_2)_nCH_2OH]^+$ were found to undergo a gas phase dehydrogenation, dependent on n, with oxidation of the terminal OH group [2].

2.1.2 *Complexes with mixed nitrogen and oxygen donor ligands*

The volumes of activation for the dissociation by hydroxide ions of the cations of several iron(II) diimine complexes, including those with phen and bpy, in aqueous solution have been measured using spectrophotometry at atmospheric and elevated pressures [3]. The positive values of ΔV^* of between +10 and +16 cm^3mol^{-1} are rationalised as arising from significant loss of electrostricted water from the hydroxide ion as it reacts associatively with the iron(II) ion.

The complexes of several 3*d* transition metals (Mn(II) to Zn(II)) with the unsymmetrical Schiff's base ligand, 2-(2,5,8-triaza-1-octenyl)phenol, as the monoperchlorate salt have been studied using XPS [4]. In particular, the binding energy of the nitrogen atoms was investigated, and it was found that the asymmetric N 1*s* electron spectra could be deconvoluted to give two components, the one of higher binding energy corresponding to the amine nitrogens, the lower to the imine nitrogen.

The complexes formed with iron(II), nickel(II), copper(II) and zinc(II) and the Schiff's base ligand formed from 2,4-dihydroxybenzaldehyde and thiosemicarbazone were studied spectroscopically and their bactericidal and superoxide dismutation activities were assessed [5]. Overall, none of the complexes was significantly more effective than the ligand on its own. In a similar study, the activities of the related iron(II) and copper(II) complexes formed with the Schiff's

base from 2,4-dihydroxybenzaldehyde and semicarbazone were found to be greatest for iron(II) and least for the free ligand [6]. The iron(II) compound might have a dinuclear structure arising from phenolate bridging of two five-coordinate (NO_3 from the ligand plus one coordinated water) iron centres.

The formation constants of ternary complexes of iron(II) with $cdtaH_4$ as primary ligand and indole-3-butyric acid as secondary ligand have been determined, and show that the iron(II) complex is not as stable as the complexes with other divalent metals [7].

In the reaction of neat hydrazine hydrate with 1,1'-diacetylferrocene, the dihydrazone [$H_2NN(Me)CC_5H_4FeC_5H_4C(Me)NNH_2$] results in almost quantitative yields after 72 h at room temperature [8]. Increasing the reaction time or treating the dihydrazone with fresh hydrazine causes the iron to be stripped from the metallocene and bis(hydrazine)bis(hydrazinecarboxylato-*N',O*)iron(II) (**1**) crystallises. The dihydrazone can be cyclised in the presence of Ba^{2+} or Mo^{2+} ions to give the cyclic diazine [-N(Me)$CC_5H_4FeC_5H_4C$(Me)N-] with the liberation of hydrazine.

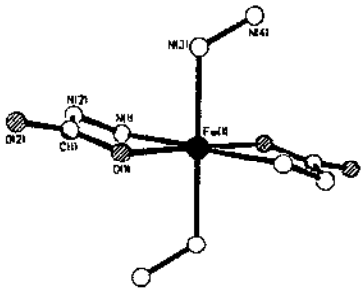

(**1**)

Four high spin ferrous polydentate Schiff's base complexes were prepared and characterised by IR, X-ray absorption and Mössbauer spectroscopies and variable temperature magnetic susceptibility measurements [9]. The Schiff's base ligands were prepared by the condensation of 5-nitrosalicylaldehyde with 2-(aminoethyl)pyridine (base = 5-NO_2-salaep) or tetraamines. The structure of the complex formed with 5-NO_2-salaep (**2**) was determined by X-ray crystallography and reveals that the iron(II) is coordinated by two tridentate ligands. Structure (**2**) models many of the features thought to be present at the iron site of the "ferroquinone complex" of photosystem II. The EXAFS and XANES spectra reported could only be fitted to the suggested structures for the other complexes with difficulty. The Mössbauer spectra are consistent with the distortion observed about the iron centre in the complexes. The variable temperature magnetic data suggest that there is appreciable zero-field splitting of the ground states in these complexes. One of the complexes exhibits what has been assigned as a thermally induced $^5T_{2g} \geq {}^1A_{1g}$ spin conversion, with the spin conversion apparently taking place in two steps which are separated by a 30 K broad spin equilibrium domain where high and low spin molecules coexist in a 1:1 mixture.

The electrocatalytic reduction of the nitrite ion by edta complexes of iron(II) and ruthenium(II) has been investigated [10]. In the case of iron(II) it is the $[Fe^{II}(edta)(NO^{+})]^{-}$ species which acts as an effective electrocatalyst for the reduction of NO_2^- or HONO to give N_2O, N_2, NH_3OH^+, or NH_4^+. Product selectivity can be introduced by pH control. The mechanisms proposed find parallels with those of nitrite reduction by water-soluble porphine complexes of iron, and the system thus models the enzyme-based system for nitrite reduction.

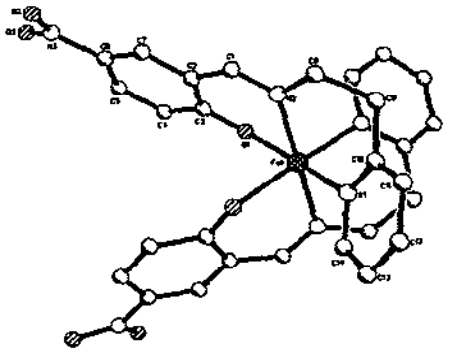

(2)

The iron(II) compound formed with 1-(3-sulfophenyl)-3-methyl-4-(5-chloro-2-hydroxy-3-sulfophenylazo)pyrazol-5-one was characterised by X-ray powder diffraction, TGA and spectroscopic measurements, and assigned a square pyramidal structure with N_2O_2-donation from the ligand and one coordinated water [11]. In addition, it was concluded that the ligand is in the lactam-hydrazone tautomeric form.

In a solution state study on the complexation of first row transition metals by the ligands tris(2-pyridyl)carbinol and bis(2-pyridyl)phenylcarbinol, the results obtained on the iron(II) system were somewhat complex [12]. Three different complexes formed between iron(II) and tris(2-pyridyl)carbinol were identified, which were suggested to correspond to symmetric binding of six pyridine moieties from two ligands with *N,N',N''*-binding, and two complexes where the oxygen atom of the carbinol group binds in either a protonated or deprotonated form to give *N,N',O*-binding. The bis(2-pyridyl)phenylcarbinol ligand, with only two pyridine moieties, is expected to bind in an *N,N',O*-fashion.

2.1.3 Complexes with nitrogen donor ligands

Iron(II) monomers in an N_6- or N_4-environment continue to be of interest by providing models for testing theories of structure and bonding as well as some examples of spin crossover systems, underlining the influence the electronic structure of the ligand can have on the stabilisation of the electronic structure at the metal centre. The N_4-complexes can also be relevant as models for iron in haem environments, and generally are capable of coordinating one or more extra ligands to give five or six coordinate iron centres. Examples of such complexes are also considered here.

2.1.3.1 Complexes with N_6-coordination

The complexation of iron(II), as well other divalent metals, by the hexadentate ligand (3) has been investigated using potentiometric titrations [13]. The results were compared with those for other similar N_6 donors and it was concluded that this ligand forms strong complexes, probably as a result of adopting what is described as a "hemi-cage" structure around the metal ion.

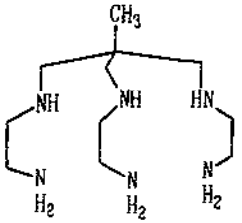

(3)

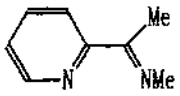

(4)

The isomeric forms of the tris Schiff's base complex formed between iron(II) ions and the Schiff's base (4) derived from 2-acetyl pyridine and methylamine have been investigated in kinetic and spectroscopic, particularly ^{1}H NMR, studies and the structure of the *mer* isomer has been confirmed by X-ray crystallography [14]. The solution studies indicate that the *trans* isomer is also important. The kinetics of base hydrolysis and the solvation of the complex have also been studied.

A rather unusual route to N_6-metal complexes involves the reaction of the powdered metal and solutions of elemental sulfur in *N*-methylimidazole [15]. The method was successful for metal M = Mg, Mn, Fe, and Ni, to give [M(*N*-MeIm)$_6$]S$_8$ complexes. The structure of the nickel(II) complex was determined. The cation is analogous to other hexakis(imidazole) complexes.

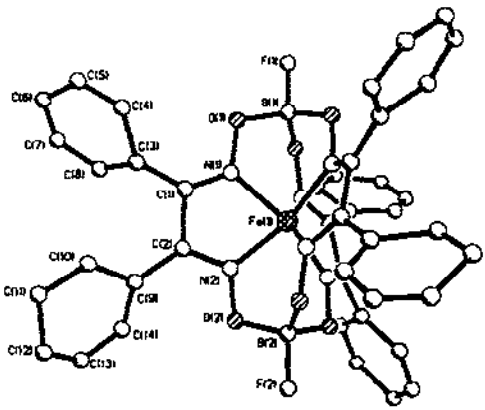

(5)

Studies on macrobicyclic boron-containing *d*-metal oximates have included characterisation by FAB mass spectometry [16]. In these complexes, which were reported previously, the metal is

encapsulated in the ligand cavity to give a clathrochelate. The fragmentation patterns of the iron(II) complexes indicate that the introduction of substituents on to the outside of the clathrate framework has a destabilising effect on the complex. A new iron(II) example (5) of a macrocyclic fluoroborate-containing clathrate has been structurally characterised using X-ray crystallography [17]. In common with the other structures reported, the iron(II) is contained in an N_6 coordination sphere provided by the inner cavity of the ligand.

A template condensation of a number of aliphatic, aromatic, and alicyclic dioximes containing tin(IV) tetrachloride on iron(II) was used to synthesise anionic clathrate chelate complexes of general formula $[FeD_3(SnCl_3)_2]^{2-}$ with D^{2-} = dioxime dianion [18]. The seven new complexes were characterised by elemental analysis, IR, electronic absorption, ^1H, $^{13}C\{^1H\}$, ^{119}Sn NMR and ^{57}Fe, ^{119}Sn Mössbauer spectroscopies. On the basis of these measurements, the complexes are thought to have the general structure shown in (6).

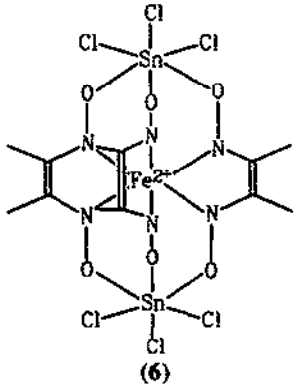

(6)

The N_6-macrocyclic ligand hexacyclen (the nitrogen analogue of 18-crown-6) forms a complex with iron(II) ions. The complex appears to undergo a thermally controlled intramolecular reverse electron transfer to an iron(III) state as revealed by the analysis of Mössbauer and EPR spectra, and magnetochemical measurements [19]. The data were interpreted in terms of an equilibrium between iron(II) intermediate (S = 1) spin and iron(III) high ($S = {}^5/_2$) spin.

The effect on complexing properties of methyl substituents adjacent to the donor nitrogen atoms in a family of tridentate (N_3) heterocyclic ligands was explored [20]. The FeN_6-complexes which form with these ligands are high spin (S = 2) and their paramagnetically shifted ^1H NMR spectra were used to characterise the complexes in solution. The magnitude of 10 D_q was found to decrease as steric bulk increases. Cyclic voltammetric studies revealed reversible one-electron Fe(III)-Fe(II) couples at high potentials (1.06 - 1.22 V vs. SCE).

The complex anion $[Fe^{II}(pzB)_2]^-$ dissolved in dichloromethane was found to be highly effective in inducing the aerial oxidation of methyl linoleate, in a manner somewhat like that of lipoxygenase [21].

A series of eight dinuclear iron(II)-vanadium(IV) complexes of the two general types, $[FeL_3VO(acac)]$ and $[FeL_3VO(diam)]PF_6$, with HL = PhN=NC(R)=NOH R = Ph, Me, diam = bpy, *o*-phen, 3,5-dimethyl-1-(2-pyridyl)pyrazole has been prepared with the compound

[Fe(PhN=NCPh=NO)$_3$VO(bpy)] characterised by X-ray crystallography [22]. These contain low spin iron(II) in an N_6-environment from the tris-chelates, and the three pendant oximato oxygen atoms bind to the vanadium atom which is further bonded to an oxo oxygen and the bpy nitrogen donors. The complexes behave as one-electron paramagnets due to the VO^{2+} centre and the EPR spectra are axial with $g_{\parallel} < g_{\perp}$.

The MLCT excitation of ruthenium(II) and iron(II) complexes formed with the aromatic *N*-heterocyclic acceptor ligands pyridine, pyrazine, 2,2'-bipyridine and 1,10-phenanthroline, has been studied using quantum mechanical calculations [23]. The results are compared with structural (mostly on ruthenium((II) complexes) data and it is suggested that there is delocalisation of the charge-transferred electron over the whole ligand in the excited state. Spectroelectrochemical studies on $[Fe(phen)_3]^{2+}$ and $[Fe(bpy)_3]^{2+}$ show that the reductions of these complexes to +1 and 0 oxidation states occur via ligand based processes, with the additional electrons probably localised on separate ligands [24].

The lipophilic complex $[Fe^{II}L_3]^{2+}$ for L = 4,4'-di-t-butyl-2,2'-bipyridine, was prepared as a carrier for the transport of electrons form an aqueous oxidising to an aqueous reducing phase across a CH_2Cl_2 bulk liquid membrane [25].

An iron(II) complex was used to organise a synthetic peptide into three helical bundles [26]. A bipyridyl function was attached to the terminus of the chain of the 15 residue synthetic peptide, and three of these were allowed to react with iron(II) from $Fe(NH_4)_2(SO_4)_2.6H_2O$. The resulting "complex" apparently contains the peptides coiled into helices, as supported by the CD data, which are consistent with an 85% α-helical character. The fact that the metal organisies these bundles is further supported by the CD spectra of the peptide without the metal present, which only has 35% α-helical character. The stoichiometry of the complex was confirmed using spectrophotometric measurements.

2.1.3.2 Complexes with N_4-coordination and N_4-coordination with axial ligands

Iron(II) complexes of 1,10-phenanthroline ligands substituted at the 2,9-positions or monosubstituted at the 2-position by phenyl moieties with *ortho* substituents were prepared and characterised and found to be bis-$[FeL_2]^{2+}$ complexes [27].

The divalent transition metal-mediated condensation of *o*-phenylenediamine with 4,9-dimethyl-5,8-diazadodeca-4,8-diene-2,11-dione gave 14-membered tetra-aza-macrocyclic six coordinate complexes of general formula $[M(mac)Cl_2]$ and $[M(mac)SO_4.H_2O]$ (M= Fe, Co, Cu; mac = macrocyclic ligand) [28]. The metal ion is thought to be coordinated by four azomethine nitrogen atoms, which are bridged by acetylacetone moieties. The spectroscopic and magnetic data are interpreted in terms of high spin iron(II) centres.

Ligands containing dioximate groupings provide a planar imine N_4-environment for iron(II) and stabilise it as a low spin ion. The iron can accommodate ligands in axial sites, as an $[FeN_4L_2]$ compound, and the substitution of weakly bound ligands such as thf, dmf, dmso, tht, and a number of nitriles by carbon monoxide in iron(II) difluoro(dioximato)borate complexes has been studied using MLCT spectroscopy [29]. The kinetics of the reactions with CO were determined by flash

photolysis and the order of lability of the axial ligands found to be thf > dmf > dmso > nitriles ≥ tht >> py. The potential application of these systems in CO scrubbing and detection is discussed. The CO binding by the anion substituted derivatives of this system, $[FeN_4LX]^-$, was also investigated [30], and it was found that the affinity for CO to give a $[FeN_4X(CO)]^-$ complex was much greater than in the case of the neutral compounds, in the order CN >> NCS > Cl > Br, a fact which was attributed to the *trans* labilising effect of the anions. In another study, the effect of the weak donor and anionic ligands on the axial ligand reactions of *trans*-$[FeN_4L(CO)]$ were investigated, and it was found that in reactions with 1-MeIm two dissociative pathways corresponding to CO and L loss contribute for the weak donor ligands, but only the CO loss pathway is important for the anions or sterically hindered donors [31]. The relative binding constants of L to $[FeN_4L_2]$ are CN^- > MeIm > py > 2-MeIm >> Cl^- > Br^- > MeCN and the relative rates of CO dissociation *trans* to L are CN^-, MeIm < py < MeCN, 2-MeIm < Cl^-, Br^-.

The iron(II) centred oxygen carrier system based on a lacunar cyclidene complex can be modified to enhance dioxygen carrying properties by the incorporation of extra steric bulk on the saturated rings of the parent molecule (7). The approach was tested on a number of derivative iron(II) and nickel(II) cyclidene complexes, and it was found that dioxygen affinities could be enhanced dramatically by placing a bulky group to the rear of the cavity within which the O_2 binds, whereas they decreased if the group was placed near the entry. The interpretations were based on the results of a crystal structure determination on a nickel(II) complex, and molecular modelling studies [32].

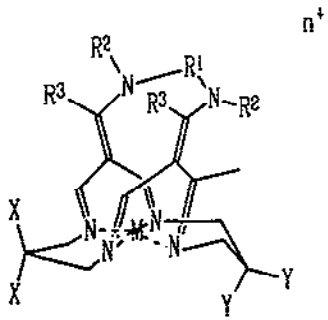

(7)

The complex $[Fe^{II}(cyclam)(CF_3SO_3)_2]$ (cyclam = 1,4,8,11-tetraazacyclotetradecane) acts as an effective catalyst for alkene epoxidation [33]. This system, and ones formed with related ligands, all give high turnovers and high yields, based on H_2O_2, for epoxidations performed in acetonitrile or methanol, and represent unusual examples of non-porphyrin catalysts for this reaction. Presumably this is the result of a favourable N_4-equatorial coordination, akin to that found in porphyrin systems.

2.1.4 Complexes containing cyanide ligands

The photoinduced redox reactions of $[Fe(bpy)(CN)_4]^{2-}$ in aqueous solutions were investigated and it was found that hydrated electrons formed in the light induced reaction react with

the ground state compound to form $[Fe(bpy)(CN)_4]^{3-}$ which was characterised by its absorption spectrum and reactivity [34]. The partial molar volumes for a series of $K_2[Fe(diimine)(CN)_4]$ salts have been determined using density measurements, adding useful data for such iron(II) complexes to the literature [35]. In another study it was found that, rather surprisingly, the activation volumes for the dissociation of the pentacyanide complexes, $[Fe(CN)_5L]^{3-}$, for L = pyrazine, 4-phenylpyridine, 4-(1-butylpentyl)pyridine and N-(n-pentyl)pyrazinium, were found to show no correlation to ligand volume, a fact which the authors admit needs further investigation [36].

The solvent effects on the redox reactions between the ionic species sulfite and hexacyanoferrate(III) and peroxodisulfate and hexacyanoferrate(II) were studied and it was concluded that solvent parameters are important in determining the kinetics of the reactions [37].

The dinuclear complex anion $[(CN)_5Fe^{II}HNC_6H_4NHFe^{II}(CN)_5]^{6-}$ was isolated from an oxygenated solution of *p*-phenylendiamine and $Na_3[Fe(NH_3)(CN)_5]$ [38]. The spectral features are consistent with a quinonediimine structure for the bridging ligand. Dinuclear $[(CN)_5Fe^{II}(pyCN)Ru^{II}(NH_3)_5]^-$ complexes can be prepared in two forms, dependent on the isomer of the bridging cyanopyridines used (4- or 3-) [39]. Chemical and electrochemical oxidation yields the mixed valence compounds, which appear to be valence trapped Fe^{II}/Ru^{III} species on the basis of their spectroscopic and electrochemical properties.

The iron(II) isocyanide complexes $[Fe(CN)_2(CNR)_2]$ and $[Fe(bpy)(CN)_2(CNR)_2].2H_2O$, with R = Me, Et, were prepared by esterification of $[Fe(CN)_2(CNH)_2].4Et_2O$ and $[Fe(bpy)(CN)_2(CNH)_2].2H_2O$. The esterification used Mitsunobo conditions, with the presence of triphenylphosphine and diethyl azocarboxylate to give a redox condensation under mild conditions. The products were characterised from their IR spectral characteristics [39a].

2.1.5 Complexes with unusual magnetic properties

The complexes $[Fe^{II}(4,4'\text{-dpb})_2X_2]$ (4,4'-dpb = 4,4'-diphenyl-2,2'-bipyridine; X = SCN, SeCN) have been synthesised and their magnetic properties investigated [40]. The variable temperature (6 to 460 K) susceptibility, and Mössbauer and FT-IR spectroscopic data indicate that the complexes have S = 1 ground states, and belong to the class of "spin crossover" compounds. These ground states are probably the consequence of a severe distortion from octahedral geometry allowing for a near degeneracy of the d_z2 and d_{xy} orbitals around the metal.

The X-ray crystal structures of the spin crossover complex $[Fe^{II}(bpy)_2(NCS)_2]$ in the high spin (298 K) and low spin (175, 110 K) forms were determined and it was found that on average the Fe-N bond lengths are 0.17 Å shorter in the low spin state [41]. The pressure dependence of the absorption spectra was also followed, and showed that high to low spin conversion could be induced by the application of pressure.

The crystal structure of the spin crossover compound $[Fe^{II}(4,4'\text{-bi-}1,2,4\text{-triazole})_2(SeCN)_2].H_2O$ has been determined at room temperature and found to be isomorphous with the analogous thiocyanate compound [42]. The iron centre is in a distorted octahedral N_6-environment created by the four triazole ligands which are coordinated to further iron centres in a 2D array. There are two *N*-bonded SeCN ligands. The EPR and NMR spectroscopic properties of

the two complexes were measured, and in particular, the NMR spectral data indicate that the spin transition occurs in domains rather than in a statistically random way.

The tris chelate complexes of a number of substituted 2,2'-bipyridyl and 1,1'-isoquinoline ligands have been synthesised. In particular, the isolated solid complexes formed with dimethyl-2,2'-bipyridyl-3,3'-dicarboxylate and 1,1'-biisoquinoline have Mössbauer spectroscopic and magnetic properties consistent with spin-equilibrium behaviour [43]. The two related ligands 2,2'-bipyridine-6-carbaldehyde phenylhydrazone and 2,2'-bipyridine-6-carbaldehyde 2-pyridylhydrazone form FeN_6 complexes of different spin states (low and high respectively) [44]. The tridentate ligands 2,6-di(thiazol-2-yl) pyridine, 2,6-di(4-thiazol-2-yl) pyridine and 2,6-di(2-imidazolin-2-yl) pyridine form N_6-complexes, for which only the 2,6-di(4-thiazol-2-yl) pyridine complex is high spin, undergoing a thermally induced spin transition [45].

The two complexes $[Fe(1\text{-methyl-1H-tetrazole})_6](CF_3SO_3)_2$ [46] and $[Fe(1\text{-propyl-tetrazole})_6](BF_4)_2$ [47] were reported as the second and third examples of LIESST (light induced spin-state trapping) systems in which irradiation of a high spin state results in a transition to a low spin state.

The tetragonal pyramidal nitrosyl complexes [M(NO)(L)], for M=Co(II) or Fe(II), and L is the Schiff's base produced by condensation of 2-hydroxy-1-naphthaldehyde with 1,2-diaminoethane, *o*-phenylenediamine or 4-methyl-*o*-phenylenediamine have been prepared by reaction of the metal salt with the Schiff's base under an atmosphere of NO [48]. The iron complexes have temperature independent magnetic moments corresponding to the presence of three unpaired electrons ($S = {}^3/_2$) and showed no sign of spin pairing to give an $S = {}^1/_2$ state as temperature was lowered to 87 K. Both types of behaviour have been observed in previously reported iron(II)/Schiff's base/nitrosyl complexes.

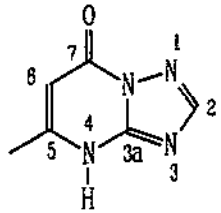

(8)

The synthesis and spectroscopic properties of a series of polynuclear metal coordination compounds of general formula $[MX_2(mtpH)_2]$ with M = Mn, Fe, Co, Ni, Cu, Cd; X = Cl, Br; mtpH = 5-methyl[1,2,4]triazolo[1,5-*a*]pyrimidin-7-ol (8) have been reported [49]. The IR spectra and X-ray powder diffraction patterns suggest two structural types within the series. Iron(II), in common with all the other metals except manganese and cobalt, forms a complex in which there is a pseudo-octahedral geometry about the metal from four bridging anions, which are part of a linear chain structure, and two *N*-coordinated mtpH ligands. This is deduced on the basis of the ligand field spectra and magnetic properties. The iron(II) complex shows a strong ferromagnetic interaction between the metal ions with $\theta = 22.7$ K.

The magnetic properties of the two dimensional antiferromagnetically coupled iron(II) system [Fe(4-imidazoleacetate)$_2$].2CH_3OH (9) have been investigated [50]. The compound was synthesised from ferrous acetate and the sodium salt of the ligand, and its structure confirmed by X-ray crystallography. The six coordinate iron atom is in a rhombically distorted environment. The magnetic moment of 5.2 BM at room temperature indicates that the iron ion is in a high spin state. The temperature dependence of the susceptibility down to 15 K can be explained in terms of antiferromagnetically coupled iron centres with a spin-orbit coupling contribution. At 15 K there is a magnetic phase change, and the susceptibility reaches a maximum. This weak ferromagnetism was confirmed by studying the ac susceptibility and Mössbauer spectra. The origin of this effect can be understood from the crystal structure, in which the relevant orientations of the adjacent ferrous coordination polyhedra result in the presence of two spin sublattices. In this way a canting of the spins results which gives rise to the three dimensional ferromagnetic ordering below 15 K.

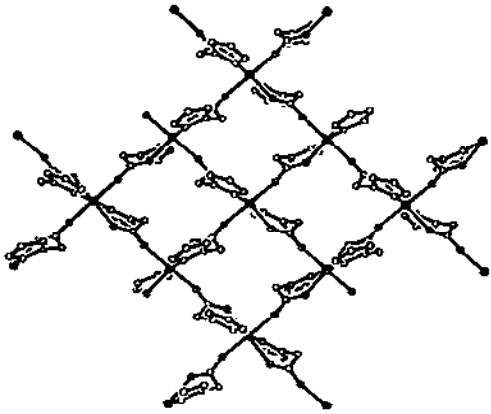

(9)

The crystal structure and magnetic properties of $[Fe^{II}(pyz)_2(NCS)_2]_n$ have been reported [51]. The crystal structure reveals that iron centres are six-coordinate with four pyrazine ligands which bridge to other iron centres to give an infinite 2D square array, and two axial *N*-bonded thiocyanate ligands. This goes some way to explaining the well-known magnetic behaviour, by incorporation of an interlayer interaction parameter which improves the fit of the low temperature behaviour.

2.1.6 Complexes with other donor sets

The preparation of complex cation $[Fe(N_2H_5)_2(H_2O)_2Cl_2]^{2+}$ and three other analogous hydrazinium metal chlorides (with M = Co, Ni, or Cu) proceeds easily in aqueous solutions containing the metal chloride and hydrazine hydrochloride [52]. The X-ray structure of the iron(II) complex shows that the iron centre is in an octahedral environment, with all sets of ligands *trans* to each other.

The complex $[Fe(L)_2]$, where HL = antimony bis(thiolactate), has been synthesised and characterised by microanalysis, magnetic measurements and reflectance spectroscopy [53].

The use of dimethyl telluride as a ligand for divalent metals has been investigated [54]. Solutions of Me_2Te and $M(SO_3Cl)_2$ in acetonitrile produce compounds of the formula $[M(TeMe_2)_2(SO_3Cl)_2]$ for M = Cr, Mn, Fe, Co, Ni, or Cu. On the basis of a comparison of the diffuse reflectance spectra and magnetic susceptibility data, it is suggested that each metal atom is in an octahedral environment with a high spin electron configuration and ligation by two telluride molecules and two didentate chlorosulfate groups. The magnetic moment for the iron(II) complex is 5.43 BM.

The *cis*(H)(H_2) complex $[(PP_3)Fe(H)(H_2)]BPh_4$ where $PP_3 = P(CH_2CH_2PPh_2)_3$, has been synthesised using a variety of routes, including a one pot reaction containing an aqueous solution of an iron(II) salt, PP_3 and excess formic acid [55].

The Mössbauer spectral parameters of a series of six-coordinate low-spin iron(II) complexes containing didentate phosphine ligands have been reviewed and discussed [56]. Partial quadrupole splittings are used to classify the complexes as *cis* or *trans* and a correlation between these splittings and cone angle is also suggested. In another study, the Mössbauer spectra of a range of low spin iron(II) complexes, $[FeX(Y)(diphosphine)_2]^{n+}$, n = 0, 1, X and/or Y = Cl, Br, MeNC, H, N_2, H_2 CO, were measured [57]. These authors concluded that whereas partial isomer shifts were of limited value in classifying the compounds, the partial quadrupole splittings were more informative.

The reaction of NaSH with $[Fe^{II}(dmpe)_2Cl_2]$ at low temperature yielded the six-coordinate compound *trans*-$[Fe^{II}(dmpe)_2(SH)_2]$, as confirmed by X-ray crystallography [58].

Adducts of 2'-deoxyadenosine (dado) with the chlorides of a number of transition metal dihalides, including $FeCl_2$, were formed from mixtures of the ligand and metal halide under reflux conditions [59]. Compounds containing two equivalents and one equivalent of the ligand per metal were obtained. The 2:1 compounds were assigned as tetrahedrally or octahedrally coordinated monomers (no example isolated for iron(II)), whereas, those which were 1:1 in ligand and metal were assigned as polymeric species bridged via the dado ligands on the basis of their spectroscopic and magnetic properties. The IR spectrum of $[Fe(dado)Cl_2]$, for example, exhibits absorptions characteristic of terminal Fe-Cl stretching modes. The room temperature magnetic moment of 5.19 BM suggests that there is no magnetic interaction between the high spin iron centres, which is also in accord with the polymeric structure arising form bridging by the dado ligands, rather than by chloride bridges.

The reaction of $FeCl_3$ with $SnCl_2$ in thf yields the salt $[Fe_2(\mu_2\text{-}Cl)_3(thf)_6][SnCl_5(thf)]$, which contains two six-coordinate iron(II) centres 3.0862(2) Å apart linked by three chloride bridges, as revealed in a single crystal X-ray diffraction study [60]. The compound undergoes partial decomposition under reflux to give $[Fe_4(\mu_3\text{-}Cl)_2(\mu_2\text{-}Cl)_4(thf)_6]$ and $[SnCl_4(thf)_2]$.

A route to the synthesis of polynuclear iron(II) compounds from iron(II) chloride and oxygen donor ligands has been reported [61]. In order to obtain a reactive solution of iron(II) chloride in thf, $FeCl_3$ and metallic iron were mixed in the solvent. This resulted in the isolation of crystals of the tetranuclear iron(II) compound $Fe_4Cl_8(thf)_6$ (**10**). The structure shows iron atoms in

two different environments. One has the iron centre in a trigonal bipyramidal coordination geometry with three chloride ligands in the equatorial plane and a thf ligand and μ_3-Cl occupying the axial sites. The other has the iron centre in an octahedral environment, with two thf ligands *cis* to each other and four further chloride ligands. The room temperature magnetic moment of the compound can be interpreted as arising from non-interacting high spin iron(II) ions with μ_{eff}/Fe = 5.40 BM.

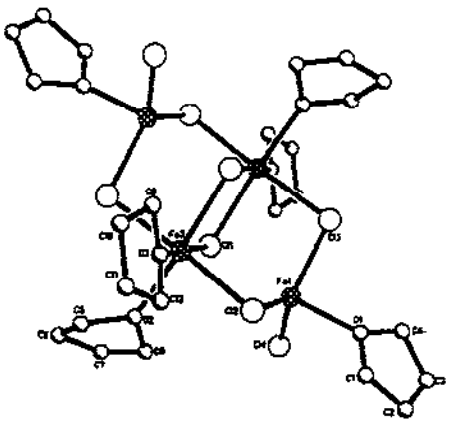

(10)

This same synthetic route was employed in the synthesis of $[FeCl_2(OPMe_3)]_\infty$ and $[FeCl_2(OPMe_3)_2]$, this time with the addition of PMe_3 to the $FeCl_3$/Fe/thf solution [62]. The X-ray crystal strucutres reveal that the polymer consists of infinite chains of $FeCl_2(OPMe_3)$ units with four bridging chlorine atoms and one phosphine per iron atom resulting in a trigonal bipyramidal coordination geometry about the metal centre. The monomer has the expected tetrahedral geometry. The magnetic moments per iron of 4.90 and 5.51 BM, respectively, are in the range expected for uncoupled high spin iron(II).

The syntheses and properties of a number of first row transition metal pterin and pteridine complexes formed in non-aqueous media have been described [63]. The X-ray crystal structures of three copper(II) complexes were determined. An iron(II) complex with 2-(ethylthio)-4-oxopteridine, H_2L, can be isolated in 83% yield as a deep purple solid on reaction of the deprotonated ligand with iron(II) chloride in methanol as $[FeL(MeOH)_2].MeOH$.

Thorium bromide clusters with interstitial transition metal atoms have been prepared, including the iron compound $FeTh_6Br_{15}$. This has an octahedral core of thorium atoms surrounding the iron atom and overall a structural type closely related to Nb_6F_{15} as revealed by X-ray diffraction [64].

2.1.7 Complexes with low coordinaton numbers

The use of sterically demanding dinucleating ligands to produce low coordination number metal centres has been explored by Power and coworkers. The synthetic strategy involves reacting

transition metal bis(trimethylsilyl)amides, $M\{N(SiMe)_2\}_2$, with the source of a bridging ligand. In this way, the dinuclear iron(II) complex, $\{Fe\{N(SiMe_3)_2\}(\mu\text{-}PMes_2)\}_2$ could be formed. This complex has phosphido bridges and terminal amido groups, with the iron(II) centres being three coordinate. However, the corresponding reaction with $HAsMes_2$ produced $Mes_2AsAsMes_2$ in contrast to the case for manganese(II) which gives the arsenido-bridged analogue of the iron(II) phosphido compound [65]. The structures were confirmed by X-ray crystallography. A similar strategy was used to produce the aryloxide-bridged dimers $\{Fe\{O(2,4,6\text{-}t\text{-}Bu_3C_6H_2)\}\{\text{-}O(2,4,6\text{-}t\text{-}Bu_3C_6H_2)\}\}_2$ and $\{Fe\{N(SiMe_3)_2\}\{\mu\text{-}O(2,4,6\text{-}t\text{-}Bu_3C_6H_2)\}_2$ as well as the adduct $[Fe(OCPh_3)_2(thf)_2]$ starting from $Fe\{N(SiMe)_2\}_2$ [66]. The manganese(II) analogues were also prepared and all structures were confirmed by X-ray crystallography. The results suggest that the overall reaction proceeds via the formation of the intermediate $\{Fe\{N(SiMe_3)_2\}\{\mu\text{-}O(2,4,6\text{-}t\text{-}Bu_3C_6H_2)\}\}_2$ and that in the case of the previously discussed reaction [65], the phosphido bridged complex represents a stable intermediate state from which it did not seem possible to proceed under normal conditions. The first examples of homoleptic transition metal boryloxides were produced by reacting $M\{N(SiMe_3)_2\}_2$, (M = Mn or Fe), with sterically crowded boronous acids [67]. For iron(II), the compound formed was $[Fe(OBMes_2)(\mu\text{-}OBMes_2)]_2$ which has two three-coordinate iron centres with one terminal boryloxide ligand linked by the oxygen atoms of two bridging ligands, as revealed in the single crystal X-ray structure. Finally, the structures of the amido-bridged dimers $\{Fe(NR_2)(\mu\text{-}NR_2)\}_2$, where R = $SiMe_3$, C_6H_5, and the Lewis base adduct, $[Fe\{N(SiMe_3)_2\}_2(thf)]$ have been reported [68]. The monomer/dimer equilibrium was investigated using variable temperature ^1H NMR spectroscopy and it was concluded that dimerisation of the monomeric species occurs at temperatures below 30°C.

2.2 IRON(III) COMPOUNDS

The chemistry of iron(III) is dominated by complexes containing oxygen donor ligands, and also by hydrolytic processes. The oxo-bridged species resulting from the latter are considered in section 2.3. Since a major area of interest in the chemistry of iron(III) mononuclear complexes is the production of siderophores (iron chelators) for clinical use, these have been separated out as a subsection organised in a similar way to the subsequent review of other mononuclear complexes.

2.2.1 Siderophore model complexes

The recognition that naturally occurring chelating agents called siderophores are used by bacteria to sequester iron(III) from the environment in the form of highly stable iron(III) mononuclear complexes, has led to the design and synthesis of a vast array of similar chelating agents, often with a view to their possible use in iron overload therapy. The most commonly occurring siderophores contain hydroxamate and catecholate moieties, arranged along an organic backbone to give O_6-coordination of the iron centre on complexation. In general, it has not yet been possible to produce a synthetic siderophore which matches all the properties of the naturally occurring ones. Success here would allow for the production of cheaper drugs for the treatment of iron overload, most of which, such as desferrioxamine, are currently isolated from bacteria.

2.2.1.1 Siderophore complexes with oxygen donors

The iron binding properties of three tetradentate and one hexadentate 3-hydroxy-2-methylpyrid-4-one chelators (**11**)-(**14**) intended for clinical use have been studied using visible spectrophotometry by Job plot estimations, and compared with the iron binding by desferrioxamine (DFO) [69]. At low pH, the chelators all form a mixture of complexes of ligand:iron stoichiometries of 1:1, 1:2 and 2:3. At pH 7.4, complexes with a 3:2 ratio form. This is in contrast to desferrioxamine, which forms 1:1 chelates at both low and neutral pH. Overall, these chelators display a higher binding capacity for iron than desferrioxamine, but the complex stabilities have not been investigated.

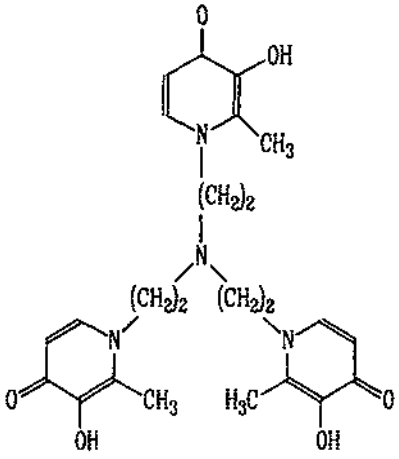

(11)

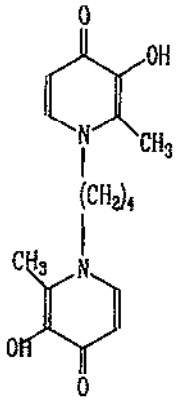

(12)

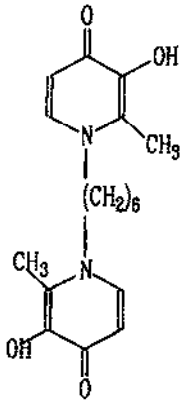

(13)

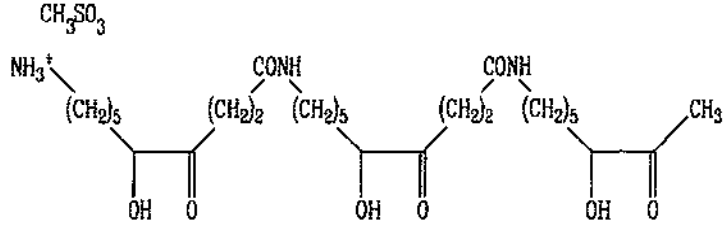

(14)

The incorporation of three 2,2'-dihydroxybiphenyl subunits in a macrobicycle produced six convergent phenolate groups as coordination sites for iron(III) in the ligand (**15**) [70]. The chelate can be synthesised in a stepwise fashion or using the template synthesis route originally developed by

Raymond and coworkers [71] using 2,2'-dihydroxybiphenyl, $N(CH_2CH_2NH_2)_3$ (tren), $FeCl_3$, Et_3N, dmf, and 4-dimethylaminopyridine, which produces the iron(III) complex, which can then be demetallated. Competition experiments indicated that the chelator produces a more stable iron(III) complex than either desferrioxamine or edtaH_4. A similar template route was used by Raymond and coworkers to produce the iron(III) complex (**16**) of the tricatechoyl amide-based ligand, "bicappedTRENCAM" The structure of this complex was confirmed by X-ray crystallography [72]. Related ligands can be synthesised by substituting tren with $N(CH_2NH_2)_3$ and varying the substituents on the catechoyl amide. The protonation constants were found to be quite low and the electrochemical studies performed on aqueous solutions of the iron(III) complexes show reversible reduction potentials of –0.89 to –0.97 V vs. NHE. Although the ligands are highly selective for iron(III), with ratios of formation constants of iron(III) to iron(II) complexes ranging from 28.1 to 29.5, they display a slight stabilisation of the iron(II) complex relative to related tripodal compounds such as the siderophore enterobactin.

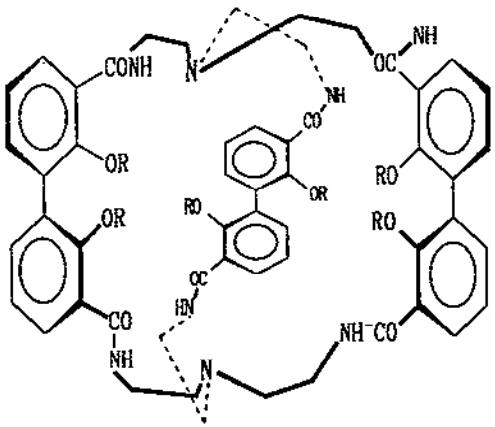

(15a) R = H **(15b)** R = Me

Solution state studies on the thermodynamic stability and iron transport properties of the hydrolysis products of enterobactin have been reported [73]. One aim of the study was to shed light on the mechanism for iron release from siderophores. The stability constant of the iron(III) complex of enterobactin itself has log $K_f \approx 49$, which raises the question of how iron can be released from this complex. One suggestion is that the ligand portion of the complex undergoes hydrolysis to give a less stable iron complex from which iron can then be removed. Enterobactin can be viewed as a cyclic trilactone formed from the amide monomer *N*-(2,3-dihydroxybenzoyl)serine (DHBS) (**17**), and the study involved the determination of the equilibrium constants for metal complexation of the monomer, dimer and trimer ligands using electronic and CD spectroscopy, spectrophotometric and potentiometric titrations and calorimetry. The enterobactin and DHBS were isolated from a culture supernatant of *E. coli*. A comparison of the results for the linear trimer, corresponding to the first hydrolysis product from the cyclic lactone, and for enterobactin led to the suggestion that the

exceptionally high stability of iron(III)/enterobactin complexes against tris-catecholate analogues (or models) is one third enthalpic and two thirds entropic in origin. It was also found that trimer and dimer hydrolysis products are active as transport agents for iron, as indicated by radioactively labelled iron tracer studies in whole *E. coli* cells.

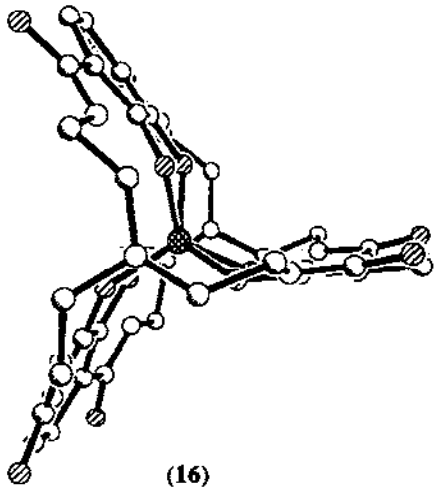

(16)

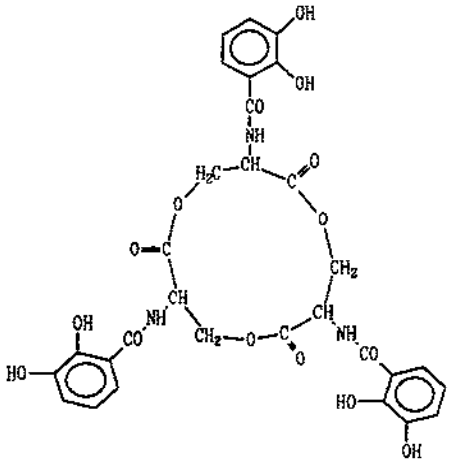

(17)

The solution thermodynamics of enterobactin and its iron complex have been studied using UV spectrophotometry and results have been compared with the data for the synthetic analogue, MECAM (*N,N',N''*-tris(2,3-dihydroxybenzoyl)-1,3,5-tris(aminomethyl)benzene) [74]. The similarity between the values obtained for the *o*-hydroxyl protonation constants of enterobactin and MECAM suggests that MECAM is a good synthetic model for this siderophore. However, MECAM is not

susceptible to hydrolysis, unlike enterobactin, as discussed above. Complexes with other trivalent metals were also studied and it was found that the order of protonation (from highest pK_a to lowest) was Al > Fe > Sc > Ga >> In. Additionally, metal uptake studies on *E. coli* indicate that there is some mechanism in operation which distinguishes between iron/enterobactin complexes and those with other metal ions. The elucidaton of this discrimination should be of relevance to toxicological research.

Single crystal polarised absorption and magnetic circular dichroism (MCD) spectroscopy have been used in probing the electronic structure of the iron(III) tris(catecholate) complex $[Fe(cat)_3]^{3-}$ to shed light on the bonding in siderophore complexes [75]. In addition, $[Fe(TRENCAM)]^{3-}$ and the iron(III) tris-chelate complex $[Fe(eta)_3]^{3-}$ formed with 2,3-dihydroxyethylterephthalamide (H_2eta), were studied using MCD in order to gauge the effect of a perturbation on the electronic structure of $[Fe(cat)_3]^{3-}$ and as a comparison for the bonding in the three complexes. Although previous theoretical models predicted that the ground state of the $[Fe(cat)_3]^{3-}$ complex should be low spin, with $S = {}^1/_2$, the analysis of the charge transfer and ligand field spectra supports the evidence from EPR, magnetic and Mössbauer spectroscopic data which all suggest that the iron is high spin, $S = {}^5/_2$. The CT bands in such complxes arise from ligand-π to metal *d* transitions and indicate that a significant contribution to the Fe-O interaction is made by π-bonding, which may in turn explain the high stabilities of these complexes relative to similar FeO_6-complexes such as $[Fe(ox)_3]^{3-}$. It was also found that the spectroscopic characteristics of the enterobactin complex were essentially the same as those for the model TRENCAM complex, and therefore the spectroscopic methods employed are of direct relevance to the probing of biological systems.

A series of dihydroxamate ligands formed in the condensation of 2,6-pyridine dicarboxylic acid with protected *N*-aminopropyl-*N*-acetylhydroxylamine, which are analogues of the siderophore rhodotorulic acid, has been prepared for complexing iron(III) as contrast agents in Magnetic Resonance Imaging [76]. 3-Nitrobenzohydroxamic acid forms a tris-chelate with iron(III) ions which is suitable for use in the spectrophotometric determination of iron [77]. The complexation of iron(III) (and other metal) ions by the aminohydroxamic acid ((aminoiminomethyl)amino)-*N*-hydroxypentamide has been studied by spectrophotometry and potentiometry [78, 79]. The iron centre has an FeO_6-coordination sphere. The open chain analogues (**18**) of tris(hydroxamic acid) cryptands have also been synthesised and the stability constants of these ligands and the cryptand with both iron(III) and gallium(III) determined [79]. It was found that the stability constants for the cryptates were higher than for the tris(hydroxamate) chelates.

The molecular structures of $[Fe(mpa)_3]$ and $[Fe(mbb)_3]$, where Hmpa = *N*-(4-methylphenyl)acetohydroxamic acid and Hmbb = *N*-methyl-4-methylbenzohydroxamic acid, as well as their gallium(III) analogues have been determined by X-ray crystallography [80]. A consideration of the structural differences between the complexes led to the conclusion that the gallium complexes are more stable than the iron complexes, which, when the large differences in free energy of formation for the aqueous ions are taken into consideration, is in agreement with the observations that the formation constants for the iron compounds are larger, and that iron can displace gallium from its complexes.

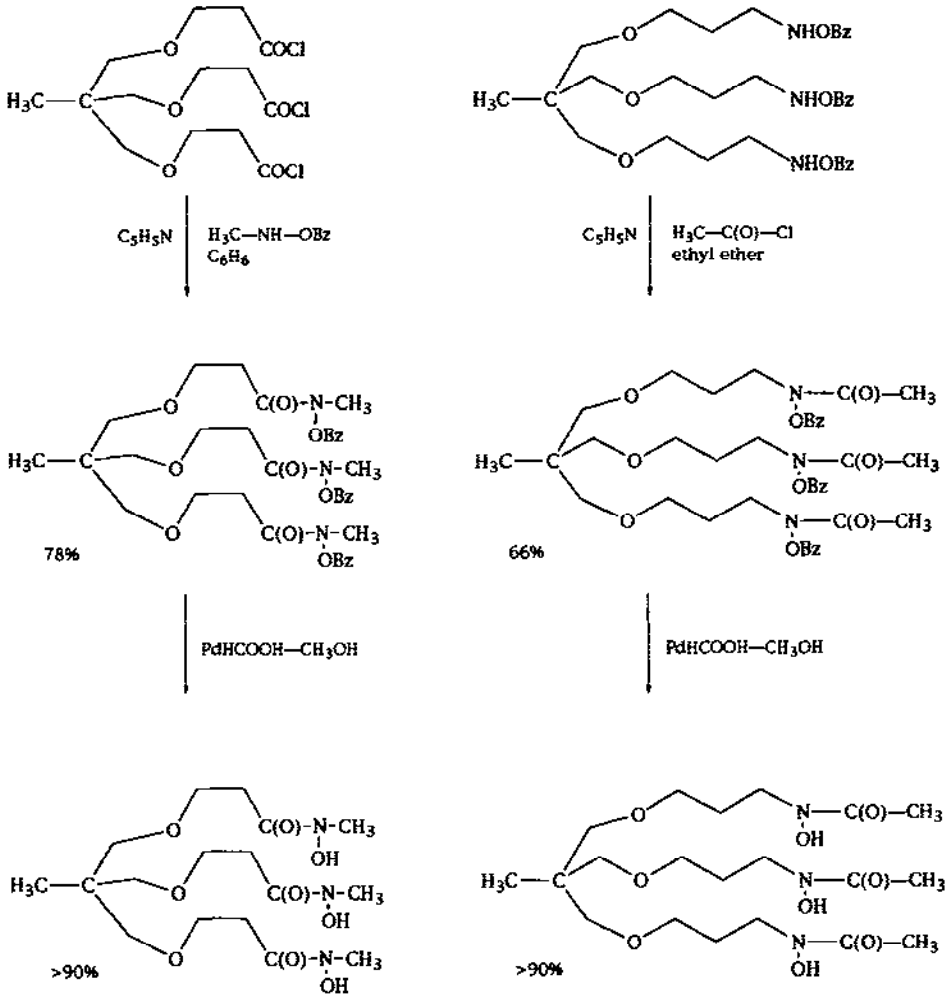

Tris(hydroxamic acid) with terminal CH_3NOH donors

Tris(hydroxamic acid) with terminal CH_3CO donors

(18)

The complex-formation equilibria and relative stability constants of the iron(III) and copper(II) complexes present in aqueous solutions of metal and L-leucinehydroxamic acid (2-amino-4-methylpentanehydroxamic acid) were determined using spectrophotometric and potentiometric titrations [82]. In the case of the iron(III) complexes, it was concluded that the coordination shell was O_6 with both oxygen atoms of the hydroxamate group chelating the metal, with the expected tris complex only forming at very high ligand concentrations. A number of protonated intermediate 1:1 and 1:2 metal:ligand species were postulated.

The effect of pressure on the complexation of iron(III) by hydroxamic acids was investigated [83]. Activation and reaction volumes for the formation and aquation of (acetohydroxamato)iron(III) complexes and the activation volumes for the formation of the complex of iron(III) with desferrioxamine were obtained from high pressure stopped-flow and UV-VIS spectral measurements. The activation volumes exhibit opposite signs for the complexation of $[Fe(H_2O)_6]^{3+}$ and $[Fe(H_2O)_5(OH)]^{2+}$ with acetohydroxamic acid (negative) and desferrioxamine (positive), indicating associative and dissociative modes of activation respectively.

The protonation and iron(III) binding constants of the ligand 1,2-dimethyl-3-hydroxy-4-pyridinone have been reported [84]. The ligand is an effective iron chelator in moderately dilute solution (~10^{-3} M), but probably as a result of the 1:3 stoichiometry of the metal:ligand complex, there is extensive dissociation in very dilute solution (~10^{-6} M). The results were compared with those from other relevant iron(III) tris-chelate complexes (such as $[Fe(cat)_3]^{3-}$) as well as the multidentate ligand systems including the MECAM and DFO iron complexes and the transport protein transferrin. The comparison underlined the importance of taking dilution into consideration when assessing the effectiveness of siderophores in capturing iron(III). Thus, it was found that whilst the ligand was more effective than transferrin at binding iron(III) ions at 10^{-3} M, at high dilution the speciation diagrams and pM values for the ligand, indicate that it would not be able to remove iron from transferrin under these conditions. The failure of many researchers to investigate dilution as a parameter in similar studies might result in misleading information with regard to the effectiveness of synthetic siderophores.

2.2.1.2 Siderophore complexes with mixed oxygen/nitrogen donors

A number of N/O (usually as N_3O_3-ligands) donating hexadentate ligands have been developed for use in the treatment of iron overload, as well as for possible use as paramagnetic contrast reagents for magnetic resonance imaging. Six such ligands (**9**) can be regarded as hydroxyaromatic derivatives of edtaH_4. The stability constants of the complexes formed between three of these ligands, for which the synthesis was recently reported [85], and gallium(III), indium(III) and iron(III) were measured and compared with the constants found for the three parent ligands [86]. It was found that the effect of methylation of the benzene ring was to increase stability, whereas quaternisation of the pyridine nitrogen decreased metal chelate stability by about two orders of magnitude. The stability constants of the same three metals with the hexadentate macrocycle 1,4,7-triazacyclononane-*N,N'N''*-triacetic acid were measured [87]. The stability constants of the gallium(III) and iron(III) complexes were higher than that of the indium(III) complex, indicating a

preferential interaction of the ligand with small metal ions. The species distribution curves show that the iron(III) and indium(III) complexes dissociate to form their hydroxides above pH 7.5. The gallium(III) ligand system is soluble at all pH values as a result of the formation of the tetrahydroxo gallate ion at pH 10.4 and above. In the case of the related ligand system, *N,N',N''*-tris(3,5-dimethyl-2-hydroxybenzyl)-1,4,7-triazacyclononane, very stable chelates are formed by the coordination of iron(III), gallium(III) or indium(III) by the three basic nitrogen donors of the macrocycle and the very basic phenolate oxygen atoms [88]. The log of the stability constant for the iron(III) complex determined by competition with edtaH_4 in an ethanol/water mixture (3:1) was found to be 51.3. This compares with a value of 26.3 for the iron(III)/edta system in the same medium and a value of 28.3 for the iron(III)/1,4,7-triazacyclononane-*N,N'N''*-triacetic system in water.

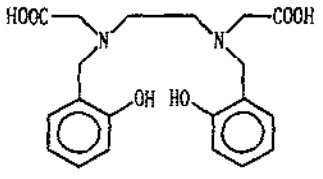

1 HBED. H_4L

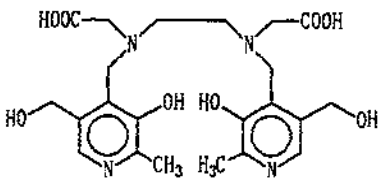

2 PLED. H_4L

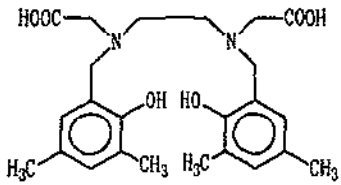

3 TMHBED. H_4L

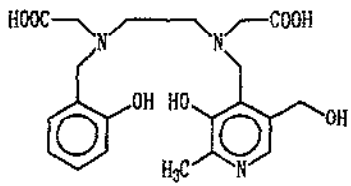

4 HBPLED. H_4L

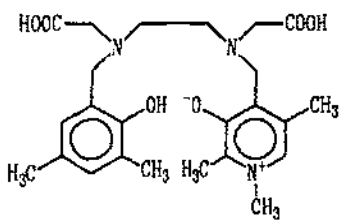

5 Me_4HBED. H_3L

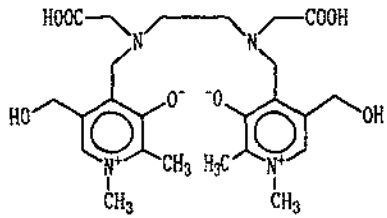

6 DMPLED. H_2L

(19)

The stability constants of trivalent metal ions, including iron(III), with a series of tetra-azamacrocyclic tetra-acetates (**20a**)-(**20c**) have been determined [89]. Although there are obvious structural similarities for these three ligands, there was no obvious trend in the pattern of stability

constants determined. It was found that all of the trivalent metal ion complexes studied form precipitates at neutral and higher pH, but are soluble in acidic solution.

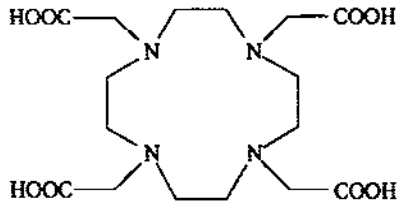

(20a)

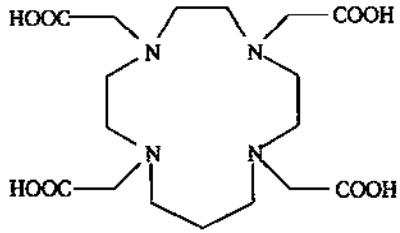

(20b)

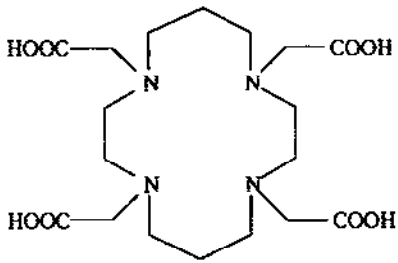

(20c)

The ligands methyl (*E*)-2-(1-alkyl/aryl-4,5-dihydro-1*H*-tetrazol-5-ylidene)-2-cyanoacetates and the corresponding 1-(1-alkyl/aryl-1*H*-tetrazol-5-yl)-2-alkanones (**21**) are efficient chelating agents for both iron(III) and aluminium(III) [90]. The metal complexes were prepared by extracting the trivalent metal from the aqueous phase into an ethereal phase containing the ligand. On the basis of the EPR and Mössbauer spectra of the iron(III) complexes and the ^{13}C NMR spectra of the aluminium species, it was concluded that the only the statistically most probable (Δ)/(Λ)-*mer*-isomers were formed with the metal ion in a rhombically distorted N_3O_3-environment.

2.2.1.3 Siderophore complexes with mixed oxygen/sulfur donors

A less commonly occurring functional group found in siderophores is thiohydroxamic acid. Hexadentate thiohydroxamate ligands derived from 2-mercaptopyridine-6-carboxylic acid 1-oxide and triamines provide an O_3S_3-coordination environment for the iron(III) centre, as revealed in the X-ray structure of *N,N',N''*-tris((1,2-didehydro-1-hydroxy-2-thioxopyrid-6-yl)carbonyl)-2,2',2''-triamino-triethylaminato)iron(III).$^1/_2CHCl_3$ (**22**) [91]. The coordination geometry about the iron centre is intermediate between octahedral and trigonal prismatic.

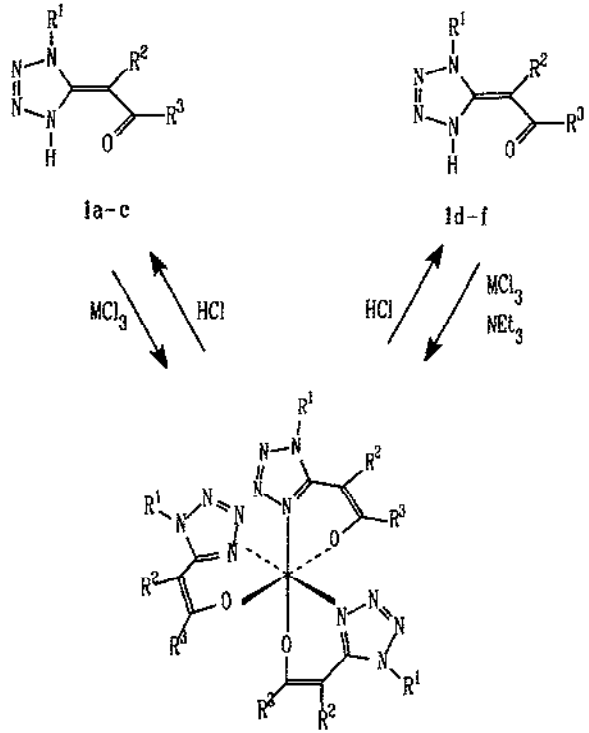

	a	b	c	d	e	f
R^1	Me_3CCH_2	$PhCH_2$	4-EtC_6H_4	Et	$Me(CH_2)_2$	Me_3C
R^2	CN	CN	CN	H	H	H
R^3	OMe	OMe	OMe	Ph	Ph	Ph

(21)

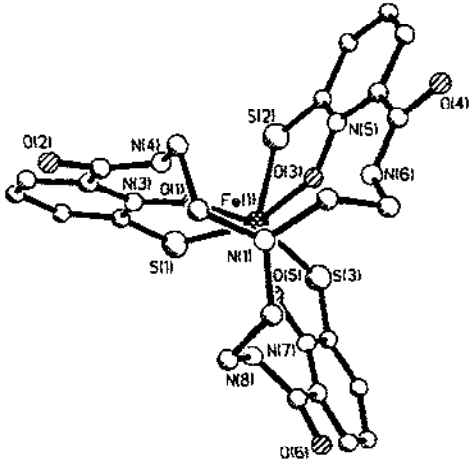

(22)

2.2.2 *Other iron(III) complexes*

2.2.2.1 *Complexes with oxygen donor ligands*

The complex which forms between iron(III) chloride and gallic acid is known as iron gallic ink. Crystals of the complex could be obtained from gels and the structure was found to consist of an infinite iron(III) gallate 1:1 framework (**23**) with each iron atom in an octahedral O_6-coordination geometry provided by two didentate deprotonated phenolate groups from two ligands, and two monodentate carboxylates from another two ligands [92].

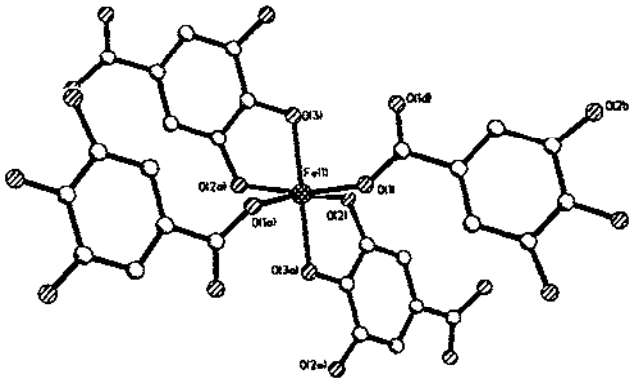

(**23**)

The complex formation between iron(III) and oxalic acid (ethanedioic acid) was studied by potentiometry in dmso solution [93]. This solvent was chosen partly to avoid complications introduced into the system when water is used as solvent through the formation of hydrolytic iron(III) species. The ligand behaves as a weak diprotic acid in dmso. The speciation of the iron is relativley simple, with the major species being 1:1, 1:2 and 1:3 metal:ligand complexes. There was no conclusive evidence for the presence of protonated ligand species nor for any oxalato-bridged metal complexes. The electrochemistry of the system was also explored in order to explain why dmso solutions of the tris-chelate are stable over several weeks, showing no signs of photodecomposition to iron(II) oxalate, unlike the aqueous system. It was found that the value for the Fe^{3+}/Fe^{2+} couple in water was +0.55V as against +0.30V in dmso, which, coupled with the fact that the oxidation of oxalate occurs more easily in water, suggests a less thermodynamically favourable redox process in dmso.

The irradiation of a [Fe(acac)$_3$] and 2-nitroso-1-naphthol mixture in ethanol led to complete ligand exchange, as determined from the changes in the visible absorption spectrum [94].

The equilibria and kinetics of the reactions of iron(III) with heptane-2,4,6-trione, 1-phenylhexane-1,3,5-trione and 1,5-diphenylpentane-1,3,5-trione were investigated in water/methanol solutions using spectrophotometric and potentiometric titrations [95]. It was found that hydrolytic

iron(III) species, such as $[Fe(L)OH_2]$, needed to be taken into account and that $[Fe(H_2O)_5OH]^{2+}$ is an important reacting species.

A study to investigate the dynamics of the water protons in concentrated iron(III) aqueous solutions, as well as gallium(III), aluminium(III) and dysprosium(III) solutions, using incoherent quasi-elastic neutron scattering (IQENS) presents a new method of probing the aqueous speciation of metal ions [96]. The lifetime of protons in the primary coordination sphere of aquated iron(III) was found to be $\tau_1 \geq 5 \times 10^{-9}$ s, which is in agreement with the results from ^{17}O NMR spectroscopy. The value for dissociated protons was $\tau_1 < 5 \times 10^{-9}$ s, which is shorter than that determined previously from ^1H NMR spectroscopic and electric field relaxation experiments. The best fits to the measured data are obtained for a model where exchange is slow and a degree of hydrolysis is assumed.

The iron(III) chlorite system in aqueous solution was investigated [97]. From the results of rapid-scan spectrophotometric and one-wavelength stopped-flow experiments the formation of a $[FeClO_2]^{2+}$ complex was substantiated.

Spectrophotometric and stopped-flow kinetic studies on the iron(III)/squaric acid (3,4-dihydroxy-3-cyclobutene-1,2-dione = H_2sq) system in aqueous media can be interpreted in terms of the formation of two iron(III) complexes, $[Fe(OH_2)_5(sq)]^+$ and $[(OH_2)_6Fe_2(OH)_2(sq)]^{2+}$ [98]. The mode of coordination of the squarate anion is open to conjecture, particularly in the dinuclear system, for which monodentate, bridging didentate, chelating didentate and bridging tetradentate coordination modes are all possibilities. A consideration of bite angles led to the formulation with a dihydroxo bridge and didentate chelating squarates being favoured by the authors. The squaric acid ligand has obvious analogies with ascorbic acid which is also known to form several iron(III) complexes, and has a tendency to reduce the iron to the iron(II) state. This latter fact is proposed as an explanation for the observation that the previously reported blue $[Fe(OH_2)_5(sq)]^+$ compound fades over time and this is inhibited by iron(II) ion.

The formation of a deep blue complex is also observed in acidic solutions of iron(III) with L-dopa (L-3-(3,4-dihydroxyphenyl)alanine = H_2LH) which bleaches over time. The reactions in anaerobic acid solutions of L-dopa and iron(III) ions were investigated using stopped-flow spectrophotometric, spectroscopic and chronoamperometric methods [99]. The data can be interpreted in the following way. The two complexes which form, $[FeLH]^+$ and $[FeHLH]^{2+}$, both decompose *via* an intramolecular electron transfer to yield iron(II) and dopasemiquinone, which in turn is oxidised by iron(III) to dopaquinone. The quinone then cyclises by an intramolecular Michael addition to give the UV-transparent leucodopachrome, explaining the bleaching observed and also why the presence of iron(II) ions can inhibit this process.

The presence of triethanloamine was found to inhibit the iron(III) catalysed decomposition of hydrogen peroxide, with the effect increasing for increasing triethanolamine concentration, probably because of the saturation of the coordination sphere of the iron [100]. The reaction appears to involve the formation and breakdown of a peroxo intermediate from kinetics measurements.

The effects of the presence of an aminosugar on the reduction of iron(III) to iron(II) ion by D-galacturonic acid when copper(II), uranium(IV), lead(II), nickel(II) or cadmium(II) ions are present

in solution have been investigated by potentiometry [101]. The results are suggested as important in modelling the mobilisation and bioavailability of iron in biological systems, and in particular as the root-soil interface. The removal of various mono-, di- and oligosaccharides from aqueous solution by adsorptive binding to freshly precipitated iron(III) hydroxide was found to be highly selective in respect of the stereochemistry and chain length of the sugar, presumably as a direct result of the iron/sugar complex which forms [102].

Three ligands which all possess the 1,4-dihydroxyanthraquinone function (qzH_2) (**24**) were used to complex iron(III) to give $[(H_2O)_4Fe^{III}(qzH)]$ and $[\{(H_2O)_4Fe^{III}\}_2(qz)]$ compounds, as determined from spectrophotometric data [103]. Stopped-flow kinetics studies indicated that the reaction is biphasic with successive formation of the two complexes. Hydrolysed iron(III) species are important reactants. The work was partly aimed at investigating whether iron(III) is a carrier for molecules such as these, which can have anticancer potency, in serum.

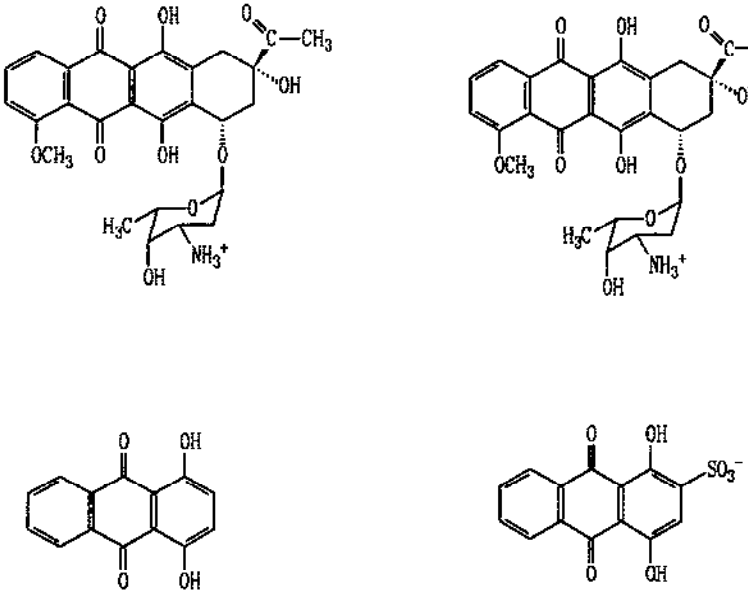

(**24**)

Iron(III) in the ammonium salt of $[Fe^{III}W_{17}H_4NaO_{56}F_6]^{8-}$ is probably distributed over many octahedral sites by analogy with the isomorphous and isostructural cobalt(II) compound. A single crystal X-ray structure determination suggests that it replaces tungsten(VI) centres in the conventional $X_2W_{18}O_{70}$ formulation [104]. The single crystal X-ray structure of the heteropolyanion compound $Ba_2H[\alpha\text{-}FeO_4W_{12}O_{36}].26H_2O$, solved from a twinned crystal, displays the α-Keggin structure, with the central iron(III) ion in a distorted tetrahedral environment [105]. Reaction of lacunar heteropoly undecatungstates with various first row transition metals and lanthanides gave compounds of the general formula $[TiW_{11}M(H_2O)O_{39}]^{n-}$ [106]. In the case of aluminium and gallium heteropoly-undecatungstates, complexes of the general formula $[XW_{11}M(H_2O)O_{39}]^{n-}$ form, where M = Al, Ga

and X is Fe(III), Cr(III), Co(II), or Cu(II), [107]. Their spectroscopic properties and X-ray diffraction patterns suggest that their structures derive from the Keggin structure. Iron(III)-containing Dawson polytungstates, $[\alpha_2\text{-}P_2W_{17}O_{61}(Fe^{3+}Br)]^{y-}$, which provide inorganic porphyrin models are discussed in section 2.4.2.1 [108,109].

The inoferrate, $K_2Na_4[(Fe^{III}O_3)_2]$, forms as single crystals from well ground mixtures of $KFeO_2$ and Na_2O heated for 29 days at 500°C followed by a further five days at 400°C, and has a structure isotypic with the gallium(III) analogue with the iron atom in a distorted tetrahedral environment of oxygen atoms, as revealed in a single crystal structure determination [110].

The compound $FeAsO_4$ was synthesised in a new hydrated form and its crystal structure determined. The structure contains a tetrameric unit of iron octahedra consisting of a pair of FeO_6- and a pair of $FeO_5(H_2O)$-units that share edges. These tetramers are interconnected by AsO_4 tetrahedra to create a network structure with channels containing the water molecules bound to the iron centres as well as the lattice water molecules. Magnetic susceptibility measurements indicate that there is antiferromagnetic ordering below 49 K, and this is in agreement with the Mössbauer spectroscopic data [111]. The crystal structure of $Fe_2(SeO_4)_3$ synthesised under hydrothermal conditions has been reported [112]. It is isostructural with the same monoclinic modification of $Fe_2(SO_4)_3$ with two different iron(III) and three different selenium(VI) atomic positions; FeO_6-octahedra share corners with SeO_4-tetrahedra thereby building a framework structure.

The reaction of iron(III) chloride with $ClOTeF_5$ yields $Fe(OTeF_5)_3$. The adduct $Fe(OTeF_5)_3.3SO_2ClF$ can be crystallised from SO_2ClF solutions [113]. The single crystal X-ray structure reveals that the iron centre is in a distorted FeO_6-environment provided by three SO_2ClF oxygen atoms and three $[OTeF_5]^-$ ligands. The solvate free complex appears to be trigonal planar from Mössbauer spectroscopic data.

2.2.2.2 Complexes with mixed oxygen/nitrogen donor ligands

Mixed *N,O*-ligation often mimics the coordination of iron(III) centres found at the active sites of metalloproteins. Often the iron atom is linked to another iron centre, as discussed in section 2.3, but there is a growing number of cases where a monomeric iron site has been identified. One example is the enzyme protocatechuate 3,4-dioxygenase which has an iron centre in a trigonal bipyramidal geometry with an axial and equatorial tyrosinate (*i.e.* phenolate), an axial and equatorial histidine (*i.e* imidazole) and the remaining equatorial site occupied by a solvent molecule. The complex bromobis[2-(2-hydroxyphenyl)benzothiazolato]iron(III) (**25**) is suggested as a model for this site [114]. The X-ray crystal structure reveals that the two didentate hydroxyphenylbenzothiazolato ligands bind with their phenolate and thiazole moieties *trans* to each other. The trigonal bipyramidally coordinated iron centre thus has two equatorial phenolate ligands and two axial thiazole ligands. The third equatorial site is occupied by a bromide ligand. The complex was formed by an unexpected two electron oxidative rearrangement of the bromo iron(III) complex of the Schiff's base $N_2O_2S_2$-ligand 2,2'-bis(salicylideneaminophenyl) disulfide which was first formed. This conversion must have involved the reductive cleavage of the S–S bond in the ligand and the oxidative formation of two thiazole rings, presumably catalysed by the iron centre. Although the axial and equatorial positions of

all of the ligands are not exactly analogous to the situation in the native system the crystallographic details help in understanding the active site structure. EXAFS data on the native system, which reveal that there is an Fe/N/O shell of three scatterers at 1.90 Å, can be understood as arising from the tyrosinate ligands and coordinated solvent interactions, whilst the Fe-N interactions in the model compound, as is usual in high spin iron(III) complexes, are somewhat longer at *ca.* 2.2 Å.

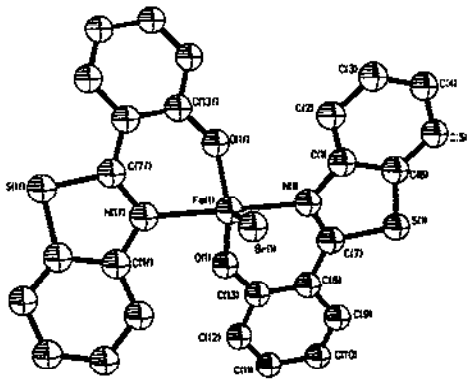

(25)

Que and coworkers have also synthesised and characterised by X-ray crystallography a functional model for the catechol coordinated active site of this enzyme, $[Fe^{III}(TPA)(DBC)](BPh_4)$, where TPA = tris(2-pyridylmethyl)amine and DBC = 3,5-di-*t*-butylcatecholate [115]. The coordination at the iron centre is not directly as would be found in the native enzyme; this would be as described for the preceding complex with a catechol coordinated in place of the solvent molecule. The complex is found to react with dioxygen within minutes to afford the expected intradiol cleavage of the catechol in 98% yield giving 3,5-di-*t*-butyl-1-oxacyclohepta-3,5-diene-2,7-dione (60%) and 3,5-di-*t*-butyl-5-(carboxymethyl)-2-furanone (38%). Kinetic studies revealed that the complex is the fastest reacting of all the [Fe(L)(DBC)] complexes studied. The high specificity and fast kinetics are suggested to be the result of the high Lewis acidity of the iron(III) centre in this complex. Also, compared with other complexes, the iron–catecholate interaction is significantly stronger as indicated by the short Fe–O bonds, the lower energy catecholate LMCT bands in the electronic spectrum, and the isotropic shifts of the DBC protons in the ^1H NMR spectrum. This indicates an increased semiquinone character. Since one proposal for the mode of action of this enzyme is *via* a semiquinone intermediate in the cleavage reaction, this might explain the enhanced reactivity of the model compound. The complex consists of a six-coordinate iron centre with four nitrogen donor ligands from the TPA ligand, and two oxygen donors from the didentate catechol-based ligand.

Iron(III) complexes of this same ligand were used by Que and coworkers to model the iron-mediated C–X bond formation in β-lactam antibiotic biosynthesis [116]. The $[Fe^{III}(TPA)X_2]$ complexes (TPA = tris-(2-pyridylmethyl)amine; X = Cl, Br, N_3) were used to catalyse the alkane functionalisation reactions of cyclohexane to give $C_6H_{11}X$ in the presence of *t*-butyl-4-methylphenol.

Although the native systems are known to involve iron(II) metal centres, the results of this work suggest that an important feature in the reaction is the formation of a high valent iron-oxo intermediate with a coordinated X ligand. Evidence for the formation of a high valent (TPA)Fe-oxo intermediate in acetonitrile solutions was also found by these workers [117]. This results from the reaction of $[\{Fe^{III}(TPA)\}_2O]^{4+}$ with hydrogen peroxide to give an iron-oxo species best formulated as $[(TPA)^{+\bullet}Fe^{IV}{=}O]^{3+}$, on the basis of EPR and Mössbauer spectroscopies. As such, it represents an unusual example of an oxo-ferryl species in a non-haem environment.

Further studies of the formation of iron-peroxide species have been undertaken using iron(III) ions coordinated by Schiff's base ligands such as H_2acen (H_2acen = ethylenebis(acetylacetoneimine)) [118], and by tripodal ligands such as $N(BzIm)_3$ [118, 119]. A side-on bound iron(III) peroxide species is postulated, which would explain why the H_2acen derivatives do not give any evidence for the formation of peroxide-bound iron. The tripod ligand complexes react with t-butylhydroperoxide to give purple species with spectral features reminiscent of those of purple lipoxygenase [119]. A similar study was performed on dinuclear iron compounds [120].

The unsymmetric polydentate ligands 1-(2-hydroxy-phenyl)-2-aza-3,5-bis(benzimidazol-2-yl)pentane and 1-(2-hydroxy-5-bromo-phenyl)-2-aza-3,5-bis(benzimidazol-2-yl)pentane (**26**) were prepared by the condensation reaction of the primary amine function of 1,3-bis(benzimidazol-2-yl)propylamine with salicylaldehyde or 5-bromosalicylaldehyde to give the Schiff's base. The imine was reduced *in situ* to afford the desired ligands. These were then reacted with iron(III) ions, (and similarly with copper(II) ions), to yield iron(III) complexes with a ligand:metal stoichiometry of 2:1 plus two uninegative anions per iron atom [121]. The ligands are capable of providing a mixed phenolate/imidazole coordination environment for the metals, although the exact mode of coordination is hard to predict in the absence of a crystal structure.

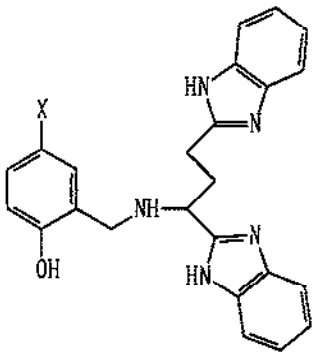

X = H
X = Br

(26)

The complexes formed with iron(III), chromium(III) and copper(II) ions and bis(trifluoroacetylacetone)ethylenediimine were studied potentiometrically, spectroscopically and by X-ray powder diffraction [122]. It was concluded on the basis of the IR spectral data that for the iron(III) compound, one of the two carbonyl groups is not coordinated.

The ligand *o*-phenylenediamine-*N,N,N',N'*-tetraacetic acid ($phdtaH_4$) is analogous to $edtaH_4$, but has a more rigid $-NC_2N'-$ linkage which is provided by the phenylenediamine moiety. The crystal structure of the potassium salt of $[Fe(OH_2)(phdta)]^-$ has been determined [123] and reveals that the iron atom is seven coordinate, with six sites taken by the four carboxylates and two amine nitrogen donors of the ligand, and the seventh site occupied by a coordinated water molecule. This is directly analogous to the situation found in the majority of iron/edta monomers. The water exchange rates at the iron(III) centre in the complex were studied as a function of temperature and pressure by the ^{17}O NMR spectral line-broadening method. The activation parameters for water exchange were determined (at 25°C) as $k = (1.2 \pm 0.2) \times 10^7\ s^{-1}$, $\Delta H^{\ddagger} = 26 \pm 3\ kJ\ mol^{-1}$, $\Delta S^{\ddagger} = 22 \pm 9\ kJ\ mol^{-1}$ and $\Delta V^{\ddagger} = 4.6 \pm 0.2\ cm^3\ mol^{-1}$. The positive activation volume indicates that the water exchange proceeds *via* a dissociative interchange mechanism, in contrast to the situation for the hexaaquairon(III) ion for which the process is associative. The water exchange in this complex is much faster than for the hexaaquairon(III) ion, perhaps as the result of the electron donating properties of the $phdta^{4-}$ ligand increasing the electron density on the metal centre and leading to a weakening of the metal-water bond through bound-ligand effect. This effect is probably also responsible for the lengthening of iron-water bonds compared with those in the hexaaquairon(III) ion which is commonly observed in such complexes.

Another ligand related to $edtaH_4$ is 1,3-propanediaminetetraacetic acid and this was used in a Raman and NMR spectroscopic and pH titration study of the complexation of iron(III) ions in aqueous solutions [124]. The increased space between the amine nitrogen atoms is suggested as allowing for a large enough chelate ring to be formed so that the complex is six, rather than seven, coordinate as has been previously demonstrated in crystal structure determinations. The results of the study indicate that in solution the six-membered chelate ring of the trimethylenediamine backbone prefers a twist-boat conformation and also there is a considerable decrease in the stability of the iron(III) complex compared with the iron(III)/edta system.

The ligand pyridine-2,6-dicarboxylic acid (also known as dipicolinic acid = H_2dipic) forms a 2:1 complex with iron(III) of formula $(H_5O_2)[Fe(dipic)_2]$ with the ligands adopting a *mer* configuration about the six-coordinate iron atom, as revealed by an X-ray crystal structure determination [125]. The $(H_5O_2)^+$ counter-ion was also confirmed by Raman spectroscopy. The variable temperature magnetic susceptibilty data indicate that the high spin complex has a weak ferromagnetic interaction, with μ_{eff} increasing from 5.91 B.M./Fe at room temperature to about 7.5 B.M./Fe at 30 K. The plot of reciprocal susceptibility *vs.* temperature shows that the compound follows a Curie-Weiss behaviour with $\theta = 20$ K.

Three complexes which form with iron(III) and diethylenetriaminepentaacetic acid (H_5dtpa) were characterised by single crystal X-ray diffraction [126]. A previous report on the structure of $[Fe(Hdtpa)]^-$ revealed the iron ion to be seven-coordinate with three ligand nitrogen donors and four ligand oxygen atoms in the coordination sphere. The three solid state structures were obtained on compounds isolated from aqueous solutions with varying pH values. At low pH the compound $[Fe(H_2dtpa)]_2.2H_2O$ forms. This contains two six-coordinate iron centres with two nitrogen donors and three carboxylate donors originating from one ligand. The third carboxylate is provided by the

pendant aminocarboxylate arm from the ligand on the other iron centre and one further protonated carboxylate does not participate in the bonding at all as shown in structure (27). At intermediate pH, (achieved by the addition of $NaHCO_3$ or ethylenediamine), the compound $[Fe(dtpa)]^{2-}$ can be isolated. The structure of this complex (28) is seven-coordinate, with the ligand providing N_3O_4-ligation, and the fifth (deprotonated) carboxylate arm free. Thus, as for the iron/edta system, the speciation of the iron is strongly pH dependent. Some of the spectroscopic properties, (such as EPR), of the low pH complex are also characteristic of the iron environment in lipoxygenase. The reaction of an iron(II)/dtpa complex with dioxygen was also studied and compared with the same reaction for the iron(II)/edta system, for which an iron(III) peroxide adduct was postulated. Only the formation of a simple iron(III) complex was observed for the dtpa case [127].

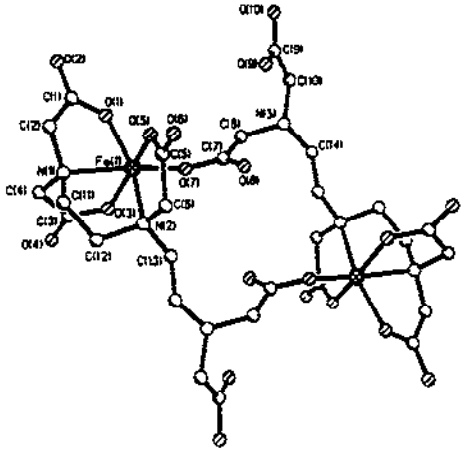

(27)

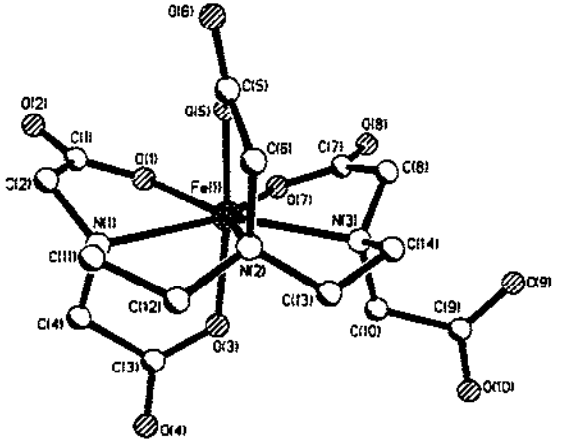

(28)

The effect of substituents on acen-type ligands on the ease of oxidation of the axial ligands (L_{ax}) in $[Fe^{III}(Racen)(L_{ax})_2]^-$ was investigated for R = CH_3, 4-X-C_6H_4, for X = H, Cl, Br, CH_3, CH_3O, and $L_{ax} = N_3^-$ [128]. The electronic properties of the equatorial Schiff's base ligand are modulated by R and affect the efficiency of the oxidation of the azide, as followed by photoreduction using UV light.

The solution state chemistry of iron(III) (as well as nickel(II) and copper(II)) complexes with the Schiff's bases *N,N'*-ethylenebis(salicylideneimine) (salen) and the related *N*-(2-aminoethyl)salicylideneimine as well as their organic fragments, salicylaldehyde and ethylenediamine, has been studied using potentiometric titration methods [129]. The equilibria involved in the synthesis of Schiff's bases are shown to lie much further towards the side of the products when metals are present (template syntheses). The iron/salen complex can be demetallated with ligands such as catecholate *via* the formation of $[Fe(salen)(cat)]^-$. The anion $[Fe(salen)(C_2O_4)]^-$ is a six-coordinate complex, as revealed by X-ray crystallography, with a high spin iron configuration [44]. The related nitrilotriacetate complex is also high spin.

The catalytic decomposition of H_2O_2 in the presence of the Schiff's base complex *N,N'*-bis(salicylidene)-*o*-phenylenediamineiron(III) ($[Fe(salph)]^+$) sorbed on to Dowex-50W resin was studied [130]. The reaction is first order with respect to $[H_2O_2]$ and is suggested to proceed *via* the formation of an $[Fe^{II}(salph)(OH)(HO^{\bullet}_2)]^-$ radical intermediate.

Iron(III) complexes with sulfathiazole, sulfamethoxazole, sulfadiazine, sulfapyridine and sulfadiimidine with metal:ligand stoichiometries of 1:2 have been prepared from iron(III) chloride and characterised by elemental analysis and electronic absorption, IR, Mössbauer and EPR spectroscopies, as well as conductivity, TGA and X-ray powder diffraction measurements [131]. On the basis of their IR spectra it appears that they all have very similar coordination geometries, with the terminal amino group of the sulfa-molecules not involved in the coordination. The EPR and Mössbauer spectra indicate that the iron centre is high spin. The thermogravimetric analyses indicate that the complexes contain coordinated water and the conductivity measurements show that that they are non-electrolytes. An octahedral $N_2O_2Cl(H_2O)$-coordination sphere for the iron with one nitrogen donor from the thiazole group and one oxygen atom from the sulfa-group of each ligand is postulated. The antibacterial activity of all of the complexes was found to be higher than that of the free ligands.

The complexation of iron(III) by simple peptides has been followed potentiometrically, and some evidence for polynuclear species was found [132].

2.2.2.3 Complexes with nitrogen donor ligands

The hexadentate polyamine macrocycle 6,13-dimethyl-1,4,8,11-tetraazacyclotetradecane-6,13-diamine (diammac) reacts with iron(II) ions in aqueous solution to form the low spin iron(III) complex $[Fe(diammac)]^{3+}$. The structure of this cation (**29**) as a mixed perchlorate/chloride salt was determined by X-ray crystallography [133]. The ligand provides an N_6-octahedral coordination environment for the iron. The complex is stable indefinitely in aerated aqueous solution and provides a rare example of a stable non-aromatic amine iron(III) complex, the only other common example

being the $[Fe(tacn)_2]^{3+}$ complex. The $^2T_{2g}$ ground state was confirmed from an analysis of the electronic spectrum and also the EPR spectrum measured at 77 K is consistent with a low spin iron(III) state, although the spectrum could not be observed at room temperature, presumably because of short spin-lattice relaxation times. The magnetic moment determined by the Evans method, gave a moment of 2.20 B.M. consistent with the expected orbital contribution to the $S = {}^1/_2$ spin state. Interestingly, the iron(II) analogue could not be isolated. The reversible Fe^{III}/Fe^{II} couple occurs at a potential of –0.35 V *vs.* Ag/AgCl and is probably the reason why the iron(III) state is favoured. A further paper reports in more detail on the EPR spectra of the complex as the triperchlorate salt [134]. The angular overlap model was used to interpret the rhombic g tensors measured and the orientation of these tensors related to the way in which the ligand field deviates from octahedral symmetry.

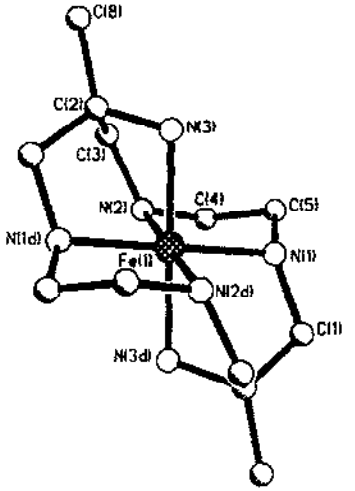

(29)

The structure of $[Fe(pzB)_2]^+$ as the nitrate salt has been determined and is a low spin iron(III) N_6-complex with average Fe-N bond lengths of 1.954(5) Å, considerably shorter than in high spin iron(III)/pzB complexes [135].

2.2.2.4 Complexes with cyanide ligands

The charge transfer transitions of $[Fe(CN)_5(3\text{-pyrazinecarboxylate})]^{4-}$ and $[Fe(CN)_6]^{3-}$ were studied in different electrolyes, and it was concluded that the electrolyte can affect the transition energies either indirectly, by changing the polarity of the medium, or directly through ion-pair formation [136]. The kinetics of replacement of 4,4'-bpy and 4-cyanopyridine by cyanide in $[Fe(CN)_5L]^{3-}$ complexes were studied in binary aqueous mixtures containing *t*-butanol, methanol, glycerol, ethylene glycol and sucrose [137]. Linear plots of the logarithms of the limiting rate constants *versus* the mole fraction of water, which are of different slope for different combinations, were obtained and interpreted as arising from multiparameter solvent effects. Kinetic, thermodynamic

and spectral data have been measured for the formation $[Fe(CN)_5L]^{2-}$ complexes from $[Fe(CN)_5(H_2O)]^{2-}$ with L = cytosine, cytidine and cytidine-5'-monophosphate [138]. With excess ligand present *pseudo* first order kinetics are followed with a dissociative mechanism. The oxidation of benzenediols by $[Fe(CN)_4(bpy)]^-$ has been followed in kinetics studies and it was found that the volumes of activation were substrate dependent and that the oxidations proceed more rapidly with increased pressure. An outer-sphere electron transfer mechanism is operative [139]. The interaction of $[Ru^{III}(edtaH)Cl]^-$ with $[Fe^{III}(CN)_6]^{3-}$ results in the formation of $[(edtaH)Ru^{III}NCFe^{III}(CN)_5]^{3-}$, which could be isolated as a tripotassium salt [140]. Such bridged hetero-nuclear systems are regarded as superior to the mononuclear compounds as catalysts in the oxidation of organic compounds. The osmium(VIII)-catalysed oxidation of glycols by $[Fe(CN)_6]^{3-}$ was found to follow zero order kinetics with respect to ferricyanide, and first order dependence in $[OsO_4]$ [141].

2.2.2.5 Complexes with other ligands

The amidinato complex $[PhC(NSiMe_3)_2]_2FeCl$ was prepared from FeOCl and the amidine $PhC(NSiMe_3)[N(SiMe_3)_2]$ in acetonitrile/thf. The crystal structure, IR and Mössbauer spectra were measured [142]. The iron atom has a distorted trigonal bipyramidal geometry with one chloride and two nitrogen donors from different ligands occupying the equatorial sites and the apical sites occupied by the remaining nitrogen atoms. The Mössbauer spectral parameters are in accordance with the distorted bipyramidal description of the structure, rather than a square-based pyramidal one.

The previously reported and structurally characterised $[Fe(py)_3Cl_3].py$ complex has been studied using Mössbauer spectroscopy [143]. The complex can be regarded as a charge transfer complex of $[Fe(py)_3Cl_3]$ and pyridine and the interpretation of the Mössbauer data led to the conclusion that crystals of the complex system can be deficient in pyridine. Crystals undergo a phase transition from orthorhombic to monoclinic at 200 K.

Catalytic studies of the Diels-Alder reaction using the ligand, L, 2,2-bis[2-{4(*S*)-phenyl-1,3-oxazolinyl}]propane as a chiral controller to complex iron(III) halides (FeX_3) have been performed [144]. The active complex, $[Fe(L)Cl_2I]$ was treated with the didentate dienophile 3-acrylolyl-1,3-oxazolidin-2-one and cyclopentadiene and gave the endo adduct with 90% or better enantioselectivity. In the light of this, the chelation of the dienophile is expected to be on one axial and one equatorial site of the iron complex.

The seven coordinate iron(III) complex, dichloro(6,13-bis(2-hydroxyethyl)-6*H*,13*H*-tripyrido[*cd,fg,lm*][1,2,4,7,9,10,13]heptaazapentadecine)iron(III), whose structure was confirmed by X-ray crystallography, can only be prepared by aerial oxidation of the iron(II) complexes. This and related planar macrocyclic ligands can be produced by template condensations at iron(II) centres. The structure of the iron(III) complex (30) reveals that the iron is coordinated equatorially by five nitrogen atoms from the macrocycle, and axially by two chloride ions. The iron(II) complexes were isolated as various derivatives from the reaction mixtures and were assigned as seven coordinate $[Fe^{II}(L)X_2]$ species on the basis of previous experience. They were found to be high spin from magnetic susceptibility studies. The iron(III) complexes are also high spin, with temperature independent magnetic moments of 5.95 B.M. over the range 93 to 294 K [145].

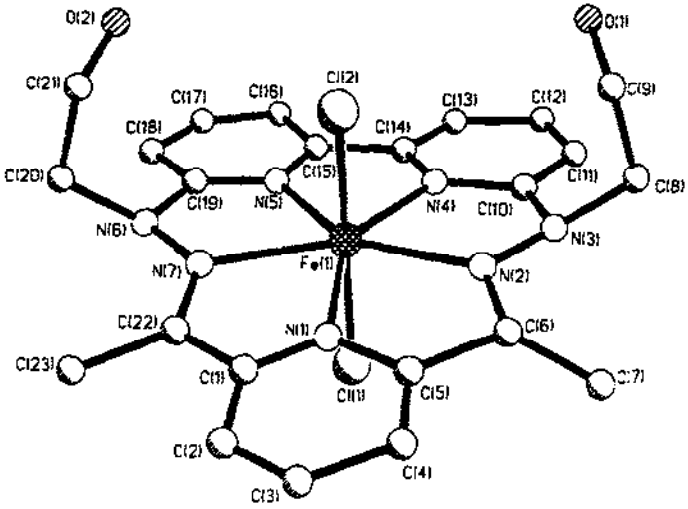

(30)

The reaction of iron powder with $PhMe_2PBr_2$ initially yields a white iron(II) complex which is oxidised by traces of oxygen to the purple compound $[FeBr_3(PMe_2Ph)_2]$ which has a trigonal bipyramidal coordination geometry with the phosphines occupying the axial positions [146].

A stopped-flow kinetic study on the anaerobic oxidation of cysteine (H_2L) by iron(III) was performed over the pH range 2.5 to 12 [147]. Three reactive complex species were identified as $[FeL]^+$, [Fe(OH)L], and $[Fe(OH)L_2]^{2-}$. The first two species are formed *via* an initial reaction of $[Fe(OH)]^{2+}$ with H_2L, the final product depending on pH. $[Fe(OH)L_2]^{2-}$ is formed at high pH from [Fe(OH)L] and L^{2-}.

The charge transfer complex $[(TTF)_2FeCl_3]$, and its bromo analogue as well as the corresponding ruthenium(III) compounds and an iridium(IV) example, can be prepared from solutions of tetrathiafulvene (TTF) and the metal halide. Magnetic susceptibility measurements and electronic, vibrational, XPS and EPR spectroscopic evidence all support the hypothesis that the iron compounds consist of stacked $TTF^{\delta+}$ radicals with the $FeX_3^{\delta-}$ entities bound to the sulfur donor atoms of the $TTF^{\delta+}$ stacks [148].

Iron trichloride forms 1:1 and 1:3 compounds with 1,2,4-triazole-3-thione and its 1- and 5-phenyl, and 5-methyl substituted derivatives [149]. The compounds were characterised by Mössbauer, IR and UV spectroscopies.

The compound $[FeWO_4Cl]$ was prepared by heating a mixture of WO_3, Fe_2O_3 and $FeCl_3$, the latter acting as a chemical transport reagent, and shown to be isomorphous with the analogous molybdenum compound by X-ray powder diffraction [150]. Solution of the powder data shows that the iron atom is coordinated in a square pyramidal fashion by four basal oxygens and an apical chloride ligand.

The compounds $Cs[M^{III}F_4(H_2O)_2]$, for M = Al, Cr, Fe, and Mn, have been prepared and characterised by X-ray powder diffraction, showing that they are isomorphous, and a single crystal structure on the aluminium compound. This reveals the metal to have octahedral coordination with the two aqua ligands *trans* to each other and forming strong hydrogen-bonds between the anions [151].

The variation in bond length for first row transition metal di- and trihalides has been discussed in the light of the structural information. Unlike the Cr(III)/Cr(II) case, where the Cr(III)-F distance is much shorter than that for Cr(II),as expected, for iron(III) and iron(II) the distances are the same within experimental error [152]. It is concluded that this is a consequence of the spherical high-spin d^5 configuration of the iron(III) centre.

2.2.3 Complexes with unusual magnetic properties

West and coworkers have been studying semicarbazone complexes, which can lead to spin equilibrium and spin crossover compounds. Metal complexes of 2-acetylpyridine N-oxide thiosemicarbazone (L) and the *N*-methyl (L') and 3-azabicyclononyl (L") derivatives were prepared and characterised [153]. The thiosemicarbazone can act as a neutral didentate ligand to give *ON*-coordination or as a deprotonated tridentate ligand to give *ONS*-coordination. The latter is the case for the iron(III) complexes reported. The EPR spectra indicate that whereas the Fe/L complex is high spin, the Fe/L' and Fe/L" complexes are low spin. The iron(III) complexes of the ^4N-ethyl and ^4N-diethyl derivatives were also prepared and characterised by the same workers [154]. The EPR spectra indicate that the complexes contain low spin cations. The chemical and antifungal properties of the ^4N-diethyl and ^4N-dipropyl derivatives are described in a further paper in this series [155]. The antifungal action of the iron(III) complexes was found to be negligible.

The complexes $[Fe^{III}(L)_2]Cl$, where L = pyridoxal 4-phenyl-, pyridoxal 4-ethyl- or pyridoxal 4-methyl-thiosemicarbazone, exhibit a discontinuous spin transition between high and low spin configurations, with the magnetic moments showing a thermal hysteresis of width $\Delta T \approx 9$ K with the transition occurring at 299 K for increasing temperature, and 290 K for decreasing temperature [156].

Variable temperature single crystal structure determinations have been performed between 120 and 311 K on BPh_4^- and PF_6^- salts of the spin-crossover compound $[Fe(acpa)_2]^+$, where Hacpa = *N*-(1-acetyl-2-propylidene)(2-pyridylmethyl)amine [157]. The Mössbauer spectra can be resolved into quadrupole doublets from the high and low spin systems, and the variable temperature susceptibility behaviour is indicative of a gradual transition between the $^6A_{1g}$ and $^2T_{2g}$ states. The structures are sensitive to spin state, with generally shorter iron-ligand bond lengths for the low spin forms with the greatest difference in the Fe-N lengths. Overall the system can be classified as a spin-equilibrium, rather than spin-transition, spin-crossover system.

Two other examples of spin-equilibrium spin-crossover complexes are $[Fe(bzpa)_2]ClO_4$ and $[Fe(acen)(NC_5H_3Me_2\text{-}3,4)_2]BPh_4$, where Hpzba = (1-benzoylpropen-2-yl)(2-pyridylmethyl)amine and H_2acen = ethylenebis(acetyl-acetoneiminate), which were characterised by X-ray structure determinations at room and low (140 or 120 K) temperature [158]. In both, the iron atom has a N_4O_2-coordination sphere, with the oxygen donor atoms *cis* and with the iron-ligand bond lengths

shorter by an average of 0.069 Å in the bzpa and 0.104 Å in the acen complexes in the low spin structures. The Mössbauer spectra are "time-averaged" for the two spins states in both cases, and the magnetic moments show a continuous variation with temperature.

The spin-crossover iron(III) complex [FeL]BPh_4.acetone, where L is the hexadentate Schiff's base ligand derived from triethylenetetraamine and salicyaldehyde, has been structurally characterised by X-ray crystallography at 290 K [159]. The Mössbauer spectra indicate that at this temperature the compound is in spin equilibrium. A second crystal form of the compound which is twinned, is apparently high spin over the range 78 to 320 K.

An imidazolate bridged trinuclear Cu-Fe-Cu system is proposed on the basis of magnetic data for the reaction of copper complex of the ligand 4-(6-methyl-8-oxo-2,5-diazanonane-1,5,7-trienylimidazole) with Schiff's base compounds (acen or salen) of iron(III) [160]. It was concluded that iron(III) is low spin for the acen compound, with ferromagnetic coupling between the heterometals, and high spin for salen, with antiferromagnetic coupling.

2.2.4 Complexes with anionic (not oxo) bridges

The crystal structures of the iron(III) compounds $FeSCl_7$, $FeSeCl_7$, $FeSeBr_7$, $FeTeCl_7$ and $FeTeCl_7$ reveal that they all exhibit the iron centre in a distorted tetrahedral coordination environment. The four donors are the four halides, one of which bridges to the chalcogen, which in turn is in an octahedral environment of three bridging and three terminal halides [161].

The polyselenide iron(III) compound $[Ph_3PNPPh_3][Fe_2Se_2(Se_5)_2]$.2dmf (**31**) (as well as the cobalt(III) compound $[PPN][Co_3(Se_4)_6]$.2dmf) was prepared by reaction of sodium polyselenide solutions with $FeCp(CO)_2I$ [162]. The crystal structures of both compounds were determined and contain alternating layers of cations and anions. The iron centres are bridged by two selenium donors, and further coordinated by chelating Se_5-ligands to give chair conformation $FeSe_5$-rings and an approximately tetrahedral geometry at the irons.

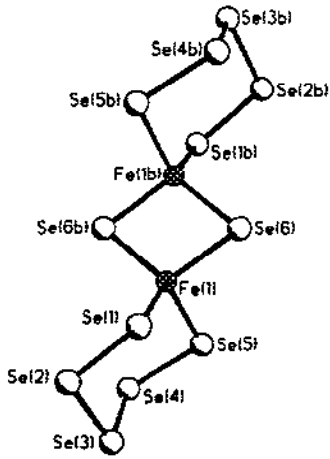

(31)

A complex formulated as [Fe_2(3,4-dihydroxyphenyl-propionate)Cl_2].2KCl.2H_2O was synthesised from alcoholic solutions containing iron(III) chloride, the ligand (dihydrocaffeic acid) and KOH [163]. Copper (II), cobalt(II) and nickel(II) complexes were also prepared. On the basis of magnetic and spectroscopic studies on all of the complexes, it is suggested that the metal ions are tetrahedrally coordinated. It is possible that the structures consist of dichloro-bridged dimers with one didentate catecholate-like ligand per metal.

The reaction of $Fe_2(SO_4)_3$ with KSCN in methanol yielded $K_2[Fe_2(NCS)_8(CH_3OH)_2]$, whereas the same reaction in water gave $[Fe_2(NCS)_6(H_2O)_4]$ and $Fe(NCS)_3$ as determined from analytical, IR and UV-VIS spectroscopies, conductivity and solvation measurements as well as magnetic data. Results are indicative of antiferromagnetic coupling for the two dinuclear compounds *via* N-bridging thiocyanates [164].

The structure of catena-{$(H_2O)_2$(1-MeIm)$_2$Mg(-CN)$(CN)_4$(1-MeIm)Fe^{III}].H_2O consists of $\{(CN)_5Fe^{III}(1\text{-MeIm})\}^{2-}$ units linked in extended chains through bridging cyanides, *cis* to the imidazole, to six-coordinate magnesium(II) counter-ions [165]. The Mössbauer spectra have very large quadrupole splitting parameters (2.62 $mm.s^{-1}$ at 291 K) supporting the suggestion that there are strong -bonding interactions between the imidazole and the low spin iron(III), in which the imidazole acts as a -director to align the electron hole in the $d\pi$ iron orbitals along the Fe-N(1-MeIm) axis.

Three fluoride bridged iron(III) structures have been reported. An X-ray crystal structure determination on the compound $(Me_4N)[FeF_4]$ reveals that the lattice contains difluoro-bridged $[Fe_2F_8(H_2O)_2]^{2-}$ (**32**) anions [166]. There are strong hydrogen bonding interactions between the protons of the coordinated waters and coordinated fluorides.

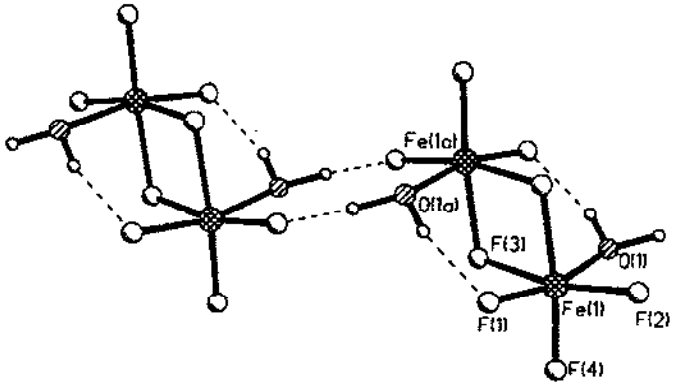

(32)

In contrast, the crystal structure of the iron/fluoro complex formed in the reaction between iron chloride and $[(CH_3)_4N]F$ contains face-sharing bioctahedral $[Fe_2F_9]^{2-}$ units (**33**) [167]. Lastly, the crystal structure of $Sr_5Fe_3F_{19}$ contains $\{Fe_2F_{10}\}^{4-}$ units as well as monomeric $[FeF_6]^{3-}$ units [168].

The structure of the dimeric units is similar to that of $[Fe_2F_8(H_2O)_2]^{2-}$ with the coordinated waters replaced by fluoride ligands.

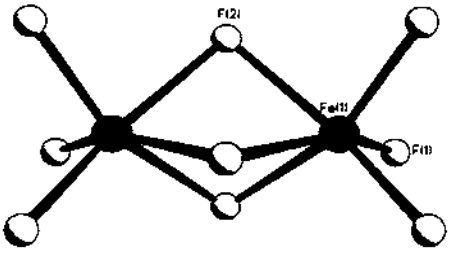

(33)

2.3 *IRON DIMERS AND CLUSTERS LINKED BY OXY-BRIDGES*

In recent years the recognition that the structural motif of iron centres linked by oxy bridges is a commonly occurring feature in natural systems has led to the blossoming of a rich coordination chemistry incorporating this feature. Whilst some compounds have been synthesised with the aim of modelling specific biological systems, others have been prepared in order to explore the hydrolysis reactions of iron, predominantly in the +3 state, and yet others to create cluster systems with unusual magnetic properties.

2.3.1 *Dinuclear singly μ_2-oxo-bridged iron compounds*

Some of the first structurally characterised oxo-bridged diiron compounds were those formed with Schiff's base ligands, such as $[\{Fe^{III}(salen)\}_2O]$. A facile one-step synthesis and the crystal structure of the dimer formed with the sterically more rigid salphenH_2 ligand, $[\{Fe^{III}(salphen)\}_2O]$.dmso, as well as some of the properties of the compound have been reported [169]. The structure consists of two five coordinate square-based pyramidal iron(III) sites with the salphen ligand providing the N and O donors of the base and an oxide bridge joining the two irons at the apices. The ∠Fe-O-Fe angle = 146.7° which compares with 144.6° for $[\{Fe^{III}(salen)\}_2O]$ and 142.5° for $[\{Fe^{III}(salen)\}_2O].CH_2Cl_2$. The room temperature magnetic moment of 2.05 BM/Fe suggests strong antiferromagnetic coupling of the iron centres. No ESR spectrum could be observed. The Mössbauer parameters are in the range observed for the salen compounds, with $\delta = 0.33$ mm.s^{-1} and $\Delta E_q = 0.77$ mm.s^{-1}

The oxo-bridged compound $[(Fe^{III}L)_2O]$, where L is the Schiff's base ligand from two equivalents of salicylaldehyde and one of isothiosemicarbazone, can be oxidised by molecular iodine to give a structure which was assigned as consisting of equal quantities of heterovalent (Fe^{III} and Fe^{IV}) and homovalent (diferric) oxo-bridged clusters on the basis of X-ray diffraction and charge balance [170].

The reaction of *S*-methylisothiosemicarbazide hydroiodide, acacH and sodium carbonate with iron(III) nitrate in ethanol gives a monomeric compound formulated as [FeLI], which can be hydrolysed in ammoniacal methanol solution to give the compound $[(FeL)_2O]$, where L = pentane-2,4-dione bis(*S*-methylisothiosemicarbazonato)(3-) [171]. The structure of this dinuclear compound was determined by X-ray crystallography. Each of the two iron centres has a square pyramidal geometry, with the basal plane consisting of N_2O_2-coordination from the tetradentate ligand, and the oxo-bridge forming the apex. On the basis of the stoichiometry, structure, electronic and NMR spectra, and magnetic measurements, which reveal that the compound is diamagnetic, a formal oxidation state of +4 was assigned to the iron centres in the complex.

NMR spectroscopic spin relaxation studies on iron(III)/edta systems at high pH have been performed [172]. The reduction in relaxation efficiency was interpreted in terms of the dual effects of the formation of the oxo-bridged dimer at these pH values leaving only an outer sphere contribution to the relaxation rate, and also the decrease in μ_{eff} because of the antiferromagnetic coupling in the dimer.

The reaction of the $[Fe^{II}(N_4)(MeCN)_2]$ system, described in section 2.1.3.2 [29], with dioxygen yields an oxo-bridged diiron(III) system formulated as $[\{Fe^{III}(N_4)(MeCN)\}_2O]$ [173]. The compound is assigned as a low spin iron(III) system, partly on the basis of the spectroscopic properties of the mononuclear iron(III) complexes, which can be isolated by anion cleavage of the oxo bridge, *e.g.* $[Fe^{III}(N_4)(Cl)_2]^-$. The rates of reduction of the oxo-bridged compound were studied by following the formation of the iron(II) monomer spectrophotometrically using a variety of reducing agents, such as hydroquinones, catechols, substituted phenols, anilines and phosphines [174]. The results are consistent with coordination of the reductant *trans* to the oxo bridge by replacement of the labile MeCN ligand.

The oxo-bridged phthalocyaninato complex $[\{Fe^{III}(pc)(MeIm)\}_2O]$ crystallises in conjunction with bis-imidazole iron(II) phthalocyaninato adduct and acetone solvate molecules [175]. The Fe-O-Fe angle is 175.1° and each iron centre is in a low spin state.

2.3.2 Dinuclear systems which model protein sites and reactions

2.3.2.1 Structural models

The modelling of the diiron sites known to exist in a variety of proteins has become more refined in its approach to producing realistic models. The work has also spawned a wealth of coupled iron systems which themselves are models for testing out theories of electronic structure, bonding and magnetic properties. The effect of changing the bridging dicarboxylate unit of the $[Fe^{III}_2O(OOCR)_2]^{2+}$ core has been investigated [176]. The dicarboxylic acid 3-phenyldipropionic acid (H_2MPDP) was used in the synthesis of $[Fe_2O(MPDP)\{HB(pz)_3\}_2]$ (**34**) and two complexes with terminal didentate ligands, B, $[Fe_2O(MPDP)B_2Cl_2]$ where B = 4,4'-Me_2bpy (**35**) or bis(1-methylimidazol-2-yl)phenylmethoxymethane (**36**). The X-ray structures of these complexes revealed that the coordination of the iron atoms was similar to that found for the acetate analogue for the $HB(pz)_3^-$ ligand. For the didentate B ligands, dinuclear iron cores also resulted, in contrast to

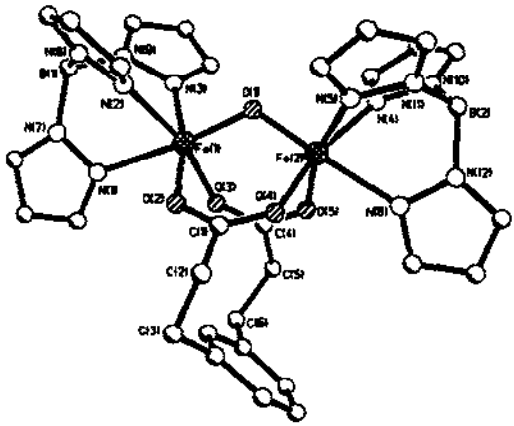

(34)

the situation found for monocarboxylate ligands where only tetranuclear compounds could be isolated. Most importantly, these dinuclear compounds possess two free coordination sites (one on each iron) *cis* to the oxo bridge, the position where exogenous ligands and dioxygen bind in the invertebrate respiratory protein haemerythrin, and additionally, the imidazole ligation from the bis(1-methylimidazol-2-yl)phenylmethoxymethane ligand provide a more accurate model of the histidyl coordination found in the native protein. It was found that the didentate ligands could be exchanged with $HB(pz)_3^-$ ligands:

$$[Fe_2O(MPDP)B_2Cl_2] + 2KHB(pz)_3 \rightarrow [Fe_2O(MPDP)\{HB(pz)_3\}_2] + 2KCl + 2B$$

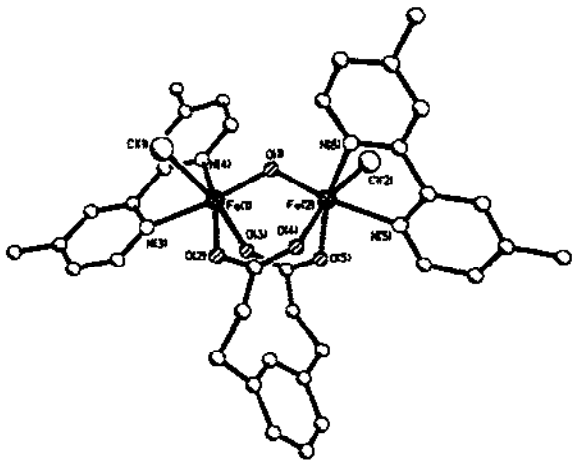

(35)

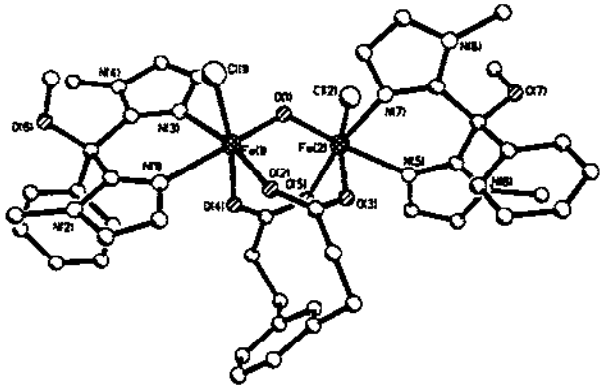

(36)

A dinuclear compound was also prepared with the didentate ligand tris(1-methylimidazol-2-yl)methoxymethane as well as a monomeric compound with this ligand. On the basis of the shifts in the ligand field bands in the electronic spectra, the order of ligand field strengths of the ligands was assigned as N_3(pz) (698 nm) > N_2(im)Cl (682 nm) > N_2(pyridine)Cl (665 nm). Magnetic and Mössbauer spectral data are also given, and these are useful additions to the library of data on such systems.

An example of a dinucleating phenolic oxygen donor is provided by the compound formed between catechol and $FeCl_3$ in methanol, $[FeCl_2(cat)]_2^{2-}$ [177]. The X-ray crystal structure (**37**) reveals that two five coordinate iron(III) centres are linked by bridging catecholate ligands, which are also chelating, with the rest of the coordination sphere being made up by two terminal chlorides. The co-ordination of iron(III) ions by catechol is of interest in modelling the intermediates of catechol oxidation by intra and extradiol dioxygenase enzymes. Electrochemical reduction of the compound is irreversible at the iron at –1.86 V *vs.* Fc/Fc$^+$ and there are two irreversible oxidations at –0.56 and +0.33 V corresponding to oxidations of the catecholate ligands.

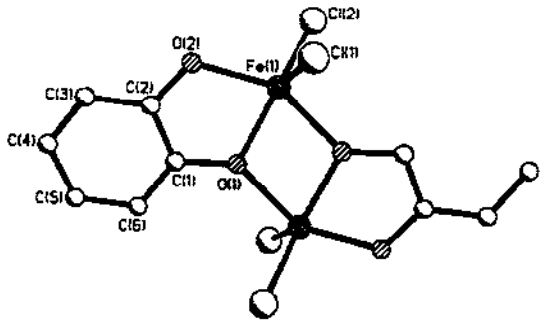

(37)

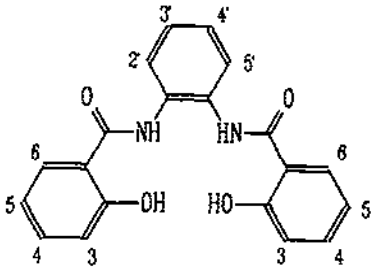

(38)

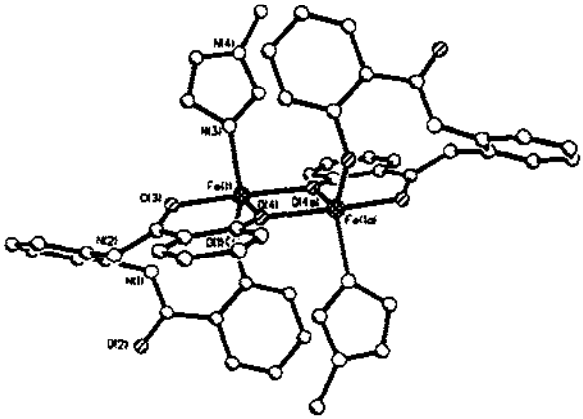

(39)

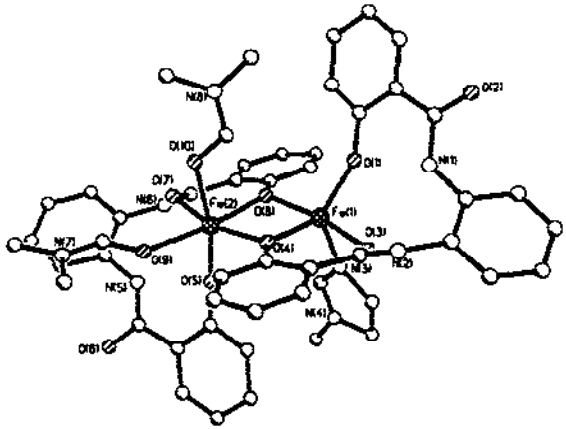

(40)

The X-ray crystal structure of dichloro[2,6-diacetylpyridine bis(salicyloylhydrazonato)]-bis(ethanol)diiron(III), which was one of a series of mono and dinuclear iron(III) complexes formed with 2,6-diacetylpyridine bis(acylhydrazone) ligands, contains two non-equivalent iron atoms in which the tetradeprotonated hydrazone ligand displays a bridging heptadentate behaviour [178]. One iron centre is exclusively *O*-coordinated by the salicylhydrazone part of the ligand and two coordinated ethanol molecules in an O_6-fashion. The catecholate moieties bridge to the seven-coordinate iron, which is further coordinated by the nitrogen donors of the ligand and two chloride ions.

A further example of a dinuclear complex with non-equivalent iron(III) coordination was confirmed by X-ray crystallography for the complex $[Fe_2(L)(OMe)(Cl_2)(MeOH)]$, where L = *N,N'*-bis(salicylidene)-1,3-diaminopropan-2-ol [179]. The iron centres are bridged by the alkoxide function of the ligand and by a methoxide from the methanol solvent. One is further coordinated to the didentate chelate of the imine nitrogen and phenoxide oxygen of one arm of the ligand plus a chloride ion, giving five coordination, whilst the other iron centre has an additional methanol coordinated to give six-coordination. They are weakly antiferromagnetically coupled ($J = -10.6$ cm^{-1}). A similar complex formulated as $[Fe_2(L)(OH)(Cl_2)]$, where L = *N,N'*-bis(salicylideneimine)-1,5-diaminopentan-3-ol, was also isolated. Cyclovoltammetry on these complexes suggests that mixed valence forms relevant to models for asymmetrically coordianted diiron proteins should be accessible, although the diferrous form was not stable.

A bridging alkoxide moiety from the ligand L = *N,N,N'N'*-tetrakis(2-benzimidazolylmethy)-2-hydroxy-1,3-diaminopropane holds together two iron(III) centres in another example of an asymmetrically coordinated diiron compound [180]. The cationic complex $[Fe_2Cl_2\{O_2P(Ph)_2\}(L)(MeOH)]^{2+}$ was formed in the reaction of iron(III) perchlorate, the ligand and diphenylphosphate in methanol. The coordination spheres of the iron centres differ in that where one has a coordinated methanol, the other has the phosphate ligand. It is the first example of a diiron compound with a terminally coordinated phosphate group and could be relevant to the inactive diferric form of Purple Acid Phosphatase

The active sites of dinuclear iron-oxo centres in proteins often involve iron in the +2 oxidation state. The dinuclear iron(II) compounds $[Fe_2(H_2Hbab)_2(N\text{-MeIm})_2]$ and $[Fe_2(H_2Hbab)_2(dmf)_2(N\text{-MeIm})]$, where H_4Hbab = 1,2-bis(2-hydroxybenzamido)benzene (**38**) were synthesised and their structures determined by X-ray crystallography [181]. The complex $[Fe_2(H_2Hbab)_2(N\text{-MeIm})_2]$ consists of two equivalent $FeNO_4$-trigonal bipyramidal coordination spheres composed of two amide oxygen atoms, a terminal and a bridging phenolate oxygen and a single nitrogen from N-MeIm (**39**). $[Fe_2(H_2Hbab)_2(dmf)_2(N\text{-MeIm})]$ (**40**), however, possesses inequivalent iron sites: one $FeNO_4$-sphere with the same coordination as before, and one FeO_6-site, where the *N*-MeIm has been displaced by two dmf molecules. The spectroscopic properties (electronic absorption, epr, Mössbauer) of these compounds compare with those of fully reduced methane monoxygenase (MMO) and the B2 subunit of ribonucleotide reductase (RRB2). They also exhibit a weak ferromagnetic coupling. Cyclic and square voltammetric studies of $[Fe_2(H_2Hbab)_2(dmf)_2(N\text{-MeIm})]$ in dmf gave two quasi-reversible one-electron oxidation steps at –500 and –250 SCE corresponding to $[Fe^{2+}, Fe^{2+}] \rightarrow [Fe^{2+}, Fe^{3+}]$ and $[Fe^{2+}, Fe^{3+}] \rightarrow [Fe^{3+},$

Fe^{3+}] core oxidation state transformations. Overall the compounds provide reasonably good models for the properties of the sites in MMO and RRB2, although the known coordination of the iron centres in RRB2 is not reproduced accurately. The use of a ligand-derived phenolate to mimic a bridging hydroxide is probably a useful first approach to stabilising dinuclear iron(II) sites.

Another possible model for RRB2 is the dinuclear compound $[\{Fe^{III}(bpma)\}_2(\mu_2\text{-}O)(\mu_2\text{-}OAc)_2]^{2+}$, where bpma = bis(2-pyridylmethyl)amine, which has been structurally characterised [182]. Both iron atoms in this complex are octahedrally coordinated by three oxygen atoms from the bridging groups with the bpma ligands coordinating facially. The pendant pyridyl groups of the ligands are *cis* to the μ_2-oxo bridge.

2.3.2.2 Catalytic and oxygenation studies

A dinucleating alkoxide function from the ligand *N,N,N',N'*-tetrakis(2-benzimidzolylmethyl)-2-hydroxy-1,3-diaminopropane (HPTB) plus a bridging hydroxide group hold together the two iron(III) centres in $[Fe_2(HPTB)(\mu\text{-}OH)(NO_3)_2](NO_3)_2$ [183]. This structure was confirmed by an X-ray diffraction study, although problems were encountered with crystal decomposition and the data could only be refined to an R value of 17%. EXAFS studies were used to help confirm the structure and refine the iron environments. The complex reacts irreversibly with H_2O_2 to form a 1:1 adduct which has a new feature at 600 nm in the electronic spectrum. From resonance Raman studies, this is assigned as a peroxide-to-iron charge transfer band. Studies using $H_2{}^{18}O_2$ and D_2O solutions suggest that the peroxide oxygen atoms are not protonated, since no changes were detected in the spectra. On the basis of the spectroscopic, structural and magnetic data presented, it was concluded that the peroxide binds by replacing the bridging hydroxide to give a $(\mu\text{-}\eta^1,\eta^1\text{-}$peroxo)diiron(III)centre. As such, this is a better model for the dioxygen interactions in MMO and RRB2 than in haemerythrin.

A five-coordinate diferrous complex, which binds dioxygen reversibly, has been reported in a review of dicopper and diiron μ-peroxo complexes [184]. A differic μ-oxo compound which can add dioxygen to alkanes, and thus models MMO, is also reported.

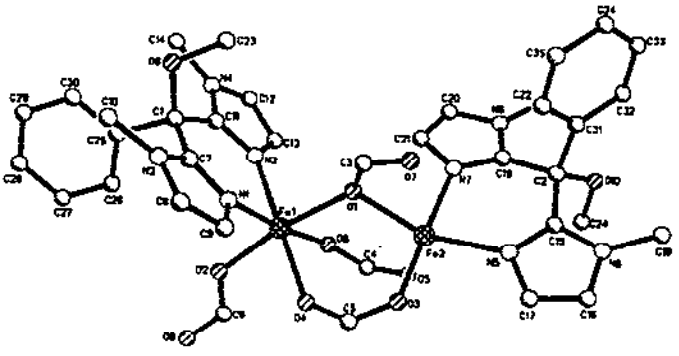

(41)

The asymmetric triply carboxylate bridged diiron(II) complex $[Fe_2(OOCH)_4$(bis(1-methylimidazol-2-yl)phenylmethoxymethane)$_2]$ (41) displays a structure of relevance to modelling the sites in diiron oxo proteins [185]. The X-ray structure determination reveals that the two ferrous centres are unsymmetrically coordinated. They are bridged by one monodentate and two didentate formate ligands, and each has one didentate imidazolate ligand. One of the iron atoms has an additional monodentate formate ligand, making it six-coordinate. There is a weak interaction of the five coordinate iron atom with the free oxygen donor of the monodentate formate bridge. The magnetic data suggest that there is very little interaction between the iron centres. The EPR spectrum has an unusually shaped integer spin signal at $g \sim -16$ cm^{-1}, which is the same value as that observed for MMO and RRB2. Furthermore, the complex reacts with dioxygen to give the dinuclear oxo-bridged iron(III) compound $[Fe_2O(OOCH)_4$(bis(1-methylimidazol-2-yl)-phenylmethoxymethane)$_2].H_2O$, which was structurally characterised by X-ray crystallography and possesses two octahedral iron(III) centres coordinated by the didentate ligand, one monodentate formate ion, a bridging oxide and two bridging formate ligands. Proof that the oxide bridge derives from dioxygen and not adventitious water was provided using resonance Raman studies on the symmetric Fe-O-Fe stretching vibration after treatment of the diferrous complex with $^{18}O_2$. There was some evidence for the formation of mixed valence species in the EPR spectra of rapidly frozen reaction solutions.

Solutions of iron(III) in the presence of nta have long been known to catalyse a variety of biological-type reactions. A dark green complex which can be isolated from solutions containing $[Fe^{III}_3(\mu_3\text{-}O)(\mu_2\text{-}OOCCH_3)_6(H_2O)_3]^+$ and nta has been formulated as $[Fe^{III}_2(\mu_2\text{-}O)(\mu_2\text{-}OOCCH_3)_2(nta)_2]^{3-}$ and is proposed as a possible catalyst in such reactions [186].

The biomimetic oxidation reactions of a variety of hydrocarbons with iron(III), Fe^{III}_2O and $Fe^{III}_4O_2$ complexes using H_2O_2/O_2 were studied [187]. It was found that all three types of iron compound were capable of acting as oxygen transfer reagents.

Two iron(III) complexes can be formed with the ligand 2,2'-dihydroxy-3,3'-diacetyl-5,5'-dichlorodiphenylmethane, one of which is expected to be mononuclear and the other dinuclear on the basis microanalytical and Mössbauer spectroscopic data [188]. The formation of complexes with copper(II), nickel(II), cobalt(II), and vanadium(V) are also described. The iron compounds can be used as catalysts for the oxidation of 3,5-di-*t*-butyl-1,2-dihydroxybenzene.

The di- and trinuclear complexes $[Fe_2OCl_6]^{2-}$, $[Fe_2O(phen)_4(H_2O)_2]^{2+}$, and $[\{Fe(alanine)_2(H_2O)\}_3O]^{7+}$, were shown to be efficient in the transfer of oxidising equivalents from *t*-butyl hydroperoxide to cyclohexane [189]. The presence of excess imidazole increased the yield and the ketone:alcohol ratio.

2.3.3 Trinuclear clusters containing the {M3(μ3-O)} core

The $[Fe^{II}Fe^{III}_2(\mu_3\text{-}O)]^{6+}$ core is a member of the vast family of μ_3-oxide bridged metal "triangles", which provide vehicles for testing theories of electronic exchange as well as form the building blocks of higher nuclearity clusters. Incoherent neutron scattering was used to probe the dynamics of the molecular motions in the mixed valence compound $[Fe^{II}Fe^{III}_2(\mu_3\text{-}$

$O)(OOCD_3)_6(py)_3].py$ [190]. This compound is known to undergo a number of phase changes, perhaps as a result of ordering of the solvent pyridine molecules. There was found to be a correspondence between the elastic scattering probability and the specific heat data, with a first order transition from the specific heat data coinciding with a discontinuous change in the neutron scattering probability, and a second order transition corresponding to a gradual change in scattering profile. The same compound and the $CHCl_3$ solvate analogue were investigated using variable pressure ^{57}Fe Mössbauer spectroscopy [191]. It was found that at pressures greater than 80 kbar these compounds become valence trapped, showing two doublets in the Mössbauer spectra with an area ratio of 2:1 which can be assigned to iron(III) and iron(II). The spectra at intermediate pressures can be interpreted in terms of the valence detrapped and valence trapped states, whilst those at pressures less than 20 kbar arise from the fully delocalised forms.

The effect of interstitial solvent stearate-bridged analogues of these Fe_3O triangles was gauged from X-ray diffraction patterns and Mössbauer spectroscopy [192]. The diffraction data indicate the trimers adopt layer structures with interlayer spacing depending on solvate, and the Mössbauer data show a mixed-valence state trapping for the non-solvated case, but not for the solvated examples.

The compound $[Fe^{II}Fe^{III}_2(\mu_3\text{-}O)(\mu_2\text{-}OOCH_3)_4(OOCH_3)_2(tacn)].2CHCl_3$ (**42**) can be prepared from ferrous acetate and tacn in the presence of oxygen [193]. The X-ray crystal structure reveals that two of the acetate ligands are didentate chelating rather than bridging. In addition, the structural parameters suggest that one of the carboxylato-coordinated iron ions is in the +2 oxidation state with the distances to the iron in the coordination sphere significantly longer than those for its counterpart. Valence localisation in this compound is supported by the Mössbauer spectra, which can be understood in terms of iron(II) and iron(III) sites. The cluster is antiferromagnetically coupled and the magnetic data can be fit using J values of $-16.5\ cm^{-1}$ for the Fe(II)-Fe(III) interactions, and $-41.8\ cm^{-1}$ for the Fe(III)-Fe(III) interactions, with a ground state of S = 1. The all iron(III) member of this family in the form of $[Fe^{III}_3(3\text{-}O)(2\text{-}OOBz)_6(CH_3OH)_2(H_2O)].C_6H_5CO_2$ has been crystallographically characterised [194].

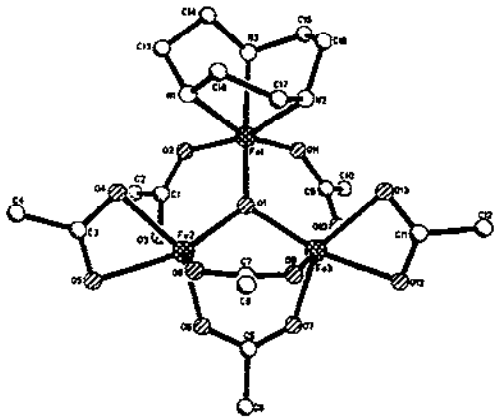

(42)

The oxidation of the hydroxyammonium ion by iron(III) ions in acetate buffers has been investigated, and it was concluded that the active species is $\{Fe^{III}_3(\mu_3\text{-}O)(OOCH_3)_6\}^+$ and the reaction stoichiometry requires one mole of iron(III) per hydroxyammonium, rather than the two previously postulated [195]. The hydroxylation of aromatic compounds by an iron(0), acetic acid, dioxygen system, which probably involves species similar to the $\{Fe_3O(OOCMe)_6\}^+$ moiety, is suggested to proceed *via* the formation of ferryl species [196].

Homo- and heterometallic trinuclear $[M^{III}_3(\mu_3\text{-}O)(OOCR)_6(H_2O)_3](NO_3)$ compounds, where R = C_7H_{15} and M_3= Fe_3, Cr_3, Fe_2Cr, $FeCr_2$, have been prepared and spectroscopic and magnetic studies are in accord with this formulation [197]. Mixed-valence states of ^{57}Fe atoms were produced by electron-capture decay in ^{57}Co labelled $[CoFe_2(\mu_3\text{-}O)(OOCH_2I)_6(H_2O)_3]$ and $[CoFe_2(\mu_3\text{-}O)(OOCH_2Br)_6(H_2O)_3]$, which were studied by Mössbauer emission spectroscopy [198]. The two compounds show temperature dependent trapped-to-averaged and trapped valence states, respectively.

2.3.4 Magnetic studies and systems with unusual magnetic properties

A series of thirty-six dinuclear iron(III) centres found in Fe_2 and Fe_3 compounds bridged by a ligand oxygen atom and at least one other bridging ligand, such as carboxylate and phosphate, has been considered [199], and a correlation between the antiferromagnetic exchange coupling constant J and a parameter, P, which is defined in Ångstroms as half the shortest superexchange pathway between the two iron centres established. The magnetostructural correlation can also be applied to tetranuclear compounds and metalloproteins, although it does not apply to (μ-oxo)diiron(III) centres unsupported by other bridging ligands. This correlation is of interest in view of the fact that other attempts to correlate J with structural parameters such as Fe-O-Fe angle and Fe---Fe distance have not proved wholly successful in the past..

The ligand 4,6-bis[*N*,*N*-bis(2'-pyridylmethyl)aminomethyl]-2-methylresorcinol was synthesised to provide a bridging ligand capable of furnishing the correct topological arrangement to favour an overall ferromagnetic interaction of two iron(III) centres [200]. It is suggested that in the complex $[Fe_2(L)(H_2O)_4]^{4+}$ each iron atom is coordinated by two pyridyl functions, the connecting amino nitrogen, two waters and one of the resorcinolate oxygen donors. In this way the central bridging favours a ferromagnetic exchange between the irons with J = +0.62(3) cm^{-1}.

The ligand L = *N*-salicylidene-2-hydroxy-5-chloro(or bromo)benzylamine, forms dinuclear iron(III) complexes, $[Fe_2(L)_2(CH_3COO)_2]$, which also display ferromagnetic coupling of the iron centres with J = +1.6 cm^{-1} [201]. The structure of the complex was confirmed by X-ray crystallography and shows that each iron is six-coordinate with an NO_5-donor set provided by two bridging acetates, two dinucleating phenolates from each ligand, and the N and O from the salicylidene. This quadruply bridged diiron centre is somewhat unusual, and might account for the positive interaction between the irons centres.

The Schiff's base ligand, $salpnH_2$, was used in the synthesis of trinuclear bridged M(II) complexes [202]. The compounds of general formula $[M_3(salpn)_2(O_2CCH_3)_2].2dmf$, with M = Co(II) and Fe(II), as well as the iron(II) complex formed with the 2,2-dimethyl-salpn analogue, were

the products formed in the attempted synthesis of M^{II}salpn complexes. The iron(II) and cobalt(II) complexes of the salpn ligand are isostructural, and consist of three metals joined in a line by bridging carboxylates and dinucleating (*via* the phenolic oxygen) salpn ligands as shown in structure (43). A similar structure has been previously observed for the a heterometallic $ZnCu_2$-system [203]. The magnetic susceptibilities at room temperature can be understood in terms of non-coupled high spin M(II) systems.

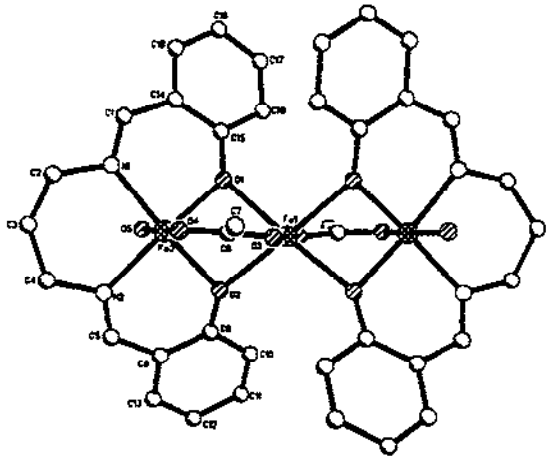

(43)

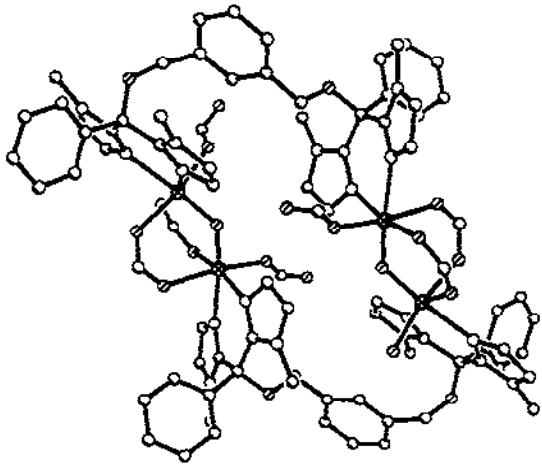

(44)

The tetranuclear iron(III) complex, $\{Fe_2$(1,3-bis((bis(1-methylimidazol-2-yl)phenyl-methoxy)methyl)benzene)$(\mu_2\text{-O})(\mu_2\text{-}HCO_2)_2(HCO_2)_2\}_2$ (44), can perhaps best be described as a

dimer of dimers (as indicated by the formulation) and has been characterised by X-ray crystallography [204]. The ligand can be regarded as two bis-imidazolate ligands bridged by a *m*-xylyl spacer, and the coordination geometry of each iron atom is essentially octahedral, with two imidazole ligands, a bridging oxo-group, two bridging formates, and one monodentate formate ligand making up the coordination sphere. In this way, the structure consists of two pairs of $(\mu_2\text{-O})(\mu_2\text{-HCO}_2)_2$-bridged diiron centres linked by the *m*-xylyl groups of the imidazolate ligands.

The $[Fe^{III}_4(\mu_3\text{-O}_2)]^{8+}$ core can be regarded as a "butterfly" made up of two $Fe^{III}_3(\mu_3\text{-O})$ triangles sharing common metals at the hinge. This approach is helpful when visualising the build up of higher nuclearity oxo-bridged clusters and also when trying to rationalise their magnetic properties. The compound $[Fe^{III}_4O_2(OOCCH_3)_7(bpy)_2](ClO_4).{}^1/_4CH_2Cl_2.H_2O$ contains this butterfly core, as revealed by a single crystal X-ray diffraction study [205]. The variable temperature magnetic susceptibility of the complex was measured to 5 K. The effective moment per molecule decreases from 4.20 BM to 0.82 BM, indicative of an S = 0 ground state. An antiferromagnetic interaction is expected in coupled iron(III) systems. The theoretical analysis of the data used two pairwise interactions to explain the observations: a wing-body and a body-body exchange as represented in (45). The wing-wing interaction was considered to be negligible in view of the greater separation of the iron centres. The analysis revealed that a wing-body exchange of $J_{wb} = -45\ cm^{-1}$ fitted the data, whereas the body-body interaction, J_{bb}, was indeterminate. The origin of this effect lies in what has often been termed "spin-frustration", that is, the situation where the relative magnitudes of the antiferromagnetic exchange interactions result in a net alignment of some of the spin vectors in a system, in this case on the two body dioxo bridge core irons.

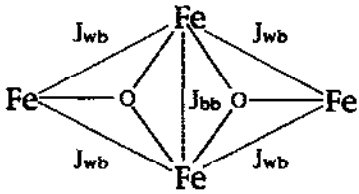

(45)

The same type of spin frustration phenomenon was observed by the same workers in a hexanuclear iron(III) complex [206, 207]. The compound $[Fe_6(\mu_3\text{-O})_2(\mu_2\text{-OH})_2(\mu_2\text{-OOCCH}_3)_{10}$(1,1-bis(*N*-methylimidazol-2-yl)-1-hydroxy-ethane)$_2].xCH_2Cl_2$ (46) forms from the reaction of the imidazolate ligand with $[Fe_3(\mu_3\text{-O})(\mu_2\text{-OOCCH}_3)_6L_3]^+$, L = H_2O, py. It can be visualised as two $Fe_3(\mu_3\text{-O})$ triangles joined by two bridging hydroxide and four bridging carboxylate groups at their bases. The magnetic susceptibility data reveal an increase in effective moment with decreasing temperature. The magnetisation data were fitted using full-matrix diagonalisation and can be understood in terms of a system with an S = 5 ground state, rather than the expected S = 0 state, this arising from a spin frustration within the core.

An alternative means of introducing unusual magnetic interactions in bridged polynuclear metal systems is to synthesise heterometallic complexes. This approach was used with the dinucleating ligand BPMP, 2,6-bis[(bis(2-pyridylmethyl)amino)methyl]-4-methylphenol, to produce

the complex $[Fe^{III}Cu^{II}(BPMP)Cl_2](BPh_4)_2$, whose crystal structure has been determined, but not yet reported [208]. The complex in acetonitrile solutions was studied using epr and Mössbauer spectroscopy, both of which show that the complex is ferromagnetically coupled with a ground state of S = 3.

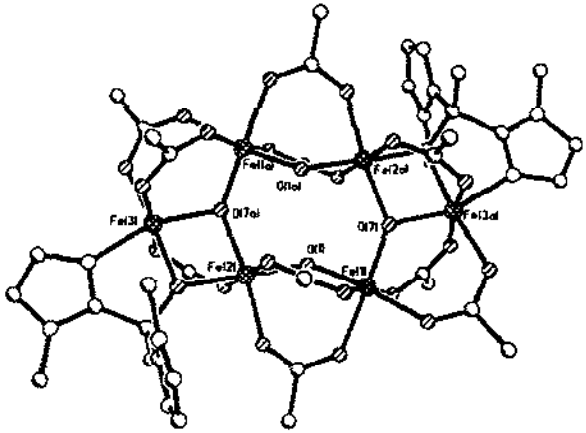

(46)

The heteropolynuclear clusters $[\{Cu(Mesalen)\}_2Fe(acac)].(NO_3)_2$ and $[\{Cu(Mesalen)\}_3Fe(acac)].(PF_6)_2$ have been prepared, and the four metal, {3CuFe}-cluster structurally characterised by X-ray crystallography [209]. Trinuclear $\{2Cu^{II}Fe^{III}\}$- and mononucler $\{Cu^{II}(Mesalen)\}$-units are arranged in helicoidal polymeric chains. Magnetic studies suggest that the different units interact weakly. Also, the Mössbauer spectroscopic data indicate that the three metal cluster also contains {2CuFe}-units.

In the trinuclear heterometallic compound $[\{(Me_3tacn)Fe^{III}\}_2(dmg)_3Ni^{II}](PF_6).{}^1/_2CH_3OH$, Me_3tacn = 1,4,7-trimethyl-1,4,7-triazacyclononane, dmgH = dimethylglyoxime, the two iron centres are joined to the central nickel atom by dimethylglyoximate bridges [210]. The crystal structure shows that the nickel atom has N_6-coordination from the dmg^- nitrogen atoms and each iron centre has N_3O_3-coordination, with the nitrogen donors from the cyclic amine ligand, and the oxygens from the dmg^- ligands as shown in (47). The trimetal unit is almost linear with an Fe-Ni-Fe angle of 179.4°. The magnetic susceptibility data were interpreted in terms of antiferromagnetic interactions between the iron and nickel centres and also the iron centres, the latter being much weaker. The overall ground spin state of the compound is S = 4. The cyclic voltammograms reveal two quasi-reversible one electron oxidations, corresponding to successive oxidations of the nickel centre up to nickel (IV), and two reversible one electron reductions, corresponding to the stepwise reduction of each iron centre down to iron(II).

The X-ray structure of $[Zr^{IV}_3Fe^{III}(\mu_4\text{-}O)(\mu_2\text{-}OC_3H_7)_6(OC_3H_7)_4(acac)_3]$ has been reported [211]. The compound is formed in the reaction of iron(III) acetylacetonate with zirconium(IV) *n*-propanolate in *n*-propanol. The four metal atoms describe a tetrahedron, with the μ_4-oxide at the centre. The iron centre is five coordinate, with the rest of its coordination sphere made up of three

didentate propanolate ligands and one terminal propanolate unit. The zirconium atoms are seven coordinate, each with a didentate acac⁻ ligand, three didentate propanolates and one terminal propanolate in addition to the μ_4-oxide.

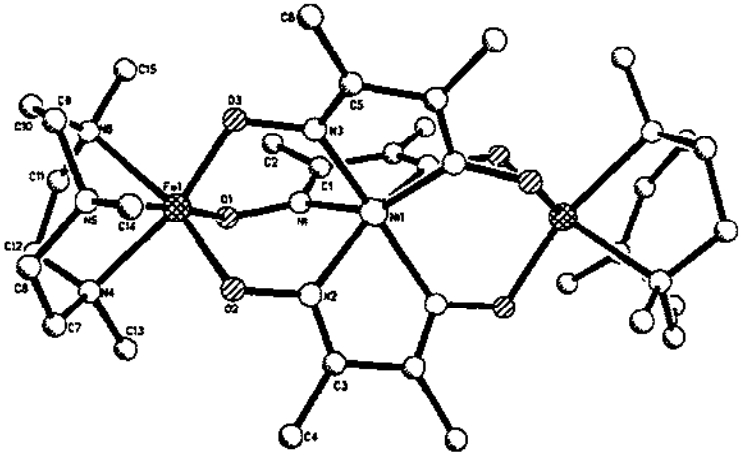

(47)

Fourteen heterometallic alkoxide clusters containing iron(III), such as $[AlFeNbZr_2(OCHMe_2)_{12}]$, have been characterised by elemental analyses, IR and reflectance spectroscopy and their magnetic behaviour [212].

An investigation into the compounds forming between iron(III) and polyalcohols in alkaline aqueous media indicated that mononuclear, oligonuclear and polynuclear iron(III) species are important [213]. It was found that the polyalcohols modified the hydrolysis of the iron(III) markedly. At high ligand concentrations, mononuclear species form, as indicated from magnetic susceptibility and electronic spectroscopic measurements. The formation of polynuclear complexes at high pH was followed using laser light scattering and kinetic measurements. In the case of sorbitol complexes, the polymerisation was found to be reversible.

2.4 IRON PORPHYRIN AND OTHER N_4-MACROCYCLES

The majority of iron/porphyrin complexes are synthesised in order to provide models for the biological haem centres found in proteins such as haemoglobin, myoglobin, the cytochromes, various catalases, peroxidases and reductases. The fact that these biomolecules are all closely related structurally, and yet fulfil a variety of functions and stabilise iron in a variety of oxidation and spin states, can be rationalised in terms of the steric environment, or pocket, provided by the folds of the polypeptide backbone of the protein, and the influence on the electronic state of the iron by axial ligands, which can be endo- or exogenous in origin. The reproduction of these features is an important aim in the synthesis of models. A second goal is to reproduce the binding or catalytic activity of the biomolecule. In many cases this involves the synthesis of functionalised porphyrins capable of placing the required steric demands on the metal.

2.4.1 Catalase and peroxidase models

Models for catalase with the required proximal oxygen binding to the iron(III) centre provided by the functionalised "basket-handle" porphyrins have been prepared [214]. The manganese(III) complexes were also synthesised. In general, their ability to catalyse the dismutation of hydrogen peroxide or the oxygenation of an alkene proved to be similar to catalysts having a proximal nitrogen ligand, provided by an imidazole ligand. However, the iron complex with the proximal oxygen was only capable of effecting the dismutation reaction leading to the suggestion that the proximal tyrosinate in catalase inhibits oxygen transfer reactions in the native enzyme. The manganese complexes were always more efficient than the iron complexes in catalysing the reactions.

The synthesis, ligand binding properties and oxidation reactions of deuterohaemin modified with an undecapeptide residue have been reported [215]. The steric effect produced by the folding of the peptide chain affects the binding of axial ligands, such that there is a markedly reduced affinity for the binding of a second imidazole ligand. The complex exhibits both catalase and peroxidase activity.

The crystal structure of [Fe^{III}(TPP)(2,6-dichlorophenoxide)] has been determined and provides a model for the phenolate binding from tyrosinate residues in catalases and also mutant haemoglobins [216]. The iron atom is five coordinate, with the phenoxide ligand coordinated in a bent fashion with the angle at the oxygen, ∠Fe-O-C = 132.6(2)°.

2.4.2 Cytochrome models

2.4.2.1 Cytochrome P450 models

The nature of the axial ligands of the water soluble iron(III) porphyrinates $[Fe(TMpyP)]^{5+}$ and $[Fe(TPPS)]^{3-}$ were examined as a function of pH by ^1H NMR spectroscopy [217]. The NMR spectroscopic shifts provide some evidence for the existence of $[Fe(TMpyP)(H_2O)_2]^{5+}$, $[Fe(TMpyP)(H_2O)(OH)]^{4+}$, $[\{Fe(TMpyP)\}_2O]^{8+}$ and $[Fe(TMpyP)(OH)_2]^{3+}$ in the $TMpyP^{2-}$ system, and $[Fe(TPPS)(H_2O)_2]^{3-}$, $[Fe(TPPS)(H_2O)(OH)]^{4-}$ and $[\{Fe(TMpyP)\}_2O]^{8+}$ in the TPPS system. Crystals of the high pH oxo-bridged $[\{Fe(TMpyP)\}_2O]^{8+}$ complex as the perchlorate salt were obtained, and the X-ray crystal structure shows the iron atoms to be pyramidally coordinated.

The first report of iron(III) porphyrins with σ-bonded tetra- and triazolato ligands includes the characterisation of two linkage isomers, [Fe(OEP)(N_4CMe)] and [Fe(OEP)(N_4CPh)] by X-ray crystallography [218]. In these, the R group on the heterocycle is either next to the σ-bound nitrogen atom, in the 5-position (isomer I, found for R = Me) , or removed from it in the 4 position (isomer II, found for R = Ph). Magnetic studies indicate that the iron is high spin. Eight different complexes are reported. These are of relevance to the phenylimidazole-inhibited complexes of cytochrome P450cam.

The first example of an iron(III) porphyrin complex with two axial chloride ligands is provided by [Fe^{III}(β-PPh_3^+-TPP)Cl_2], the structure of which was determined by X-ray

crystallography [219]. The compound is high spin, which is relatively unusual for six-coordinate iron(III)-porphyrin complexes. Another six-coordinate high-spin iron(III) porphyrin is the complex $[Fe^{III}(TMpyP)(H_2O)_2]^{5+}$ which has two axially coordinated water molecules, as revealed by X-ray crystallography [220].

The effect of pyridine binding on the spectroscopic and electrochemical properties of σ-bonded aryl iron(III) porphyrins was found to result in low spin complexes forming [221]. The spin-state was also influenced by the degree of fluorination of the aryl moiety.

The catalysis of oxidation, hydroxylation and epoxidation reactions of hydrocarbons by peroxide species using iron(III) porphyrins has been investigated using a number of systems [222-233]. These reactions are of relevance to the catalytic action of cytochrome P450, which is thought to involve an iron(IV)-oxo (ferryl) radical species. A porphyrin with twelve phenyl groups was synthesised and was found to be capable of stabilising such a ferryl radical at 8°C on reaction with 3-chlorobenzoic acid [230]. A study of acyl-carbon fission processes catalysed by cytochrome P450-type systems might also involve an $\{Fe^{III}\text{-}OOH\}$ intermediate [231]. The complex $[Fe^{III}(TPP)Cl]$ catalyses the conversion of nitrobenzene to aniline [234].

The photoredox behaviour of various *meso*-tetraarylporphyrin complexes of iron(III) was examined [235]. The study showed that the iron(III) was reduced to iron(II) on irradiation, and also that the reduction of CCl_4 was catalysed. The relevance of this to understanding the mechanism of reduction of haloalkanes by cytochrome P450 is discussed.

Electrochemical oxidation of tetrakis(2,6-difluorophenylporphinato)haloiron(III), $[(F8\text{-}TPP)Fe^{III}X]$, where X = Cl or F, was found to result in the generation of iron porphyrin radicals stable enough for spectral characterisation at room temperature [236]. ^1H, ^2H and ^{19}F spectroscopic NMR characterisation suggests that the species thus produced is the first iron(IV) porphyrin π-cation-radical complex without an axial oxo-ligand. Electrochemical oxidation of $[\{(F8\text{-}TPP)Fe^{III}\}_2O]$ yields cationic iron(III) porphyrin radical compounds.

The gas-phase synthesis of metalloporphyrin ions has been studied as a possible route to the production of the reactive intermediates of catalytic cycles such as hydrocarbon activation by cytochrome P450 [237]. $Fe(P)^+$ ions, for example, were produced by excimer laser ablation of an iron disk in the presence of the porphine vapour.

The ferric and ferryl tetramesitylporphyrinato π-cationic radical complexes were studied using resonance Raman spectroscopy in an attempt to resolve the question of the electronic structure of the Fe^{IV}=O stretching mode. It was concluded that the presence of an axial ligand affected the bonding situation [238]. The resonance Raman spectra of the carbene complexes $[Fe(TPP)CCl_2]$, $[Fe(TPP)^{13}CCl_2]$, $[Fe(TPP)CBr_2]$ and $[Fe(TMP)CCl_2]$ have been studied and the presence of a spin sensitive band, ν_2, at 1569 cm^{-1} and an oxidation state sensitive band, ν_4, at 1370 cm^{-1} led to the conclusion that the metal centre is low spin iron(IV) [239].

The complex $[Fe(TM(4)pyP)]^{5+}$ was studied as a catalyst for the oxidation of organic substrates by iodosylbenzene in organic solvents [240]. UV-VIS and EPR spectroscopies were used to identify the intermediates, which were assigned as an iron(III) rhombic species, an iron(IV) ferryl species and an iron(III) *N*-oxide species. The oxo-iron(IV) π-cation radical was not detected.

In a similar study, there was evidence that a dinuclear oxo-bridged iron(IV) radical was the catalytic species [241].

The reactions of diphenylhydroperoxyacetate with water soluble six-coordinate manganese(III) porphyrins were studied and compared with results for the iron(III) species [242]. The reactivity of the iron(III) species is much higher at low pH.

An inorganic-porphyrin analogue based on the Dawson complex, $[\alpha_2\text{-}P_2W_{17}O_{61}(M^{n+}Br)]^{y-}$ for $M^{n+} = Mn^{3+}$, Fe^{3+}, Co^{2+}, Ni^{2+} and Cu^{2+}, provides a system where the pocket about the metal ion is not as hindered as in the usual porphyrin models for cytochrome P450, and is also highly oxidation resistant [109]. The catalytic power of these complexes for alkene epoxidation and for aliphatic and aromatic hydroxylations was investigated, and it was found that the manganese(III) compound was the best catalyst, with nickel(II) and copper(II) showing virtually no activity [108]. Naturally, the iron centre is hardly in a model environment, being coordinated by oxide ligands.

2.4.2.2 Cytochrome b models

The interaction of imidazole ligands with the sterically hindered porphyrin derivative (perchlorato)(tetrakis(2,6-dichlorophenyl)porphinato)iron(III)), [Fe(T2,6Cl_2PP)($OClO_3$)], was investigated [243]. Such compounds model the bonding situation in cytochrome *b*, where the binding of axial ligands appears to modulate the spin state of the iron(III) centre, with all three possible values having been observed. It was found that the eight chloro groups did not hinder the binding of the axial ligands. The structure of the bis(1-vinylimidazole)iron(III) derivative, [Fe(T2,6Cl_2PP)(1-VinIm)$_2$]ClO_4, was determined by X-ray diffraction. The six-coordinate low spin complex has an unusual EPR spectrum at 7 K in the solid state, with both a rhombic and large *g* value being present, arising from the two different imidazole orientations observed in the crystal structure. The frozen solution spectrum shows only the rhombic signal.

The porphyrin complexes [Fe(TMP)(4-NMe_2py)$_2$](ClO_4).2C_6H_5Cl, [Fe(OEP)(4-NMe_2py)$_2$](ClO_4).CH_2Cl_2 and [Fe(TMP)(1-MeIm)$_2$](ClO_4), have been crystallographically characterised [244]. In the [Fe(TMP)(4-NMe_2py)$_2$]$^+$ complex the axial pyridine ligands have their aromatic rings bound perpendicularly, giving the configuration which is thought to be responsible for the occurrence of the large *g* value observed in certain native cytochrome *b* systems. This also leads to a ruffling of the porphyrin core. The EPR spectrum of the complex displays a feature at $g = 3.48$, consistent with this theory. The other two complexes have their axial ligands in a parallel orientation and act as controls, showing no high *g* feature and an almost planar porphyrin core. The preparation and X-ray crystal structure of bis(3-cyanopyridine)(octaethylporphinato)iron(III) perchlorate has been reported by the same group [245], and shows the axial pyridine ligands to be coordinated almost perpendicular to each other. The EPR spectrum has *g* values at 4.28 and 1.97, consistent with this configuration. The compound is either an example of a stabilised $S = 3/2$ complex, or else a complex in thermal spin equilibrium, as indicated by its magnetic properties, with the EPR spectral parameters suggesting that it is more likely to be a spin equilibrium system.

The paramagnetic $[Fe^{III}(TMP)(2\text{-MeImH})_2]^+$ complex has been studied using NOESY experiments [246]. The spectra can be understood in terms of a model with rotating axial ligands but no ligand exchange, as might be expected in view of the "cavity" structure of the iron-porphyrin complex.

The sterically hindered ligand 2-methylbenzimidazole was found to bind high spin *meso*-tetraarylporphinato iron(III) chloride compounds to give bis ligand complexes if the *meso* aryl groups carry alkyl groups at the 2,6-positions [115]. The spin states of the compounds show some evidence for $S = {}^1/_2$, $S = {}^3/_2$ admixing from the EPR spectra.

The rate of rotation of the 2-MeIm ligand in $[Fe(TMP)(2\text{-MeIm})(L)]^+$ has been studied by ^2H NMR spectroscopy and found to increase for less sterically hindered L, probably as a result of decreased interaction between L and the porphyrin [247].

2.4.2.3 Cytochrome c and c' models

The synthesis and characterisation by NMR spectroscopy of the first porphyrin-cyclam dinucleating ligand and its iron(III)/copper(II) complex have been reported [248]. The complex attempts to model the situation in cytochrome *c* oxidase where a haem iron and a copper centre interact to catalyse the reduction of dioxygen to water.

Stereoselective electron transfer reactions between ferrocytochrome *c* and cobalt(III) complexes have been studied. The results have been interpreted in terms of the degree of incorporation of the ligands of the cobalt(III) centre into a hydrophobic crevice of the protein [249].

The stability of iron(III) and iron(II) haem undecapeptides encapsulated in aqueous detergent micelles has been investigated [250]. Such haem peptides are the result of the enzymatic degradation of cytochrome *c*.

Five- and six-coordinate ferric octaethylporphyrin complexes, [Fe(OEP)X], X= ClO_4, $SO_3CF_3^{3-}$, SbF_6^- and $[Fe(OEP)(3,5\text{-}Cl_2py)_2]^+$, which were previously reported to display admixed intermediate-spin behaviour, have been studied using NMR, EPR and MCD spectroscopies to assess their suitability as models for cytochrome *c'* [251]. In particular, the MCD spectra allow the intermediate, high and low spin states to be distinguished and reveal from comparisons with data on the protein that it probably has an intermediate, ${}^5/_2$, ${}^3/_2$ ground spin state.

2.4.3 Haemoglobin and related models

The synthesis of and oxygenation studies on haemoprotein models have been reviewed [252].

The synthesis and characterisation of double-sided porphyrinatoiron(II) complexes have been described [253]. These have pockets of different sizes on each side of the porphyrin ring. Four-coordinate complexes can be produced, as well as five-coordinate monosubstituted imidazole complexes, which are capable of binding dioxygen reversibly. The oxygen affinity for the iron(II) complexes increases as the steric bulk on the rear side of the porphyrin is decreased. The changes in oxygen affinity were ascribed to the strength of the π-electron donation from the imidazole to the iron centre.

The kinetics of the binding of O_2 and CO to double-sided iron(II) porphyrin complexes indicate that the affinity is affected by steric repulsions between the axial imidazole ligand and the ester groups inside the pocket as well as the polarity within the oxygen- or carbon-monoxide-binding cavity [254]. Further spectroscopic studies also suggest that the π-back-donation from the $d\pi$ orbital of the iron atom to the π^* orbital of the bound gaseous ligand is controlled by the strength of the iron-imidazole bond, which, in turn, is influenced by the structure of the rear pocket of the porphyrin ligand [255].

Complementary Mössbauer and spectrophotometric ligand titration studies were performed to monitor the interaction with protoporphyrin IX iron(II) with a series of aliphatic amino ligands [256]. Both methods indicated that low spin octahedral complexes were formed. All except ethanolamine displayed cooperative binding, but with approximately 1000-fold less affinity for the iron(II) than the previously studied pyridine and imidazole ligands.

Solid-state ^{17}O NMR spectroscopy was used to study the picket-fence porphyrin model for oxyhaemoglobin and oxymyoglobin, [Fe^{II}(TPivPP)(1-MeIm)(O_2)] and the results compared to those obtained on the proteins themselves [257]. The model compares well with the native systems, and the results are consistent with a predominantly spin-paired configuration in all three systems.

Resonance Raman studies using $^{16}O_2$ and $^{18}O_2$ and scrambled dioxygen adducts of Fe(TPP), Fe(TPP-d_8), Fe(TMP), Fe(OEP) and Fe(TPFPP) allowed the two isomers with side-on and end-on dioxygen binding to be identified [258]. Furthermore, two oxoferryl species were found to form as a result of homolytic cleavage of the dioxygen bond using laser irradiation. Both the radical and non-radical species were observed.

The carbon monoxide adduct of a capped porphyrin [Fe(C_2-cap)(CO)(1-methylimidazole)] has been synthesised and structurally characterised by X-ray crystallography [259]. This is the first such structure where the CO is bound inside the cap. The Fe-C-O system is only slightly displaced from linearity. The results add to the information regarding O_2/CO discrimination in such systems.

Spectrophotometry was used to determine binding constants for the coordination of cyanide ions by haemin in ethanol [260]. Two ligands were found to coordinate with no evidence for an intermediate mono-ligated species.

2.4.4 Models relevant to nitrite and nitrate reductases

The [Fe(porphyrin)(NO)] species with porphyrinH_2 = $TPPH_2$, $TPCH_2$ and $OEPH_2$ have been studied using electrochemistry and electronic and vibrational spectroscopies [261]. It was found that the complexes were reduced in three one-electron steps and the products of the first two waves, as detected by Optically Transparent Thin-Layer Electrochemistry, were assigned as [Fe(porphyrin)(NO)]$^-$ and [Fe(porphyrin)(NO)]$^{2-}$ species. The complexes were assigned as low spin ferrous species and the bonding situation in the complexes is discussed.

Five- and six-coordinate nitrosyl complexes of a series of tetrakis(4-substituted phenyl)porphyrins have been prepared in order to gauge the *cis*-effect of substituents on the axial nitrosyl ligand from EPR and IR spectroscopic analysis [262]. It was concluded that as the electron-withdrawing power of the porphyrin peripheral substituent is enhanced, the iron-to-NO

bond in both the five- and six-coordinate species is weakened and the iron-to-nitrogenous base bond in the six-coordinate complexes is strengthened.

A model for *N*-bound nitrite reductase is provided by the complex $[Fe(TPivPP)(NO_2)]^-$ which was characterised by X-ray crystallography [263]. The iron is in assigned a ferrous low spin state, as indicated by the Mössbauer spectrum, although the value of the quadrupole splitting is rather large, at 2.28 mm s^{-1}, which is comparable to that for oxyhaem compounds, and unique for low spin ferrous iron. It is unlikely, however, that an $[Fe(III)\text{-}NO_2]^{2-}$ formulation is a better description of the electronic structure. The bis(nitro)iron(III) complex has also been investigated [264]. Its reactions with pyridine and imidazole produce mixed ligand complexes, $[Fe(TPivPP)(NO_2)(L)]$, with the *N*-bonded nitrite ligand sitting in the pocket formed by the pickets of the porphyrin and the ligand coordinated to the open face, as revealed by X-ray crystallography. UV-VIS, IR, NMR, EPR, and Mössbauer spectroscopic data are reported, and are consistent with the structural data and the presence of low-spin iron(III) in a rhombic environment.

The photochemistry of a new nitrate iron porphyrin complex, $[Fe(TPP)(NO_3)]$, as well as of $[Mn(TPP)(NO_3)]$ and $[Mn(TPP)(NO_2)]$, has been studied [265]. The iron nitrite complex was not stable. Irradiation produces substrate oxidation, including CH hydroxylation suggesting $O{=}Fe^{IV}(TPP^{+\bullet})$ as the active oxidant, similar to the situation in cytochrome P450.

2.4.5 Other iron porphyrin complexes

The demetallation of a series of (5,10,15,20-tetraphenylporphyrinato)iron(III) complexes with bulky substituents on the 2-positions of the phenyl rings was studied using NMR spectroscopy and spectrophotometry in order to gain insights into the mechanism of metalloporphyrin complexation in Nature [266]. The reaction occurred simultaneously with the reduction of the iron.

The pyrolytic reactions of azidoiron(III) (and azidochromium(III)) tetraphenylporphyrin have been studied in the solid state [267]. The reaction of the ferric system resulted in the liberation of nitrogen gas and the formation of the iron(II) porphyrin.

The spectroscopy and electrochemistry of the sulfate bridged iron(III) complexes $[Fe(TPP)]_2SO_4$ and $[Fe(OEP)]_2SO_4$ have been studied. [268]. It was found that the dimers dissociate in non-coordinating solvents to yield easily reducible mononuclear species.

Monomeric aqua and hydroxo complexes of $[Fe^{III}(OEP)]^+$ in aqueous sodium dodecyl sulfate (sds) detergent micellar solutions have been studied using NMR and optical spectroscopies [269]. The micelles model the hydrophobic protein pocket interactions with the haem moiety in native haemoproteins.

Low temperature MCD and EPR spectroscopic studies have been performed on the low spin Fe(III) porphyrin complexes, $[Fe(OEP)(tht)_2]^+$, $[Fe(OEP)(ImH)_2]^+$ and $[Fe(TPP)(ImH)_2]^+$ [270]. These provide well-defined iron(III) porphyrin models for axial ligand interactions in haemoproteins. It was found that the EPR and MCD spectra of $[Fe(OEP)(tht)_2]^+$ are similar to the spectra of the haem group in bacterioferritin, providing extra support for the suggestion of the unusual bis(methionine) coordination of the haem in this protein.

Two dimensional COSY experiments on a number of paramagnetic iron complexes of porphyrins and chlorins have been reported [271]. In spite of the fact that cross peak resonances for such compounds are diminished because of relaxation and antiphase cancellation effects, it was possible to interpret the spectra for high spin ferrous complexes of *N*-methylporphyrins in terms of a spin density distribution which is as asymmetric within a pyrrole as it is between non-equivalent pyrroles.

Metalloporphyrin complexes can act as lattice clathrates, trapping solvent and other small molecules within their crystal structures. The structures of over 100 of these so-called porphyrin sponges have been considered and data on 34 new materials presented [272]. A further example of such a sponge is provided by the five-coordinate compound [Fe(III)(TPP)(SPh)] [273]. The crystal structure analysis shows that there are channels in which the solvent molecules reside. The resolution of twinning problems and disorder is also discussed.

2.4.6 Other N_4-macrocyclic complexes

The proton NMR spectra of high spin iron(III) isobacteriochlorins were studied as models for the high spin sirohaem active site in the resting state of *E. coli* sulfite reductase and spinach nitrite reductase [274]. It was possible to use the data to assign the complexes as five- or six-coordinate, a feature which should assist in the interpretation of data from the native systems.

The complex [Fe(pc)(NO_2)(py)] has been isolated as a stable crystalline material (in addition to two similar coablt(III) complexes) and it molecular and electronic structure investigated, indicating it to be a six-coordinate low-spin iron(III) species [275]. The corresponding five-coordinate species [Fe(pc)(NO)] was also studied and the dioxygen activation and oxygen transfer reactions, which were found to be catalytic and selective, of the systems investigated.

The reaction of [Fe(pc)Cl] in water containing pyridine was followed using spectrophotometry and conductometry [276]. Amongst the compounds suggested as forming, is a hydroxo species which easily dimerises to an oxo-bridged dinuclear complex, which in turn disproportionates to give [Fe^{II}(pc)$(py)_2$] and [Fe^{IV}O(pc)(py)].

A range of substituted (1,2-naphthalocyaninato) iron compounds with bis-axially coordinated isocyanide ligands has been synthesised [277].

The rarely studied *meso*-octamethyl porphyrinogen tetraanion was found to bind iron(III) ions to give a square planar environment around the metal centre, as revealed in a single crystal X-ray diffraction study [278].

The reactivity of the corrole/iron(III) complex (2,3,7,8,12,13,17,18-octamethylcorrolato)-iron(III) towards axial ligands such as pyridine, chloride and isocyanide was studied using ^{1}H NMR and optical spectroscopies [279]. The unsubstituted complex has an S = $^1/_2$ ground spin-state, whereas the pyridine adduct appears to have a mixed-spin ground state. This adds useful information to the rather small body of information on the metal complexes of these tetrapyrrolic ligands.

2.5 *IRON SULFUR COMPOUNDS AND CLUSTERS AND THEIR SELENIUM ANALOGUES*

2.5.1 *Mononuclear iron sulfur compounds.*

The continued interest in modelling mononuclear Fe/S sites found in biological systems has led to the characterisation of increasingly relevant coordination compounds. The site of the electron transfer protein, rubredoxin, has been modelled in its reduced (iron(II)) state by reacting $[Fe(II)(S\text{-}t\text{-}Bu)_4]^{2-}$ with the protected polypeptide Z-cys(SH)-pro-leu-cys(SH)-gly-NH-C_6H_4-4-X to yield $[Fe(II)(Z\text{-cys(SH)-pro-leu-cys(SH)-gly-NH-}C_6H_4\text{-4-X})]^{2-}$, where X = MeO, H, F, and CN [280]. This effort forms part of a continuing study by these workers on iron(II)/peptide complexes, aimed, in part, at elucidating the rôle played by the peptide chain in controlling redox potential. These new complexes gave positively shifted redox potentials compared with other previously reported peptide complexes. The most positively shifted potential was observed for the complex with X = CN in dmc, the complex with the most strongly electron-withdrawing *para*-substituent, and the strongest NH---S hydrogen bonds as detected by contact-shifted N-H---S-Fe resonances in the ^2H NMR spectrum.

The simpler thiolate models for rubredoxin all fail to reproduce the positive redox potentials observed for the native systems, but do have the advantage of being easily accessible to structural characterisation by X-ray crystallography and providing single crystals for spectroscopic studies, such as the low-temperature single crystal magnetic circular dichroism (MCD) and polarised absorption studies performed on $(Et_4N)_2[Fe(S\text{-}2\text{-}(Ph)\text{-}C_6H_4)]$ [281]. The analysis of the spectra for this iron(II) complex reveals that the iron is high spin and in an axial environment. It was possible to assign the $^5E \rightarrow {}^5T_2$ and $^5E \rightarrow {}^3T$ transitions to give $D_q = -350\ cm^{-1}$, $C = 2800\ cm^{-1}$ and $B = 620\ cm^{-1}$. A comparison with previously studied iron(III) thiolate complexes reveals that these exhibit much larger reductions than the 70% reduction for the iron(II) case from the free ion values for electron repulsion. It was concluded that the inverted bonding description invoked for the iron(III) complexes was not valid here. A calculation of the ground state zero-field splitting based on spin-orbit coupling to the $^5T_2$ and ^3T ligand field excited states led to a calculated value of D of $-8.7\ cm^{-1}$ which is in excellent agreement with the experimental value of D of $-8.7 \pm 0.7\ cm^{-1}$ derived from the temperature dependence of the MCD spectra reported here. The splitting of the iron(II) 3*d* orbitals is suggested to depend on the interactions with the S-Feσ bonding orbital as dictated by the αC orientation of the thiolate. This effect would account for the differences in the spectra of the model complex and ferrous rubredoxin, although it should also be recognised that MCD bands have proved hard to observe in native ferrous rubredoxin.

In a series of iron complexes with dithiolate-derived ligands, Sellmann and coworkers have been trying to elucidate the possible features of importance in oxidoreductases. Many of these contain exclusively iron and there is some evidence to suggest that the metal can exist in monomeric sites. Other examples are known with metals other than iron, such as nickel. One important and much disputed feature of these systems is whether the dithiolate ligand is actually a dithiolene ligand, which in turn brings the oxidation state of the metal into question as indicated in scheme

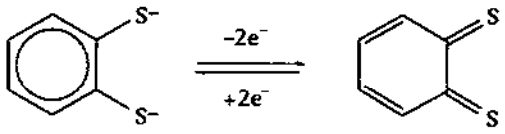

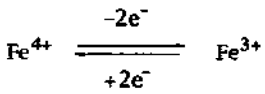

(48)

(48). This has been explored in detail *via* single crystal structure determinations for three iron complexes with the 1,2-benzenedithiolate ligand [282], two of which are concluded to consist of dithiolate complexes rather than dithiolenes, with the iron in the +4 oxidation state; these complexes are $[Fe(C_6H_4S_2)_2(PMe_3)_2]$ and $[Fe(C_6H_4S_2)_2(PMe_3)]$. The third complex is a related iron(III) dithiolate produced by reacting $FeCl_2.4H_2O$ with the ligand and excess phosphine in the presence of oxygen to give $[Fe(C_6H_4S_2)_2(PMe_3)_2]^-$, which had its structure determined as the tetramethylammonium salt. All three structures consist of strictly monomeric iron sites which are either five- or six-coordinate, depending on the number of phosphine ligands in the complexes. The assignment of these compounds as dithiolate species was made on the basis of the bond lengths of the ligand, (which do not indicate any C-S double bond character), and the Mössbauer spectra, (which have values for isomer shift and quadrupole splitting in accord with the assignments of iron(IV) and iron(III)). In a later paper [283], these workers investigated the interactions of these complexes, in addition to an iron(II) analogue, with H^+, H_2 and H^- in order to gauge their effectiveness as models for the active site in iron hydrogenases. Dihydrogen evolution was observed when $FeCl_2$, the dithiolate ligand and a protic acid were combined in methanol *via* the formation of the iron(II) species $[Fe(C_6H_4S_2)_2]^{2-}$ which yields the iron(III) species $[\{Fe(C_6H_4S_2)_2\}_2]^{2-}$ on addition of the acid. This reaction was followed using ^1H NMR spectroscopy and could be rationalised in terms of a reaction scheme involving two protonation steps of the iron(II) species. The fact that the iron(II) centre, in an environment of thiolate donors, is able to reduce protons so easily is accounted for by the increased electron density on the metal giving rise to a very negative Fe(II)/Fe(III) couple (–0.99 V *vs.* NHE). Although the reaction is an attractive model for hydrogenase activity in native systems, it is not catalytic, and the question as to the likely degree of aggregation of iron centres in such systems (if any) is still open.

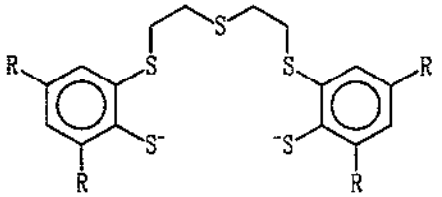

(49) R = *t*-butyl; L^{2-} = $^{t\text{bu}}S_5'^{2-}$; R = H; L^{2-} = $'S_5'^{2-}$

A related ligand system L^{2-} = (49), derived from the coupling of two dithiolate moieties by a thioether bridge, provides a pentadentate chelate and has been used to produce iron(II) complexes capable of coordinating σ–π ligands such as CO, NO, NO^+, and $P(OPh)_3$ [284], but not σ-ligands, unlike the iron(II) complexes reported for the parent ligand, L^{2-}, where R = H. The synthesis of [Fe(CO)L] yielded two stereoisomers, one with the sulfur donor atoms of the thiolates linked by the thioether *cis* to each other, and the other with them *trans*. These were easily separated owing to their different solubilities in organic solvents such as toluene, thf and CH_2Cl_2. The *cis* isomer of the NO adduct was subject to further investigation [285]. This 19-electron compound readily undergoes substitution of the nitrosyl by CO at ambient temperatures. The ease of substitution is probably a consequence of the 19th electron being delocalised over the whole molecule, and occupying an orbital which is antibonding with respect to the Fe-N and Fe-S bonds, as indicated by EPR spectroscopic studies. In contrast, the iron(III) analogue is substitutionally inert. It is suggested that the iron(II) compound provides a good model for reversible NO binding of sulfur-coordinated metal centres in nitrogenases.

The dithioether linked analogue of this ligand (50) provides a hexadentate crown thioether system. The reaction of the ligand with divalent metals (iron, cobalt, nickel, and copper) has been reported [286] and the structure of a nickel complex determined. It is likely that the iron(II) species is octahedrally coordinated by the ligand in an analogous fashion to the nickel(II) complex.

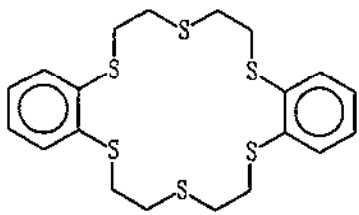

(50)

The coordination of iron(III) in the enzyme nitrile hydratase, which catalyses the hydration of nitriles to amides, from *Brevibacterium sp.*, has been investigated using resonance Raman and EXAFS spectroscopies [287]. The results can be interpreted in terms of a six-coordinate low spin iron(III) site with mixed sulfur and nitrogen or oxygen ligands, which provides an interesting synthetic challenge to chemists seeking to model this site.

2.5.2 Iron sulfur clusters

2.5.2.1 Dinuclear iron sulfur compounds

Plant type ferredoxins possess $[Fe_2S_2(S\text{-cys})_4]^{2-}$ cores with redox potentials in the range from –0.23 to –0.42 V *vs.* NHE. The model compound $(NEt_4)_2[Fe_2S_2(SC_6H_2Me_3\text{-}2,4,6)_4]$ has been synthesised and its structure determined using X-ray crystallography [288]. The steric bulk of the thiolate ligands causes the compound to adopt a restrictedly eclipsed configuration rather than the more stable staggered form.

As Power and Shoner point out in their article describing the preparation of the dimeric neutral metal thiolates, $[M(S\text{-}2,4,6\text{-}t\text{-}Bu_3C_6H_2)_2]_2$ (M = Mn, Co, or Fe), most transition metal thiolate complexes tend to be ionic, a feature which helps to prevent the formation of intractable polymeric species [289]. Although other open-shell transition metal thiolates are known, these complexes are the first well-characterised examples of low coordination number (three) neutral thiolate complexes. The single crystal X-ray structures are reported for all three compounds.

2.5.2.2 Three iron and site-differentiated four iron sulfur clusters

Most of the other work reported on iron/sulfur clusters addresses questions relating to the reactivity of the iron/sulfur cores. An area of particular interest is the reactions of $[Fe_4S_4]$ cores where one of the iron centres is labile. This is relevant to the situation recognised in an increasing number of non-redox $[Fe_4S_4]$ enzymes, such as aconitase, some dehydratases, and an amidotransferase. Holm and coworkers have extended their work on subsite differentiated cubane-type clusters and describe the ligand substitution reactions of the differentiated clusters of type (**51**). The reactions of the clusters with L = Cl and L = OC_6H_4-*p*-Br with a variety of biological and abiological ligands were monitored by NMR spectroscopic methods [290]. A set of 30 clusters of the general type (**51**) resulted from the substitution of L by these ligands. The most relevant clusters produced in terms of modelling biological sites, were those with L = O_2Me, OMe, SR, or OPh, which mimic amino acid side-chains, and a dicubane oxo-bridged species which could be detected by NMR spectroscopy, and which can be hydrolysed to give two cubane clusters with L = OH. This corresponds to the deprotonated form of the solvated aquo species, thought to be important in aconitase.

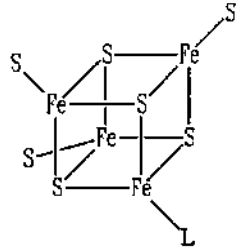

L is defined in the text
(**51**)

The X-ray structure of the protected macrocyclic polyether trithiol which has been used to capture three of the four iron sites in $\{Fe_4S_4\}$-cores, thereby leaving one site differentiated and able to undergo substitution reactions with various ligands, has also been reported [291]. The paper also describes some of the reactions of the differentiated cluster as monitored by NMR spectroscopy and comparisons are made with the other subsite differentiated clusters described above. It is concluded that both ligand systems afford a suitable simulation of the coordination in native $\{Fe_4S_4(S\text{-cys})_3\}$-clusters such as are known to exist from protein crystallography on aconitase, and, further, that neither of the tridentate ligands imposes a highly specific environment on the $\{Fe_4S_4\}$-core as evidenced by the similar reactivities of both systems.

The cluster type (**51**) was used as a basis for modelling the known bonding situation (from protein crystallography) in the site-specific cluster in the assimilatory sulfite reductase from *E. coli*, *Ec* SiR [292]. This contains a covalently bridged, magnetically coupled sirohaem assembly, with the cubane iron and sirohaem probably bridged by a cysteinyl sulfur atom (although this cannot be seen in the protein structure) as indicated in scheme (**52**). As a first step, attempts were made to produce an Fe_4S_4-Fe complex in order to demonstrate the feasibility of the method for producing bridged assemblies. It proved possible to substitute L as an alkylthiolate with pyridine thiols, coordinated *via* their sulfur atoms. These new clusters could then be reacted with the iron(II) complexes [Fe(acen)] and [Fe(tfacen)(MeCN)] to give bridged assemblies as evidenced by changes in the isotropically shifted ^1H NMR spectra of the cluster, bridge and Fe(II) complex portions of the assemblies. As part of the investigation, the binding affinities for the iron(II) complexes for pyridine and the crystal structures of [Fe(tfacen)$(py)_2$] and [Fe(tfacenpy)] were determined. Finally, evidence is also presented for binding of [Fe(II)(OEP)] to the pyridine thiol substituted cluster, which is a step closer to modelling the interaction of sirohaem moieties with Fe_4S_4 clusters such as found in native systems. In systems such as aconitase, the site differentiated iron is often also labile and can be removed as iron(II) from the cluster to give a "voided" cubane with an $\{Fe_3S_4\}$-core. The difficulties in achieving this in model systems, such as the site differentiated clusters of Holm *et al.* cited above, might stem from the problems of charge separation from anionic cluster species. In an attempt to circumvent this problem, Pohl and coworkers have explored ways of preparing neutral clusters [293]. The preparation of a mixed ligand neutral four iron sulfur cluster was achieved by first preparing [Fe$(SR)_2L_2$].PhMe from [FeI_2L_2] and KSR (R = 2,4,6-*i*-$Pr_3C_6H_2$ and L = $SC(NMe_2)_2$). This was then reacted with elemental sulfur to afford the cluster [$Fe_4S_4(SR)_2L_2$] where pairs of irons are coordinated by the two different *S*-donors (L and SR). The crystal structures of both of these compounds were determined. The thiolate ligands of these compounds can be oxidised with $[(Me_2N)_2CSSC(Me_2N)_2]^{2+}$ to afford cationic species such as $[Fe(SR)L_3]^+$ and $[FeL_4]^{2+}$ from the monomer and possibly also the cationic cluster species $[Fe_4S_4(SR)L_3]^+$ and $[Fe_4S_4L_4]^{2+}$ from the cluster.

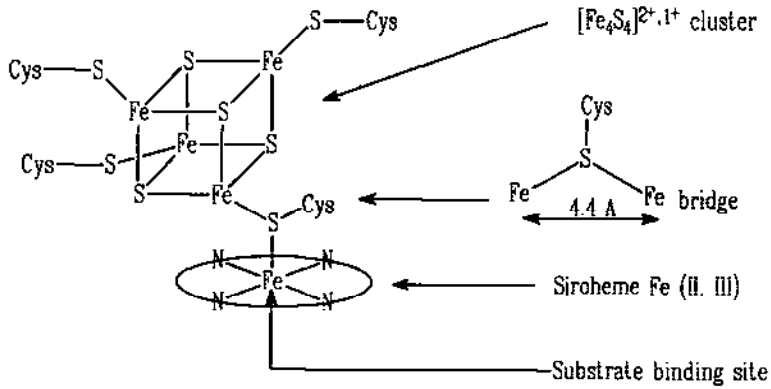

(**52**)

A similar approach was used by these workers in the synthesis of the mixed ligand clusters $[FeIL_3][Fe_4S_4I_3L]$ and $[Fe_4S_4I_2L'_2]$, where L is as before and L' = $(C_4H_9NH)_2CS$ from $[FeI_2L_2]$, $Fe(CO)_5$ and elemental sulfur [294]. The structures were confirmed by single crystal X-ray diffraction. The synthesis of $[Fe_4S_4I_3L]^-$ offers an alternative means to that of Holm *et al.* of producing four-iron sulfur clusters with one differentiated site. Such clusters are recognised as being the precursors to voided cubane clusters, although as yet, no definitive proof has been found for the formation of such species in the model work.

Experiments performed *in vitro* on the reactivity of the reduced $[Fe_3S_4]^0$ cluster in 7 Fe ferredoxin III from *Desulfovibrio africanus* show that divalent metal ions such as zinc(II), cobalt(II) and iron(II) interact rapidly to give $[MFe_3S_4]^{2+}$ clusters [295]. In addition, thallium(I) will react with both the reduced and oxidised forms to give $[TlFe_3S_4]^+$ and $[TlFe_3S_4]^{2+}$, respectively [296].

The recognition that voided cubanes can incorporate other metal centres has been used as a starting point for the synthesis of mixed metal cubane clusters which might model the biological reactions. The approach used by Ciurli and Holm still relied on the 'self-assembly' route of synthesis in order to prepare rhenium/iron/sulfur clusters [297]. In this way, the previously reported iron bridged $[Re_2Fe_7S_8(SEt)_{12}]^{2-}$ cluster was prepared from $[ReS_4]^-$, $FeCl_2$ and NaSEt in MeOH. When this is treated with dmpe in acetonitrile the single cubane cluster $[ReFe_3S_4(SEt)_4(dmpe)]^-$ can be isolated in high yield as the tetraethylammonium salt. The structure of this (**53**) was determined by X-ray diffraction and reveals that the rhenium atom is coordinated not only by a thiolate ligand, but also by the dmpe chelate to give octahedral coordination, rather than the tetrahedral coordination observed for the iron centres. This reaction involves the reduction by thiolate of the core state from $[ReFe_3S_4]^{4+}$ to $[ReFe_3S_4]^{3+}$. The cluster undergoes two electrochemically reversible processes in acetonitrile solution corresponding to the series $[ReFe_3S_4]^{2+,3+,4+}$. The magnetic properties of the new cluster were investigated and an S = 2 ground state was established, with a mean oxidation state of $Fe^{2.5+}$ suggested on the basis of the Mössbauer spectroscopy.

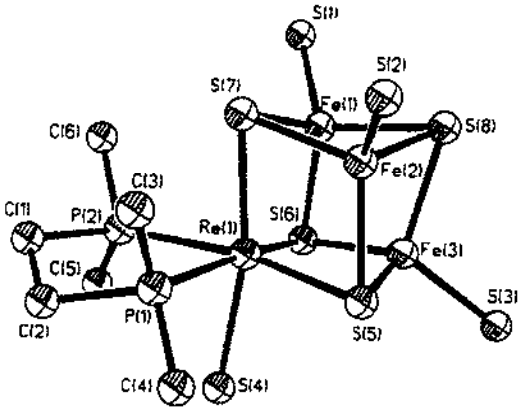

(53)

In addition, $[Fe_3CoS_4(SC_6H_2Pr^i_3\text{-}2,4,6)_4]^{2-}$ can be prepared by reacting either the four or linear three iron cluster with $CoCl_2$, and was shown to have formal oxidation states of Fe^{2+}, $2Fe^{3+}$ and Co^{2+} and $S = {}^1/_2$ from EPR and Mössbauer spectroscopies, magnetic susceptibility and cyclovoltammetry [298]. Presumably the reaction starting from the four iron cluster proceeds *via* the three iron form.

2.5.2.3 Four iron sulfur "cubane" clusters

The now 'classic' $[Fe_4S_4(SR)_4]^{n-}$ system is still subject to investigation by groups wishing to elucidate the factors important in influencing the properties of the synthetic models in order to reproduce those observed in native systems. A detailed study on the structure of the ferredoxin model $[Fe_4S_4(SPh)_4]^{2-}$ as the tetrabutylammonium salt has been performed [299]. The results of the X-ray structure determination of the cluster at 233 K are compared with previously reported results from the room temperature structure. The compound is known to undergo a phase transition at 243 K. It is concluded that the origin of the phase transition is a result of the increase in disorder of the butyl groups in the counterion, although small changes in the geometry of the iron-sulfur core could be detected.

A new tetradentate thiolate ligand has been developed to encapsulate $\{Fe_4S_4\}$ cores as 1:1 compounds by reaction with $[Fe_4S_4Cl_4]^{2-}$ [300].

The redox behaviour of Fe_4S_4-systems is of importance in assessing their suitability as model compounds. One factor often ignored is the solvent effect in these measurements. In the native systems, the redox processes happen in an aqueous environment, and this aspect has been investigated for the $[Fe_4S_4(SC_6H_4\text{-}t\text{-}Bu\text{-}p)_4]^{2-/3-}$ couple in hydrophobic and hydrophilic environments [301]. The $E_{1/2}$ value of the cluster in a CH_2Cl_2/H_2O two phase system as a near monomolecular layer on the electrode (produced by the addition of Triton X-100 to give a micellar solution) exhibits a pronounced anodic shift compared with that in CH_2Cl_2 and falls in the range of that in 4Fe and 8Fe ferredoxins. This is in agreement with the suggestion that it is the tertiary structure of the protein which provides a hydrophobic pocket and shifts the redox potential of the Fe/S clusters to such positive potentials, rather than the direct influence of the ligands themselves.

The effect of basicity of solvent in stabilising the high oxidation state 4Fe cores found in the HiPIP proteins was investigated on model $[Fe_4S_4(SR)_4]^{-}$ systems [302]. It was concluded from an examination of the electrochemical behaviour of the species with R = Ph, *t*-Bu that the stability of the cluster species is determined by the basicity rather than the polarity of the solvent and that this effect is reduced as R becomes more bulky. It thus seems that a hydrophobic environment and protection from solvent attack (water) are essential for the stabilisation of the Fe/S core in HiPIP proteins.

A potential pSR diagram has been constructed for the interconversion of $[Fe(SR)_4]^{2-}$, $[Fe_2S_2(SR)_4]^{2-}$ and $[Fe_4S_4(SR)_4]^{2-}$ and it appears that the favoured species depends on the thiolate concentration [303].

The catalytic oxidation of benzoin to benzil by *p*-benzoquinone in the presence of $\{Fe_4S_4\}$ complexes with thiolate and peptide ligands was studied [304]. The reaction in the presence of $(PPh_4)_2[Fe_4S_4(2,4,6\text{-triisopropylbenzenethiolate})]$ obeys first order kinetics. The rate constant was

found to depend on the bulkiness of the thiolate or peptide ligand. It was concluded that the methine hydrogen of benzoin is released as a proton in the rate determining step, as indicated by the observation of an isotope effect (k_H/k_D 2.5:1) on the oxidation rate of *α-C*-deuteriated benzoin. The catalytic hydrolysis of aryl esters by the iron sulfur cluster $[Fe_4S_4(SC_6H_5)_4]^{2-}$ has been investigated [305]. It was found that the cluster catalysed the hydrolysis of the esters and proposed that the role of the iron sulfur cluster in the enzyme aconitase is to provide a nucleophilic centre.

Perhaps the most exciting development in the area of Fe_4S_4 chemistry was the report of a totally synthetic 2[4Fe-4S] clostridal ferredoxin [306]. This was achieved by synthesising a 55 amino acid sequence peptide corresponding to that of *Clostridium pasteurianum* Fd using methods based on the Merrifield synthesis. The sequence homology was proved by elution of the synthetic and native apoproteins to identical positions on high resolution PAGE gels. A modification of the known method for reconstituting Fe/S clusters in apoproteins was used, with $FeCl_3$ and Na_2S in excess and incubated with the synthetic protein for 3 hours. Comparisons of the EPR, visible and CD spectra for the synthetic and native proteins all show good agreement. The reduction potential for both is –400 mV *vs.* NHE at pH 8. Although other peptide systems which ligate Fe/S clusters have been reported, these all suffer from having rather short peptide chains. This new example should give insights into the influence of the peptide chain folding on properties and also provides a complementary method to site directed mutagenesis.

2.5.2.4 Mixed metal, other four iron and higher nuclearity clusters

The mixed metal cubane cluster formed in the reactions of the highly unstable $[Mo_3S_4(H_2O)_9]^{4+}$ species which have been previously reported to yield $[MMo_3S_4(H_2O)_{10}]^{4+}$ for a variety of divalent metals, M, such as iron has been reported. From electronic spectroscopic investigations, it appears that M can be substituted by other di- and trivalent metals [307].

Another mixed metal cluster which has been reported was prepared by the reaction of $[Fe_6S_6I_6]^{2-}$ with $[NiI_4]^{2-}$ to produce $[Fe_3Ni_5S_6I_8]^{4-}$ (54) which was characterised by X-ray diffraction [308].

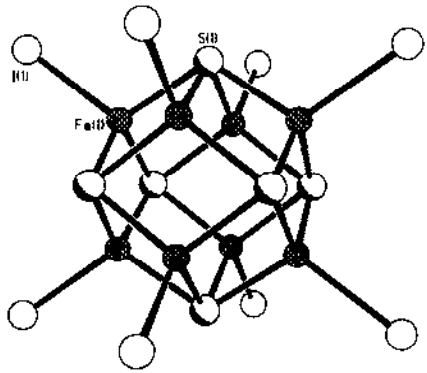

(54)

The three cluster anions $[MoFe_6S_6(CO)_{16}]^{2-}$, $[MoFe_4S_3(CO)_{13}(PEt_3)]^{2-}$, and $[Mo_2Fe_2S_2(CO)_{12}]^{2-}$ were synthesised with the structures of the first two determined in single crystal diffraction studies [309]. In $[MoFe_6S_6(CO)_{16}]^{2-}$ the Mo-Fe distance distribution is reported to approximate that found in the FeMo-cofactor of nitrogenase, but whether this will need re-examining in the light of the protein crystal structure is open to question.

The synthesis and properties of a range of cluster salts of the form $[C]^+[A]^-$ containing metal sulfide and selenide cubane type cores and including the iron compounds with C = $Fe_4(Cp)_4(S)_4$, $Fe_4(\eta^5\text{-}C_5H_4Me)_4(S)_4$, and A = $Fe_4(NO)_4(S)_4$, (both characterised crystallographically), as well as the $[C]^+[tcnq]^-$ salts (the salt with the Fe/Cp cluster was crystallographically characterised) have been reported [310].

A rather different four iron sulfur cluster, $(Et_4N)_4[Fe_4S_6(SEt)_4]$ (**55**), has been synthesised and structurally characterised [311]. This cluster can be prepared by mixing $[Fe(SEt)_4]^{2-}$ and elemental sulfur in acetone, and its formation can be regarded as either the oxidative coupling of $[Fe(SEt)_4]^{2-}$ and $[Fe_3S_4(SEt)_4]^{3-}$, or two $[Fe_2S_2(SEt)_4]^{2-}$ anions by the sulfur. The compound contains a nearly linear arrangement of iron atoms held together as part of an Fe_4S_6 chain which may be representative of soluble fractions of the $(Fe^{III}S_4)_n$ chains present in $KFeS_2$. The Mössbauer data are consistent with the presence of two different iron(III) sites. The cluster undergoes a variety of reactions to produce other known species.

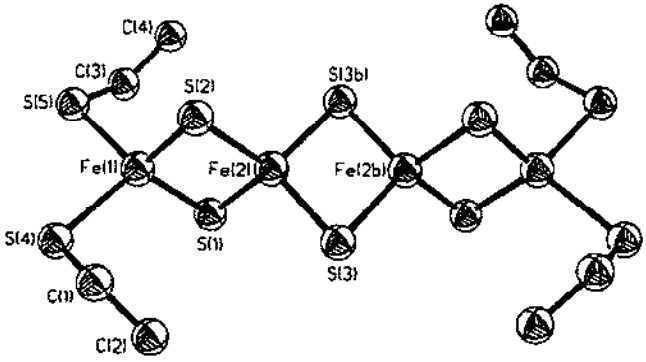

(**55**)

The electronic properties of the so-called monocapped prismane and basket iron-sulfur clusters have been studied using magnetic susceptibility, magnetisation and Mössbauer spectroscopic measurements [312]. Ground states of S = $^1/_2$ were assigned to the clusters $[Fe_7S_6(PEt_3)_4Cl_3]$ (a monocapped prismane) and $[Fe_6S_6(PEt_3)_6]^-$ (a basket) and S = 1 to $[Fe_6S_6(PEt_3)_4Cl_2]$; $[Fe_6S_6(PEt_3)_4Br_2]$; $[Fe_6S_6(PEt_3)_4I_2]$; $[Fe_6S_6(PEt_3)_4(SPh)_2]$; and $[Fe_6Se_6(PEt_3)_4Cl_2]$ (all baskets). The magnetic measurements all indicate antiferromagnetic spin coupling giving rise to the assigned ground states.

2.5.3 Iron selenium analogues

The related Fe/Se compounds and clusters often provide insights into the reactions and properties of the corresponding Fe/S systems, for example, *via* the isotope effect of the selenium in

vibrational and ^{1}H NMR spectroscopic studies. The structure of the $[Fe(SePh)_4]^{2-}$ anion has been determined and it displays the expected tetrahedral coordination [313].

Holm and coworkers report the syntheses and characterisation of a series of seven Fe/Se/SR clusters [314], namely the compounds $(Et_4N)_2[Fe_2Se_2(SEt)_4]$, $(Et_4N)_2[Fe_2Se_2(SPh)_4]$, $(Et_4N)_3[Fe_3Se_4(SEt)_4]$, $(Et_4N)_3[Fe_3Se_4(SPh)_4]$, $(Et_4N)_2[Fe_4Se_4(SEt)_4]$, $(Et_4N)_3[Fe_4Se_4(SEt)_4]$ and $(Et_4N)_4[Fe_6Se_9(SEt)_4]$. The structures of four of these were determined by single crystal X-ray diffraction, and the properties of the clusters compared with their sulfur analogues.

In a similar fashion, the double cubane complexes $[M_2Fe_6Se_8(SEt)_9]^{3-}$, $[M_2Fe_7Se_8(SEt)_{12}]^{3-}$(M = Mo, W) and $[W_2Fe_7Se_8(SEt)_{12}]^{4-}$ have been prepared, and the structure of $[M_2Fe_6Se_8(SEt)_9]^{3-}$, as the Et_4N^+ salt, has been determined [315]. Reaction of $[Mo_2Fe_7Se_8(SEt)_{12}]^{3-}$ with acetyl chloride or arylthiol yields new clusters with substitution of the terminal thiolates. The structure of $[Mo_2Fe_7Se_8(SEt)_6(SC_6H_4Cl)_6]^{3-}$ as the Et_4N^+ salt was determined. The clusters are structurally similar to the sulfur analogues and contain trigonally distorted $MoFe_3Se_4$ subclusters linked through the molybenum atoms.

The high nuclearity $[Na_9Fe_{20}Se_{38}]^{9-}$ **(56)** cluster is formed on reaction of $FeCl_3$ with Na[PhNC(O)Me] and Li_2Se in ethanol [316]. If the Na^+ ions are ignored and regarded simply being encapsulated within the cluster cavity, then the $[Fe_{20}Se_{38}]^{18-}$ core can be viewed as a bicyclic cluster of ellipsoidal shape. It is a mixed valence 18 Fe(III) / 2 Fe(II) system and has dimensions within the nanometre size range, making it important in furthering the understanding of the properties of nanometre sized particles.

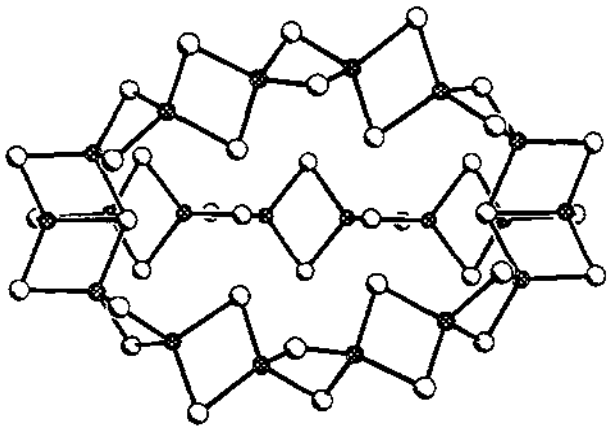

(56)

2.6 IRON IN HIGHER OR MIXED OXIDATION STATES

2.6.1 Compounds of ill-determined oxidation state

Tetraoxolene radicals can be stabilised with transition metal ions, including iron(II) and iron(III), yielding magnetically interacting compounds [317]. Initially compounds with divalent

metal ions of the general formula $[M_2(CTH)_2(DHBQ)]Y_2$, M = Mn, Fe, Ni; CTH = *dl*-5,7,7,12,14,14-hexamethyl-1,4,8,11-tetraazacyclotetradecane; H_2DHBQ = 2,5-dihydroxy-1,4-benzoquinone; Y = ClO_4, PF_6) were formed and assigned dinuclear structures with the $DHBQ^{2-}$ ligand bridging between the two metals on the basis of their spectral and magnetic properties (weak antiferromagnetic coupling). The iron(II) compound can be oxidised to the iron(III) derivative, which demonstrates EPR and Mössbauer spectroscopic data consistent with the presence of a radical species, assigned to a $DHBQ^{3-}$ radical bridge between the metals, and for which the magnetic data can be interpreted in terms of an $S = {}^9/_2$ ground state.

The iron complexes $[CpFe(CO)_2(S\text{-}CH_2\text{-}CH{=}CH_2)]$, and $[CpFe(PPh_3)(CO)(S\text{-}CH_2\text{-}CH{=}CH_2)]$ were obtained from the reaction of lithium or sodium 2-propane-1-thiolate with $CpFe(CO)_2I$ and $CpFe(PPh_3)(CO)I$ respectively [318]. They were characterised by IR and NMR spectroscopy. The iron/cyclopentadienyl derivatives, bis[(1-cinnamoylhydrazonoethyl)-cyclopentadienyl] iron [319] and ferrocenecarbonyl hydrazone [320] were used as ligands for connecting together lanthanoid centres.

The recognition that the reduction of cyclopropenes by metal hydrides has parallels with the reduction by *Klebsiella pneumoniae* prompted the investigation of the reactions of isomeric acetylenes and allenes with $[FeH(H_2)(Me_2PCH_2CH_2PMe_2)_2]^+$ in which compounds representing intermediates in the insertion of alkenes into metal-hydrogen bonds could be isolated and crystallographically characterised [321].

The nitrosyl dimer $[Fe(NO)_2Cl]_2$ reacts with didentate diphosphine ligands to give dinuclear complexes such as $[\{Fe(NO)_2Cl\}_2(\mu\text{-dppe})]$ which was structurally characterised by X-ray crystallography [322]. When excess phosphine is present, the $\{Fe(NO)_2Cl\}$ moiety undergoes halogen displacement to give $\{Fe(NO)_2(P,P')\}$ complexes and also NO substitution to give $\{Fe(NO)Cl(O,P,P,)\}$ where the phosphine has been monooxygenated by the NO.

Heterodinuclear cyanide bridged complexes of the type $[\{Fe(Cp)(dppe)\}\text{-}CN\text{-}\{Mn(CO)_2(L)(L')\}]^+$ have been prepared where L is a didentate ligand such as dppe, dppm, and L' is a monodentate phosphite or phosphane [323]. The oxidation of the compounds was studied electrochemically and the rate of electron transfer across the cyanide bridge was found to depend on the stereochemistry (*cis* or *trans*) of the carbonyl fragments.

Irradiation of $[FeH_2(dmpe)_2]$ in methane in liquid Xe at –100 °C led to the formation of a mixture of *cis* and *trans* isomers of [FeH(dmpe)Me] which decompose with the elimination of CH_4 above 0°C following solvent exchange with toluene [324]

The cleavage of proteins by iron chelates offers a means of mapping sites by the proximity of particular residues [325]. The chelate 1-[4-(bromoacetamido)-benzyl]-edta-Fe was attached to the cys-212 residue of human carbonic anhydrase I, for which there is a high resolution crystal structure, in order to gauge the steric requirements in a structurally characterised system. It was found that the protein was cleaved at one site to produce two discrete fragments in the presence of hydrogen peroxide. Controls run without the chelate proved the specificity of the method, and it was concluded that the cleavage proceeds *via* nucleophilic attack of iron-coordinated peroxo groups at carboxyl carbons of leucine residues.

2.6.2 *Comparative studies on iron(II) and iron(III)*

The electronic structures of iron(II) and iron(III) dimethylglyoximate N_6-complexes, $[Fe(dmg)L_2]^{0/+}$, for L = py, Im, have been studied [326]. A correlation between the Mössbauer spectroscopic data and the electronic configuration was found and it was concluded that the unpaired electron in the iron(III) case is in the d_{xy} orbital with the z axis of the EFG tensor perpendicular to the N_4-dioxime plane, whilst for iron(II) this axis is parallel to the plane.

The structure of $[Fe^{II}Fe^{III}_2(SO_4)_4].2H_2O$ has been determined [327]. It contains both $Fe^{II}O_6$ and $Fe^{III}O_6$ octahedra which share corners with two types of crystallographically different SO_4^{2-} tetrahedra to give a three dimensional framework.

The structure of $Fe_4(PO_4)_3(OH)_3$ contains iron(III) ions filling rows of face-sharing octahedra with a vacancy after every two iron atoms, to give Fe_2O_9 double octahedra connected by OH groups. The inter cluster antiferromagnetic interaction is probably dominant in determining the magnetic properties. Neutron diffraction confirmed the presence of the OH groups as well as showing that the nuclear and magnetic cells are equal [328]. The compound $Fe_3(P_2O_7)_2$ has been prepared and found to contain $[Fe_3O_{12}]^{16-}$ clusters connected by bent P_2O_7 groups ($\angle$P-O-P = 135°) [329]. Anhydrous iron phosphate and oxyphosphate compounds have been reviewed [330]. Several pyrophosphate complexes of divalent metals have been prepared, including $Fe_2P_2O_7$, using chemical transport reactions, with chlorine and NH_4Cl as transport reagents, and, in the case of the iron compound, the trivalent metal orthophosphate [331].

2.6.3 *Complexes stabilising other oxidation states*

The iron(I) mediated dehydrogenation of 1,3-dimethoxypropane in the gas phase using complexes of $CH_3O(CH_2)_nOCH_3$ (n = 2 to 9) has been studied using mass spectrometry [332]. The ligand 2,9-bis(*o*-methoxyphenyl)-1,10-phenanthroline, L, forms the iron(II) complex $[Fe(L)_2]^{2+}$ which can be reduced to stable iron(0) and irone(I) oxidation states electrochemically [333].

Heterodinuclear complexes $[M^{II}(phen)_3][Fe^{IV}(DED)_3]$ containing six-coordinate iron(IV) (or manganese(IV)) and divalent metals M, ($DEDH_2$ = 1,1-dicarboethoxy-2,2-ethylene dithiol) have been prepared [334]. Also, the precursor anion $[Fe^{IV}(DED)_3]^{2-}$ has been isolated. The magnetic moment for this is *ca.* 3.0 BM, suggesting that the iron atom has a low spin configuration.

The compound Sr_2FeO_4 has a K_2NiF_4 structure with the iron(IV) in a distorted octahedral environment [335], and Cs_2FeO_4 is isostructural with β-K_2SO_4 [336].

The oxidation of amino acids by iron(VI) and iron(V) was studied by stopped-flow and pulse radiolysis techniques at pH 12.4 [337]. Both were found to react preferentially with amino acids with protonated-amino groups.

REFERENCES

1. M. McCann, E. Murphy, C. Cardin and M. Convery, *Polyhedron*, 10 (1991) 2771.
2. T. Prüsse and H. Schwarz, *Helv. Chim. Acta*, 74 (1991) 1739.
3. J. Burgess, S.A. Galema and C.D. Hubbard, *Polyhedron*, 10 (1991) 703.
4. M.T. Casey, P. Guinan, A. Canavan, M. McCann, C. Cardin and N.B. Kelly, *Polyhedron*, 10 (1991) 483.

5. V. Haber and P. Ptacek, *Inorg. Chim. Acta*, 180 (1991) 267.
6. C. Sin'de, L. Chzhifen, U. Tszen'shen and Y. Tszen'khuan, *Russian J. Inorg. Chem.*, 36 (1991) 705.
7. H.T. Chu, C.F. Lao, T.S. Wu, T.H. Yen, I.G. Martynova and V.V. Sentemov, *Russian J. Inorg. Chem.*, 36 (1991) 988.
8. A. Rakotonandrasasana, D. Boinnard, J.-M. Savariault, J.-P. Tuchaugues, V. Petrouleas, C. Cartier and M. Verdaguer, *Inorg. Chim. Acta*, 180 (1991) 19.
9. C. Dash and B.K. Kanungo, *J. Inorg. Biochem.*, 42 (1991) 153.
10. M.R. Rhodes, M.H. Barley and T.J. Meyer, *Inorg. Chem.*, 30 (1991) 629.
11. B.E. Zaitsev, P.P. Pron'kin and V.A. Zaitsev, *Russian J. Inorg. Chem.*, 36 (1991) 1775.
12. R.K. Boggess, A.H. Lamson and S. York, *Polyhedron*, 10 (1991) 2791.
13. G.K. Hollingshed, G.A. Lawrence, M. Maeder, M. Rossignoli, *Polyhedron*, 10 (1991) 409.
14. M.J. Blandauer, J. Burgess, D.L. Elvidge, P. Guardado, A.W. Hakin, L.J.S. Prouse, S. Radulovic, D.R. Russell, *Transition Metal Chem.*, 16 (1991) 82.
15. S. Dev, E. Ramli, T.B. Rauchfuss and S.R. Wilson, *Inorg. Chem.*, 30 (1991) 2514.
16. Y.Z. Voloshin, V. Mosin and E.N. Karol, *Inorg. Chim. Acta*, 180 (1991) 189.
17. S. Lindeman, Y.T. Struchkov and Y.Z. Voloshin, *Inorg. Chim. Acta*, 184 (1991) 107.
18. Y.Z. Voloshin, N.A. Kostromina, A.Y. Nazarenko and E.V. Polshin, *Inorg. Chim. Acta*, 185 (1991) 83.
19. M. Mitewa, P.R. Bontchev, V. Russanov, E. Zhecheva, D. Mechandjiev and K. Kabassanov, *Polyhedron*, 10 (1991) 763.
20. S. Mahapatra, N. Gupta and R. Mukherjee, *J. Chem. Soc., Dalton Trans.* (1991) 2911.
21. M. Tachibana, K. Sasaki, A. Ueda, M. Sakai, Y. Sakaibara, A. Ohno and T. Okamato, *Chem. Lett.*, (1991) 993.
22. P. Basu, S. Pal and A. Chakravorty, *J. Chem. Soc., Dalton Trans.* (1991) 3217.
23. R. Benedix, H. Hennig and C. Nieke, *Z. Anorg. Allg. Chem.*, 605 (1991) 51 .
24. P.S. Braterman and J.-I. Song, *Inorg. Chim. Acta*, 180 (1991) 145.
25. G. De Santis, L. Fabbrizzi, A. Poggi and B. Seghi, *J. Chem. Soc., Dalton Trans.* (1991) 33.
26. M. Lieberman and T. Sasaki, *J. Am. Chem. Soc.*, 113 (1991) 1470.
27. Md. A. Masood, R. Jagannathan and P.S. Zacharias, *J. Chem. Soc., Dalton Trans.* (1991) 2553.
28. K. H. Reddy, G. Krishnaiah and Y. Sreenivasulu, *Polyhedron*, 10 (1991) 2785.
29. D.W. Thompson and D.V. Stynes, *Inorg. Chem.*, 30 (1991) 636.
30. D.G.A. Harshani de Silva, D.W. Thompson and D.V. Stynes, *Inorg. Chem.*, 30 (1991) 4865.
31. D.V. Stynes, D.G.A. Harshani de Silva and D.W. Thompson, *Inorg. Chim. Acta* 188 (1991) 139.
32. P.A. Padolik, A.J. Jircitano, N.W. Alcock and D.H. Busch, *Inorg. Chem.*, 30 (1991) 2713.
33. W. Nam, R. Ho and J.S. Valentine, *J. Am. Chem. Soc.*, 113 (1991) 7052.
34. A. Horvath, J. Szoke and W. Wojnarovits, *Inorg. Chim. Acta*, 179 (1991) 97.
35. N.J. Blundell, J. Burgess, P. Guardado and C.D. Hubbard, *J. Chem. Soc., Dalton Trans.* (1991) 1743.
36. S. Alshehri and J. Burgess, *Inorg. Chim. Acta*, 183 (1991) 153.
37. A. Rodriguez, C. Carmona, E. Muñoz, F. Sanchez and J.Burgess, *Transition Metal Chem.*, 16 (1991) 535.
38. E.H. Cutin, N.E. Katz, P.A.M. Williams and A.J. Aymonino, *Transition Metal Chem.*, 16 (1991) 155.
39. H.-Y. Huang, W.-J. Chen, C.-C. Yang and A. Yeh, *Inorg. Chem.*, 30 (1991) 1862..

39a. W. Weigand and W. Beck, *Z. Anorg. Allg. Chem.*, 600 (1991) 227.

40. D.C. Figg, R.H. Herber and I. Felner, *Inorg. Chem.*, 30 (1991) 2535.
41. M. Konno and M. Mikami-Kido, *Bull. Chem. Soc. Jpn.*, 64 (1991) 339.
42. A. Ozarowski, Y. Shunzhong, B.R. McGarvey, A. Mislankar and J.E. Drake, *Inorg. Chem.*, 30 (1991) 3167.
43. D. Onggo and H.A. Goodwin, *Aust. J. Chem.*, 44 (1991) 1539.
44. D. Onggo, D.C.Craig, A.D. Rae and H.A. Goodwin, *Aust. J. Chem.*, 44 (1991) 331.
45. A.T. Baker, P. Singh and V. Vignevich, *Aust. J. Chem.*, 44 (1991) 1041.
46. P. Gütlich and P. Poganiuch, *Angew. Chem. Int. Ed. Engl.*, 30 (1991) 975.
47. A. Hauser, *J. Chem. Phys.*, 94,(1991), 2741.
48. L.F. Larkworthy and S.K. Sengupta, *Inorg. Chim. Acta*, 179 (1991) 157.
49. M.H.B. Bol, E.J. Dirks, J.G. Hasnoot and J. Reedijk, *Inorg. Chim. Acta*, 180 (1991) 33.
50. M.-A. Martinez-Lorente, J.-P. Tuchagues, V. Petrouleas, J.-M. Savariault, R. Poinsot and M. Drillon, *Inorg. Chem.*, 30 (1991) 3587.
51. J.A. Real, G. De Munno, M.C. Muñoz and M. Julve, *Inorg. Chem.*, 30 (1991) 2701.

101. S. Deiana, C. Gessa, P. Piu and R. Seeber, *J. Chem. Soc., Dalton Trans.* (1991) 1237.
102. H. Yokoi, T. Tsutsui, Y. Mori and T. Mitani, *Chem. Lett.*, (1991) 2231.
103. S.S. Massoud and R.B. Jordan, *Inorg. Chem.*, 30 (1991) 4851.
104. S.H. Wasfi, C.E. Costello, A.L. Rheingold and B.S. Haggerty, *Inorg. Chem.*, 30 (1991) 1788.
105. H. Weiner, H.-J. Luck, J. Fuchs, B. Ziemer, R. Stosser, C. Pietzsch and P. Reich, *Z. Anorg. Allg. Chem.*, 594 (1991) 191.
106. J. Liu, W. Wang, Z. Zhu, E. Wang and Z. Wang, *Transition Metal Chem.*, 16 (1991) 169.
107. E. Wang, Q. Wu, B. Zhang and R. Huang, *Transition Metal Chem.*, 16 (1991) 478.
108. D. Mansuy, J.-F. Bartoli, P. Battioni, D.K. Lyon and R.G. Finke, *J. Am. Chem. Soc.*, 113 (1991) 7222.
109. D.K. Lyon, W.K. Miller, T. Novet, P.J. Domaille, E. Evitt, D.C. Johnson and R.G. Finke, *J. Am. Chem. Soc.*, 113 (1991) 7209.
110. K. Mader and W. Hoppe, *Z. Anorg. Allg. Chem.*, 602 (1991) 155.
111. R.J.B. Jakeman, M.J. Kwiecien, W.M. Reiff, A.K. Cheetham and C.C. Torardi, *Inorg. Chem.*, 30 (1991) 2806.
112. G. Giester and M. Wildner, *Monatsh. Chem.*, 122 (1991), 617.
113. T. Drews and K. Seppelt, *Z. Anorg. Allg. Chem.*, 606 (1991), 201.
114. J.W. Pyrz, X. Pan, D. Britton and L. Que, *Inorg. Chem.*, 30 (1991) 3461.
115. H.G. Jang, D.D. Cox and L. Que Jr., *J. Am. Chem. Soc.*, 113 (1991) 9200.
116. R.A. Leising, Y. Zang and L. Que, Jr., *J. Am. Chem. Soc.*, 113 (1991) 8555.
117. R.A. Leising, B.A. Brennan, L. Que, Jr., E. Münck and B.G. Fox, *J. Am. Chem. Soc.*, 113 (1991) 3988.
118. Y. Nishida, I. Watanabe and K. Unoura, *Chem. Lett.*, (1991) 1517.
119. Y. Nishida, and T. Akamatsu, *Chem. Lett.*, (1991) 2013.
120. M. Nakamura and N. Nakamura, *Chem. Lett.*, (1991) 1885.
121. J.D. Crane and D.E. Fenton, *Polyhedron*, 10 (1991) 1809..
122. F.M. Chyragov, G. Askerov and D.G. Gambarov, *Russian J. Inorg. Chem.*, 36 (1991) 1574.
123. M. Mizuno, S. Funahashi, N. Nakasuka and M. Tanaka, *Inorg. Chem.*, 30 (1991) 1550.
124. K. Kanamori, N. Ukita, K. Kawai, S. Taguchi, K.Goto, T. Eguchi and M. Kishita, *Inorg. Chim. Acta*, 186 (1991) 205.
125. J.F. Hesu, J.J. Chen, H.H. Wei, M.C. Cheng, Y. Wang and Y.D. Yao, *Inorg. Chim. Acta*, 184 (1991) 1.
126. D.C. Finnen, A.A. Pinkerton, W.R. Dunham, R.H. Sands and M.O. Funck, *Inorg. Chem.*, 30 (1991) 3960.
127. Y. Nishida, K. Yoshizawa and T. Takahashi, *J. Chem. Soc., Chem. Commun.* (1991) 1647.
128. J. Sima, T. Ducárová, T. Sramko and A. Kotocová, *Bull. Soc. Chim. Belg.*, 100 (1991) 193.
129. F. Lloret, M. Mollar, J. Faus, M. Julve, I. Castra and W. Diaz, *Inorg. Chim. Acta*, 189 (1991) 195.
130. M.Y. El-Sheikh, F.M. Ashmawy, I.A. Salem, A.B. Zaki and U. Nickel, *Transition Metal Chem.*, 16 (1991), 319.
131. M.K. Hassan, R.M. Hassan and M.A. Abd-Alla, *Monatsh. Chem.*, 122 (1991), 829.
132. V. I. Shcherbakova and O.B. Pankratova, *Koord. Khim.*, 17 (1991) 344.
133. P.V. Bernhardt, P. Comba, T.W. Hambley and G.A. Lawrance, *Inorg. Chem.*, 30 (1991) 942.
134. H. Stratemeir, M.A. Hitchman, P. Combe and M.J. Riley, *Inorg. Chem.*, 30 (1991) 4088.
135. S.H. Cho, D. Whang and K. Kim, *Bull. Korean Chem. Soc.*, 12 (1991) 107; *Chem. Abstr., 115 (1991) 63312s.*
136. M.L. Moya, A. Rodriguez and F. Sánchez, *Inorg. Chim. Acta*, 188 (1991) 185.
137. M.L. Moya, A. Barrios, M. del Mar Graciani, R. Jimenez, E. Muñoz, F. Sanchez and J. Burgess, *Transition Metal Chem.*, 16 (1991) 165.
138. F. Stochel and R. van Eldick, *Inorg. Chim. Acta*, 190 (1991) 55.
139. C.A. Hubbard, H.C. Baja, R. van Eldick, J. Burgess and N.J. Blundell, *Inorg. Chim. Acta*, 183 (1991) 1.
140. D. Chatterjee and A. Kr. Ghosh, *Transition Metal Chem.*, 16 (1991) 481.
141. R.C. Kapoor, R.N. Mehrotra, S.K. Vajpaiand P. Chaudhary, *Transition Metal Chem.*, 16 (1991) 65.
142. A. Zinn, H. von Arnim, W. Massa, M. Schäfer, J. Pebler and K. Dehnicke, *Z. Naturforsch.*, 46b (1991) 1300.
143. M. Januszczyk, J. Janicki, H. Wojakowska, R. Krzyminiewski and J. Pietrzak, *Inorg. Chim. Acta*, 186 (1991) 27.
144. E.J. Corey, N. Imai and H.-Y. Zhang, *J. Am. Chem. Soc.*, 113 (1991) 728.

145. E.C. Constable, M.S. Kahn, J. Lewis, M.C. Liptrot and P.R. Raithby, *Inorg. Chim. Acta*, 181 (1991) 207.
146. S.M. Godfrey, D.G. Kelly, A.G. Mackie, P.P. MacRory, C.A. McAuliffe, R.G. Pritchard and S.M. Watson, *J. Chem. Soc., Chem. Commun.* (1991) 1447.
147. R.F. Jameson and W. Linert, *Monatsh. Chem.*, 122 (1991), 887.
148. Y.I. Kim and W.E. Hatfield, *Inorg. Chim. Acta*, 188 (1991) 15.
149. B.V. Trzhtsinskaya, N.N. Chipanina, E.S. Domnina, E.B. Apakina, N.A. Khlopenko, K.G. Belyaeva and S.V. Novichikhin, *Koord. Khim.*, 17 (1991) 1083.
150. J.-H. Choy, D.-Y. Noh, H.-H. Park and J.-C. Park, *J. Chem. Soc., Dalton Trans.* (1991) 1647.
151. U. Bentrup and W. Massa, *Z. Anorg. Allg. Chem.*, 593 (1991), 207.
152. M. Hargittai, *Inorg. Chim. Acta*, 180 (1991) 5.
153. D.X. West and J.N. Albert, *Transition Metal Chem.*, 16 (1991), 1.
154. D.X. West and L.D. Barowy, *Transition Metal Chem.*, 16 (1991), 5.
155. D.X. West, C.S. Carlson and A.E. Liberta, *Transition Metal Chem.*, 16 (1991), 53.
156. N.S. Gupta, M. Mohan, N.K. Jha and W.E. Antholine, *Inorg. Chim. Acta*, 184 (1991) 13.
157. H. Oshio, K. Toriumi, Y. Maeda and Y. Takashima, *Inorg. Chem.*, 30 (1991) 4252.
158. Y. Maeda, H. Oshio, K. Tormiumi and Y. Takashima, *J. Chem. Soc., Dalton Trans.* (1991) 1227.
159. Y. Maeda, H. Oshio, Y. Tangiawa, T. Oniki and Y. Takashima, *Bull. Chem. Soc. Jpn.*, 64 (1991) 1522.
160. M. Matsumoto, H. Tamaki, K. Inoue, M. Koikawa, Y. Maeda, H. Okawa and S. Kida, *Chem. Lett.*, (1991) 1393.
161. V.B. Rybakov, L.A. Aslanov, S.V. Volkov, Z.A. Fokina and N.I. Timoshchenko, *Russian J. Inorg. Chem.*, 36 (1991) 1427.
162. U. Müller, M.-L. Ha-Eierdanz, G. Kräuter and K. Dehnicke, *Z. Naturforsch.*, 46B (1991) 175.
163. A.L. Petrou, M.V. Koromantzou and J.M. Tsangaris, *Transition Metal Chem.*, 16 (1991), 48.
164. H. Böhland and U. Witzenhausen, *Z. Anorg. Allg. Chem.*, 600 (1991), 131.
165. C.R. Johnson, C.M. Jones, S.A. Asher and J.E. Abola, *Inorg. Chem.*, 30 (1991) 2120.
166. U. Bentrup and W. Massa, *Z. Naturforsch.*, 46b (1991) 395.
167. L. Kirkiazis and R. Mattes, *Z. Anorg. Allg. Chem.*, 593 (1991), 90.
168. J. Graulich and D. Babel, *Z. Anorg. Allg. Chem.*, 597 (1991), 51.
169. F.M. Ashmawy, A.R. Ujaimi, C.A. McAuliffe, R.V. Parish and R.G. Pritchard, *Inorg. Chim. Acta*, 187 (1991) 155.
170. M.A. Yampol'skaya, Yu. A. Simonov, V.E. Zovodnik, K.I. Turte, M.S. Byrke, V.K. Voronkova, Yu. V. Yablokov and N.V. Gerbeleu, *Russian J. Inorg. Chem.*, 36 (1991) 47.
171. V.M. Leovac, R. Herak, B. Prelesnik and S.R. Niketic, *J. Chem. Soc., Dalton Trans.* (1991) 2295.
172. J. Rogalskyj and R.G. Bryant, *J. Coord. Chem.*, 24 (1991) 9.
173. D.V. Stynes, H. Noglik and D.W. Thompson, *Inorg. Chem.*, 30 (1991) 4567.
174. H. Noglik, D.W. Thompson and D.V. Stynes, *Inorg. Chem.*, 30 (1991) 4571.
175. C. Ercolani, F. Monacelli, S. Dzugan, V.L. Goedken, G. Pennesi and G. Rossi, *J. Chem. Soc., Dalton Trans.* (1991) 1309.
176. R.H. Beer, W.B. Tolman, S.G. Bott and S.J. Lippard, *Inorg. Chem.*, 30 (1991) 2082.
177. D. Zirong, R.C. Haltiwanger, S. Bhattacharya and C.G. Pierpont, *Inorg. Chem.*, 30 (1991) 4288.
178. A. Bonardi, C. Merlo, C. Pelizzi, P. Tarasconi and F. Cavatorta, *J. Chem. Soc., Dalton Trans.* (1991) 1063.
179. G.D. Fallon, A. Markiewicz, K.S. Murray and T. Quach, *J. Chem. Soc., Chem. Commun.* (1991) 198.
180. B. Bremer, K. Schepers, P. Fleischhauer, W. Haase, G. Henkel and B. Krebs, *J. Chem. Soc., Chem. Commun.* (1991) 510.
181. A. Stassinopoulos, G. Schulte, G.C. Papaefthymiou and J.P. Caradonna, *J. Am. Chem. Soc.*, 113 (1991) 8686.
182. R.J. O'Brien, J.J. Richardson and R.M. Buchanan, *Acta Crystallogr. C*, 47 (1991) 2307.
183. B.A. Brennan, Q. Chen, C. Juarez-Garcia, A.E. True, C.J. O'Connor and L. Que Jr., *Inorg. Chem.*, 30 (1991) 1937.
184. N. Kitajima and Y. Morooka, *Stud. Surf. Sci. Catal.*, 66 (1991) 259; *Chem. Abstr.*, 115 (1991) R 226612f.
185. W.B. Tolman, S. Liu, J.G. Bentsen and S.J. Lippard, *J. Am. Chem. Soc.*, 113 (1991) 152.
186. Y. Nishida, T. Akamatsu and M. Nasa, *Chem. Lett.*, (1991) 1703.

187. R.H. Fish, M.S. Konings, K.J. Oberhausen, R.H. Fong, W.M. Yu, G. Christou, R.B. Vincent, D.K. Coggin and R.M. Buchanan, *Inorg. Chem.*, 30 (1991) 3002.
188. U. Russo, B. Zarli, P. Zanonato and M. Vidali, *Polyhedron*, 10 (1991) 1353.
189. M. Fontecave, B. Roy and C. Lambeaux, *J. Chem. Soc., Chem. Commun.* (1991) 939.
190. R.D. Cannon, U.A. Jayasooriya, S.K. Koske, R.P. White and J.H. Williams, *J. Am. Chem. Soc.*, 113 (1991) 4158.
191. J.K. McCusker, H.G. Jang, M. Zvagulis, W. Ley, H.G. Drickamer and D.N. Hendrickson, *Inorg. Chem.*, 30 (1991) 1985.
192. T. Nakamoto, M. Katada and H. Sano, *Chem. Lett.*, (1991) 1323.
193. P. Poganiuch, S. Liu, G.C. Papaefthymiou and S.J. Lippard, *J. Am. Chem. Soc.*, 113 (1991) 4645.
194. V.M. Lynch, J.W. Sibert, J.L. Sessler and B.E. Davis, *Acta Crystallogr. C*, 47 (1991) 866.
195. K. Arora, P. Bhatnagar, A.P. Bhargava and Y. Gupta, *J. Chem. Soc., Dalton Trans.* (1991) 1081.
196. A.F. Duprat, P. Capdeville and M. Mauny, *J. Chem. Soc., Chem. Commun.* (1991) 464.
197. M.M. Mansurov, O.V. Semenova and S.S. Sokhibov, *Russian J. Inorg. Chem.*, 36 (1991) 1576.
198. T. Sato, K. Ishishita, M. Katada, H. Sano, Y. Aratono, S. Sagawa and M. Saeki, *Chem. Lett.*, (1991) 403.
199. S.M. Gorun and S.J. Lippard, *Inorg. Chem.*, 30 (1991) 1625.
200. H. Oshio, *J. Chem. Soc., Chem. Commun.* (1991) 240.
201. M. Mikuriya, Y. Kakuta, K. Kawano and T. Tokii, *Chem. Lett.*, (1991) 2031.
202. A. Gerli, K.S. Hagen and L.G. Marzilli, *Inorg. Chem.*, 30 (1991) 4673.
203. C. Fukuhara, T. Kazuhiko, N. Matsumoto, S. Kida, M. Mikuriya and M. Masayasu, *J. Chem. Soc., Dalton Trans.*, (1990) 3473.
204. J.L. Sessler, J.D. Hugdahl, V. Lynch and B. Davis, *Inorg. Chem.*, 30 (1991) 334.
205. J.K. McCusker, J.B. Vincent, E.A. Schmitt, M.L. Mino, K. Shin, D.K. Coggin, P.M. Hagen, J.C. Huffman, G.C. Christou and D.N. Hendrickson, *J. Am. Chem. Soc.*, 113 (1991) 3012.
206. D.F. Harvey, C.A. Christmas, J.K. McCusker, P.M. Hagen, R.K. Chadha and D.N. Hendrickson, *Angew. Chem. Int. Ed. Engl.*, 30 (1991) 598.
207. J.K. McCusker, C.A. Christmas, P.M. Hagen, R.K. Chadha, D.F. Harvey and D.N. Hendrickson, *J. Am. Chem. Soc.*, 113 (1991) 6114.
208. C. Jaurez-Garcia, M.P. Hendrickson, T.R. Holamn, L. Que and E.Münck, *J. Am. Chem. Soc.*, 113 (1991) 518.
209. I. Morgenstern-Badarau, D. Laroque, E. Bill, H. Winkler, A.X. Trautwein, F. Robert and Y. Jeanin, *Inorg. Chem.*, 30 (1991) 3180.
210. P. Chaudhuri, M. Winter, B.P.C. Della Védova, P. Fleischhauer, W. Haase, U. Flörke and H.-J. Haupt, *Inorg. Chem.*, 30 (1991) 4777.
211. R. Schmid, H. Ahamdane and A. Mosset, *Inorg. Chim. Acta*, 190 (1991) 237.
212. R. Gupta, A. Shah, A. Singh and R.C. Mehrota, *New J. Chem.*, 15 (1991) 665.
213. H.W. Rich, K. Hegetschweiler, H.M. Streit, I. Erni and W. Schneider, *Inorg. Chim. Acta*, 187 (1991) 9.
214. A. Robert, B. Loock, M. Momenteau and B. Meunier, *Inorg. Chem.*, 30 (1991) 706.
215. L. Casella, M. Gullotti, L. De Gioia, E. Monzani and F. Chillemi, *J. Chem. Soc., Dalton Trans.* (1991) 2945.
216. A.M. Helms, W.D. Jones and G.L. McLendon, *J. Coord. Chem.*, 23 (1991) ,351.
217. M.A. Ivanca, G. Lappin, W.R. Scheidt, *Inorg. Chem.*, 30 (1991) 711.
218. R. Guilard, I. Perrot, A. Tabard, P. Richard, C. Lecomte, Y.H. Liu and K.M. Kadish, *Inorg. Chem.*, 30 (1991) 27.
219. A. Malek, L. Latos-Grażynski, T.J. Bartezak and A. Zadlo, *Inorg. Chem.*, 30 (1991) 3222.
220. F.C.F. Körber, J.R. Lindsay Smith, S. Prince, P. Rizkallah, C.D. Reynolds and D.R. Shawcross, *J. Chem. Soc., Dalton Trans.* (1991) 3291.
221. K.M. Kadish, A. Tabard, W. Lee, Y.-H. Liu, C. Ralti and R. Guilard, *Inorg. Chem.*, 30 (1991) 1542.
222. G.-X. He and T.C. Bruice, *J. Am. Chem. Soc.*, 113 (1991) 2747.
223. E. Gopinath and T.C. Bruice, *J. Am. Chem. Soc.*, 113 (1991) 6090.
224. T.W. Kaaret, G.-H. Zhang and T.C. Bruice, *J. Am. Chem. Soc.*, 113 (1991) 4652.
225. E. Gopinath and T.C. Bruice, *J. Am. Chem. Soc.*, 113 (1991) 4657.
226. Y. Watanabe, K. Yamaguchi, I. Morishima, K. Takehira, M. Shimizu, T. Hayakawa and H. Orita, *Inorg. Chem.*, 30 (1991) 2581.
227. Y. Naruta, F. Toni, N. Ishihara and K. Maruyama, *J. Am. Chem. Soc.*, 113 (1991) 6865.

228. J.F. Bartoli, O. Brigand, P. Battioni and D. Mansuy, *J. Chem. Soc., Chem. Commun.* (1991) 440.
229. Y. Ito, *J. Chem. Soc., Chem. Commun.* (1991) 622.
230. S. Tsuchiya, *J. Chem. Soc., Chem. Commun.* (1991) 716.
231. D.L. Corina, S.L. Miller, J.N. Wright and M. Akhtar, *J. Chem. Soc., Chem. Commun.* (1991) 782.
232. A. Maldotti, C. Bartocci, R. Amadelli, E. Polo, P. Battioni and D. Mansuy, *J. Chem. Soc., Chem. Commun.* (1991) 1487.
233. K. Kano, H. Takagi, M. Takeuchi, S. Hashimoto and Z.-I. Yoshida, *Chem. Lett.*, (1991) 519.
234. S. Sakaki, S. Mitari and K. Ohkubo, *Chem. Lett.*, (1991) 195.
235. C. Bartocci, A. Maldotti, G. Varani, P. Battioni, V. Carassiti and D. Mansuy, *Inorg. Chem* 30 (1991) 1255.
236. A. Nanthakumar and H.M. Goff, *Inorg. Chem.*, 30 (1991) 4460.
237. K.K. Irikura and J.L. Beauchamp, *J. Am. Chem. Soc.*, 113 (1991) 2767.
238. S. Hashimoto, Y. Mizutani, Y. Tatsuno and K. Kitagawa, *J. Am. Chem. Soc.*, 113 (1991) 6542.
239. D. Lu, I.R. Paeng and K. Nakamoto, *J. Coord. Chem.*, 23 (1991) 3.
240. S. Nagakaki, Y. Iamamoto, O. Baffa, O.R., Nascimento, *Inorg. Chim. Acta.* 186 (1991) 39.
241. M. das Dores Assis, O. Serra, Y. Iamamoto and O.R. Nascimento, *Inorg. Chim. Acta*, 187 (1991) 107.
242. R.D. Arasasingham and T.C. Bruice, *J. Am. Chem. Soc.*, 113 (1991) 6095.
243. K. Hatano, M.K. Safo, F.A. Walker and W.R. Scheidt, *Inorg. Chem.*, 30 (1991) 1643.
244. M.K. Safo, G.P. Gupta, F.A. Walker and W.R. Scheidt, *J. Am. Chem. Soc.*, 113 (1991) 5497.
245. M.K. Safo, W.R. Scheidt, G.P. Gupta, R.D. Orosz and C.A. Reed, *Inorg. Chim. Acta*, 184 (1991) 251.
246. F.A. Walker and U. Simonis, *J. Am. Chem. Soc.*, 113 (1991) 8652.
247. M. Nakamura and N. Nakamura, *Chem. Lett.*, (1991) 627.
248. V. Bulach, D. Mandon and R. Weiss, *Angew. Chem. Int. Ed. Engl.*, 30 (1991) 572.
249. S. Sakaki, Y. Nishijima and K. Ohkubo, *J. Chem. Soc., Dalton Trans.* (1991) 1143.
250. S. Mazumdar, O.K. Medhi and S. Mitra, *Inorg. Chem.*, 30 (1991) 700.
251. E.T. Kintner and J.H. Dawson, *Inorg. Chem.*, 30 (1991) 4892.
252. M. Momenteau, *Bull. Soc. Chim. Belg.*, 100 (1991) 731.
253. E. Tsuchida, E. Hasegawa, T. Komatsu, T. Nakata, K. Nakao and H. Nishide, *Bull. Chem. Soc. Jpn.*, 64 (1991) 888.
254. T. Komatsu, E. Hasegawa, S. Kumamoto, H. Nishide and E. Tsuchida, *J. Chem. Soc., Dalton Trans.* (1991) 3281.
255. E. Tsuchida, T. Komatsu, T. Nakata, H. Nishide and H. Inoue, *J. Chem. Soc., Dalton Trans.* (1991) 3285.
256. M.T. Ahmet, G. Al-Jaff, J. Silver and M.T. Wilson, *Inorg. Chim. Acta*, 183 (1991) 43.
257. E. Oldfield, H.C. Lee, C. Coretsopoulos, F. Adebodun, K.D. Park, S. Yang, J. Chung and B. Phillips, *J. Am. Chem. Soc.*, 113 (1991) 8680.
258. L.M. Proniewicz, I.R. Paeng and K. Nakamoto, *J. Am. Chem. Soc.*, 113 (1991) 3294.
259. K. Kim and J. Ibers, *J. Am. Chem. Soc.*, 113 (1991) 6077.
260. H.M. Marques, *Inorg. Chim. Acta*, 190 (1991) 291.
261. I.-K. Choi, Y. Liu, D. Feng, K.-J. Paeng and M.D. Ryan, *Inorg. Chem.*, 30 (1991) 1832.
262. T.Yoshimura, *Bull. Chem. Soc. Jpn.*, 64 (1991) 2819.
263. H. Nasri, Y. Wang, B.H. Huynh and W.R.Scheidt, *J. Am. Chem. Soc.*, 113 (1991) 717.
264. H. Nasri, Y. Wang, B.H. Huynh, F.A. Walker and W.R. Scheidt, *Inorg. Chem.*, 30 (1991) 1483.
265. K.S. Suslick and R.A. Watson, *Inorg. Chem.*, 30 (1991) 912.
266. E. Hasegawa, E. Matsubuchi and E. Tsuchido, *Bull. Chem. Soc. Jpn.*, 64 (1991) 2289.
267. H. Sugaya, J. Tachibana and T. Imamura, *Polyhedron*, 10 (1991) 373.
268. P.W. Crawford and M.D. Ryan, *Inorg. Chim. Acta*, 179 (1991) 25.
269. S. Mazumdar, *J. Chem. Soc., Dalton Trans.* (1991) 2091.
270. J. McKnight, M.R. Cheeseman, C.A. Reed, R.D. Orosz and A.J.Thomson, *J. Chem. Soc., Dalton Trans.* (1991) 1887.
271. K.A. Keating, J.S. de Ropp, G.N. La Mar, A.L. Balch, F.-Y. Shiau and K.M. Smith, *Inorg. Chem.*, 30 (1991) 3258.
272. M.P. Byrn, C.J. Curtis, I. Goldberg, Y. Hsiou, S.I. Kahn, P.A. Sawin, K. Tendick and C.E. Strouse, *J. Am. Chem. Soc.*, 113 (1991) 6549.
273. M.P. Byrn and E.C. Strouse, *J. Am. Chem. Soc.*, 113 (1991) 2501.

274. E.P. Sullivan Jr., J.D. Grantham, C.S. Thomas and S.H. Strauss, *J. Am. Chem. Soc.*, 113 (1991) 5264.
275. C. Ercolani, A.M. Paoletti, G. Pennesi and G. Rossi, *J. Chem. Soc., Dalton Trans.* (1991) 1317.
276. F. Monacelli, *J. Chem. Soc., Dalton Trans.* (1991) 3373..
277. M. Hanack, G. Renz, J. Straehle and S. Schmid, *J. Org. Chem.*, 56 (1991) 3501.
278. D. Jacoby, C. Floriani, A. Chiesi-Villa and C. Rizzoli, *J. Chem. Soc., Chem. Commun.* (1991) 220.
279. S. Licoccia, M. Paci, R. Paolesse and T. Boschi, *J. Chem. Soc., Dalton Trans.* (1991) 461.
280. W.-Y. Sun, N. Ueyamaand A. Nakamura, *Inorg. Chem.*, 30 (1991) 4026.
281. M.S. Gebhard, S.A. Koch, M. Millar, F.J. Devin, P.J. Stephens and E.I. Solomon, *J. Am. Chem. Soc.*, 113 (1991) 1640.
282. D. Sellmann, M. Geck, F. Knoch, G. Ritter and J. Dengler, *J. Am. Chem. Soc.*, 113 (1991) 3819.
283. D. Sellmann, M. Geck and M. Moll, *J. Am. Chem. Soc.*, 113 (1991) 5259.
284. D. Sellmann, K. Höhn and M. Moll, *Z. Naturforsch.*, 46b (1991) 665.
285. D. Sellmann, K. Höhn and M. Moll, *Z. Naturforsch.*, 46b (1991) 673.
286. D. Sellmann, H.-P. Neuner and F. Knoch, *Inorg. Chim. Acta*, 190 (1991) 61.
287. M.J. Nelson, H. Jin, I.M. Turner Jr., G. Grove, R.C. Scarrow, B.A. Brennan and L. Que Jr., *J. Am. Chem. Soc.*, 113 (1991) 7072.
288. N. Ueyama, S. Ueno, T. Sugawara, K. Tatsumi, A. Nakamura and N. Yasuoka, *J. Chem. Soc., Dalton Trans.* (1991) 2723.
289. P.P. Power and S.C. Shoner, *Angew. Chem. Int. Ed. Engl.*, 30 (1991) 330.
290. J.A. Weigel and R.H. Holm, *J. Am. Chem. Soc.*, 113 (1991) 4184.
291. M.A. Whitener, G. Peng and R.H. Holm, *Inorg. Chem.*, 30 (1991) 2411.
292. H.Y. Liu, B. Scharbert and R.H. Holm, *J. Am. Chem. Soc.*, 113 (1991) 9529.
293. U. Bierbach, W. Saak, D. Haase and S. Pohl, *Z. Naturforsch.*, 46b (1991) 1629.
294. S. Pohl and U. Bierbach, *Z. Naturforsch.*, 46b (1991) 68 .
295. J.N. Butt, F.A. Armstrong, J. Breton, S.J. George, A.J. Thomson and E.C. Hatchikian, *J. Am. Chem. Soc.*, 113 (1991) 6663.
296. J.N. Butt, A. Sucheta, F.A. Armstrong, J. Bretton and A.J. Thomson, *J. Am. Chem. Soc.*, 113 (1991) 8948.
297. S. Ciurli and R.H. Holm, *Inorg. Chem.*, 30 (1991) 743.
298. E.K.H. Roth, J.M. Greneche and J. Jordanov, *J. Chem. Soc., Chem. Commun.* (1991) 105.
299. P. Excoffon, J. Laugier and B. Lamotte, *Inorg. Chem.*, 30 (1991) 3075.
300. C.F. Martens, H.L. Blonk, T. Bongers, J.G.M. van der Linden, G. Beurskens, P.T. Beurskens, J.M.M. Smits and R.J.M. Nolte, *J. Chem. Soc., Chem. Commun.* (1991) 1623.
301. K. Tamaka and S. Tamaka, *Bull. Chem. Soc. Jpn.*, 64 (1991) 1192.
302. H.L. Blonk, O. Kierit, E.K.-H. Roth, J. Jordanov, J.G.M. van der Linden and J.J. Steggerda, *Inorg. Chem.*, 30 (1991) 3231 .
303. P.L. Fabre, D. de Montauzon and P. Poilblanc, *Bull. Soc. Chim. France*, 127 (1991) 123.
304. T. Sugawara, N. Ueyama and A. Nakamura, *J. Chem. Soc., Dalton Trans.* (1991) 249.
305. A.K. Yatsimirsky and A.I. Dky, *Inorg. Chim. Acta*, 186 (1991) 161.
306. E.T. Smith, B.A. Feinberg, J.H. Richards and J.M. Tomich, *J. Am. Chem. Soc.*, 113 (1991) 688.
307. T. Shibahara, T. Asano and G. Sakane, *Polyhedron*, 10 (1991) 2351.
308. W. Saak and S. Pohl, *Angew. Chem. Int. Ed. Engl.*, 30 (1991) 881.
309. P.A. Eldredge, K.S. Bose, D.E. Barber, R.F. Bryan, E. Sinn, A. Rheingold and B.A. Averill, *Inorg. Chem.*, 30 (1991) 2365.
310. P. Baird, J.A. Bandy, M.L. Green, A. Hamnett, E. Marseglia, D.S.Obertelli, K. Prout and J. Qin, *J. Chem. Soc., Dalton Trans.* (1991) 2377.
311. S.A. Al-Ahmad, J.W. Kampf, R.W. Dunham and D. Coucouvanis, *Inorg. Chem.*, 30 (1991) 1163.
312. B.S. Snyder, M.S. Reynolds, R.H. Holm, G.C. Papaefthymiou and K.B. Frankel, *Polyhedron*, 10 (1991) 203.
313. J.M. McConnachie and J.A. Ibers, *Inorg. Chem.*, 30 (1991) 1770.
314. S.-B. Yu, G.C. Papaefthymiou and R.H. Holm, *Inorg. Chem.*, 30 (1991) 3476.
315. M.A. Greaney, C.L. Coyle, R.S. Pilato, *Inorg. Chim. Acta*, 190, (1991), 81.
316. J.-F. You and R.H. Holm, *Inorg. Chem.*, 30 (1991) 1431.
317. A. Dei, D. Gatteschi, L.Pardi and U. Russo, *Inorg. Chem.*, 30 (1991) 2589.
318. W. Weigand and W. Beck, *Z. Anorg. Allg. Chem.*, 600 (1991) 227.

319. H. Xiao-jun, J. Pei-sang, H. Guo-sheng and M. Yong-xiang, *Transition Metal Chem.*, 16 (1991) 314.
320. M. Yong-xiang, H. Guo-sheng, J. Pei-song and H. Xiao-jun, *Bull. Soc. Chim. Belg.*, 100 (1991) 205.
321. A. Hills, D.L. Hughes, M. Jimenez-Tenorio, G.J. Leigh, C.A. McGeary, A.T. Rowley, M. Bravo, C.E. McKenna and C.-A. McKenna, *J. Chem. Soc., Chem. Commun.* (1991) 522.
322. P. Guillaume, H. Li Kam Wah and M. Postel, *Inorg. Chem.*, 30 (1991) 1828.
323. G. Barrado, G.A. Carriedo, C. Diaz-Valenzuela and V. Riera, *Inorg. Chem.*, 30 (1991) 4416.
324. L.D. Field, A.V. George and B.A. Messerle, *J. Chem. Soc., Chem. Commun.* (1991) 1339.
325. T.M. Rana and C.F. Meares, *J. Am. Chem. Soc.*, 113 (1991) 1859.
326. A.B. Smirnov, V.I. Khelskov, K.I. Turte and F.A. Spatar, *J. Struct. Chem.*, 32 (1991) 795.
327. M. Wildner and G. Geister, *Z. Kristallog.*, 196 (1991) 269.
328. B. Malaman, M. Ijjaali, G. Venturini and C. Gleitzer, *Eur. J. Solid State Inorg. Chem.*, 28 (1991) 519.
329. M. Ijjaali, G. Venturini, R. Gerardin, B. Malaman and C. Gleitzer, *Eur. J. Solid State Inorg. Chem.*, 28 (1991) 983.
330. C. Gleitzer, *Eur. J. Solid State Inorg. Chem.*, 28 (1991) 77.
331. R. Glaum, M. Walter-Peter, D. Ozalp and R. Gruehn, *Z. Anorg. Allg. Chem.*, 601 (1991) 145.
332. T. Prusse, A. Fiedler and H. Schwarz, *J. Am. Chem. Soc.*, 113 (1991) 8335.
333. Md. A, Masood and P.S. Zacharias, *J. Chem. Soc., Chem. Commun.* (1991) 152.
334. N. Singh, R. Verma and N.K. Singh, *Polyhedron*, 10 (1991) 1803.
335. S.E. Dann, M.T. Weller and D.B. Currie, *J. Solid State Chem.*, 92 (1991) 237.
336. K. Mader and W. Hoppe, *Z. Anorg. Allg. Chem.*, 592 (1991) 51.
337. V.K. Sharma and B.H.J. Bielski, *Inorg. Chem.*, 30 (1991) 4306.